Forecast Based Risk Management for Electricity Trading Market

by

Takuji Matsumoto

SUBMITTED TO THE GRADUATE SCHOOL OF BUSINESS SCIENCES
IN PARTIAL FULFILLMENT OF THE REQUIREMENTS FOR THE DEGREE OF

DOCTOR OF PHILOSOPHY
AT THE
UNIVERSITY OF TSUKUBA

JUNE 2020

電力取引市場のための予測に基づくリスク管理

筑波大学審査学位論文（博士）

２０２０

松　本　拓　史

筑波大学大学院
ビジネス科学研究科　企業科学専攻

Forecast-Based Risk Management for Electricity Trading Market

by

Takuji Matsumoto

Submitted to the Graduate School of Business Sciences
in partial fulfillment of the requirements
for the degree of Doctor of Philosophy

Abstract

In recent years, the need for risk management in electricity trading has been increasing rapidly. Particularly, dealing with the risks posed by renewable energies has become an urgent issue on a global scale. The purpose of this research is to propose a solution based on various approaches to the problem of risk management for electricity trading, which has become complicated in recent years. The approaches can be broadly divided into three methods: forecasting methods, hedging methods, and market trading strategies.

First, we propose a prediction method for solar power producers. By combining the yearly cyclical trends of solar radiation and power output for each general weather scenario (as estimated by a generalized additive model (GAM)) with weather probability distribution (as estimated by the multinomial logit model), we propose a simple and sufficiently accurate prediction model. In the empirical analysis, we clarify the superiority of the proposed method in reducing prediction error by comparing the existing method and the method of directly substituting the weather forecast into the regression prediction formula, thereby obtaining useful suggestions to practitioners.

As for the hedging method, we first propose a method for the prediction error loss of solar power generation. Since the prediction error of renewable energy power output, such as solar power generation, increases supply and demand adjustment costs, a penalty is imposed according to the prediction error. For hedging such a prediction error loss, we propose a weather derivative on prediction error of solar radiation and demonstrate that the existing hedging method in wind power generation is effective also for solar power generation with strong seasonality. In addition, we propose a cross-hedging method using a derivative based on the absolute value of temperature prediction error and demonstrate its effectiveness.

We also propose a strategy for hedging price and volume risk simultaneously. With this strategy, we verify the effectiveness of the proposed method using different market models, such as the Japan Electric Power Exchange (JEPX) and US PJM. In particular, we develop a hedging model that effectively estimates complex, intertwined trends by combining existing non-parametric regressions from different perspectives, such as using tensor product spline functions, ANOVA decomposition, and spline functions with cross variables. Furthermore, we propose new standardized derivatives on squared temperature error and reveal their high hedging effects.

Regarding the market trading strategy, we propose an arbitrage trading method in the balancing market for retailers. We find that the effect of arbitrage on system stabilization, which was confirmed in the previous study in the European market, is also confirmed for different systems in the Japanese market. Specifically, we demonstrate some interesting market mechanisms. For example, we explain that the more predictable the imbalance amount and price, the greater the profit of the arbitrager and the system stabilizing effect. Also, we show how imposing a certain scale penalty on the generated imbalance contributes to further reductions in the imbalance of an entire system. In modeling, we propose a refined market analysis method by deriving a prediction method of a discrete approximate probability distribution based on a two-step quantile regression and by improving the previous optimization problem.

Risk management in the electricity market involves extremely complicated issues, including social, economic, and environmental factors, which should be considered at the same time. An analysis that organically connects different perspectives—such as practice and research, the Japanese market and the foreign market, as well as business strategy and policy institutional design—as is attempted in this research is thought to be a possible way to further improve economic efficiency in complex electricity markets.

Chief Thesis Advisor: Dr. Yuji Yamada
Title: Professor. Dean, Faculty of Business Sciences

Thesis Advisor: Dr. Naoki Makimoto
Title: Professor, Faculty of Business Sciences

Thesis Advisor: Dr. Koken Ozaki
Title: Associate Professor, Faculty of Business Sciences

Acknowledgments

Foremost, I would like to express my deepest gratitude to my chief thesis advisor, Professor Yuji Yamada, for his continuous support of my Ph.D. study and research, as well as for his patience, motivation, and immense knowledge. His advice has always played a decisive role in my research and in the writing of this thesis. Also, he provided me with countless opportunities for learning, including enabling me to present at multiple academic conferences, submit papers, and study abroad. I would also like to thank my associate thesis advisors, Professor Naoki Makimoto and Associate Professor Koken Ozaki, for their time and encouragement. I am also grateful to the two anonymous referees. In addition, I wish to express my sincere thanks to Professor Derek Bunn for accepting my research visit at London Business School and leading me with his superb guidance and insights. Last of all, I would like to express my heartfelt appreciation to my family for their great patience and for supporting me throughout this long research project.

Contents

List of Figures

List of Tables

List of Abbreviations

ANOVA	Analysis of Variance
AR	Auto-Regressive model
AR(I)MA(X)	Auto-Regressive (Integrated) Moving Average model (with exogenous variables)
CAPP	Central Appalachia (coal)
DA	Day-Ahead (market/price)
EMSC	Electricity and Gas Market Surveillance Commission
FIT	Feed-In Tariff Law
FOB	Free on Board
GAM	Generalized Additive Model
GARCH	Generalized Auto-Regressive Conditional Heteroskedasticity model
GPV	Grid Point Value
HH	Henri Hub (natural gas)
ICE	Intercontinental Exchange
ID	Intraday (market/price)
JEPX	Japan Electric Power Exchange
JMA	Japan Meteorological Agency
LNG	Liquefied Natural Gas
MA	Moving Average model
MAE	Mean Absolute Error
METI	Ministry of Economy, Trade and Industry
MNL	Multinomial Logit model
OCCTO	Organization for Cross-regional Coordination of Transmission Operators
OFGEM	Office of Gas and Electricity Markets (UK)
OLS	Ordinary Least Squares regression
PJM	Pennsylvania, Jersey, Maryland Power Pool
PMAE	Percent Mean Absolute Error
PRMSE	Percent Root Mean Square Error
PRSS	Penalized Residual Sum of Squares
PV	Photovoltaic (solar power)
RMSE	Root Mean Square Error
RT	Real Time (market/price)
RTO	Regional Transmission Organization
VAR	Vector Auto-Regressive model
VRR	Variance Reduction Rate
WTI	West Texas Intermediate (oil)

Chapter 1

Introduction

In 2016, the Japanese electricity market was fully liberalized in the retail market, and the need for risk management related to electricity trading has rapidly increased since then. Before 2016, the Japanese electricity market had been operated by so-called "vertically integrated" power companies and was promoted in a regional monopolistic manner under a regulated rate system called the "rate-of-return regulation." However, in the process of liberalization, which aimed to maximize social welfare (economic efficiency), the rate-of-return regulation was eliminated and transformed into a market environment where prices are determined by free competition. As a result, the need for risk management in power trading rapidly emerged, both for power companies exposed to new price fluctuation risks and for those entering the electricity retail businesses.

The factors that have increased the risk management needs in electricity trading have included more than the changes in Japan's unique market environment, as described above. In recent years, countries around the world have been responding to the new risks caused by renewable energies, which are increasingly installed worldwide to reduce global warming. The generated power outputs of renewable energies, such as solar power and wind power, are difficult to estimate in advance because they depend on the uncertain weather conditions at each power generation time. In addition, fluctuations in the amount of renewable energy output have a significant effect on fluctuations in electricity prices. Under such circumstances, responding to such risks in price and volume from renewable energy is an urgent issue for researchers and practitioners alike.

The purpose of this study is to propose solutions from different approaches to risk management issues in the electricity market that have emerged quickly from the background above. Our approaches can be broadly divided into three categories: prediction methods, risk hedging (insurance) strategies, and market trading strategies. In line with these categories, each chapter in

this thesis is structured as follows.

In Chapter 2, through a survey of previous studies, we comprehensively review past studies on each of the above three approaches to provide an overview of various research works, ranging from basic to cutting-edge research. By doing this, we understand the transition of social needs and the evolution of methodologies, and then make suggestions that can lead to the discovery and resolution of current or future issues.

After that, in Chapters 3 to 6, we propose specific risk management methods. First, Chapter 3 proposes prediction methods for solar power generation companies in which generalized additive models (GAMs) are constructed based on the intuitive and simple idea that a smooth yearly cyclical trend should be found when dividing solar radiation and solar power output by clock time and weather. In this way, we propose a sufficiently accurate prediction method that is easy to handle for new entrants, who have increased rapidly in recent years. Also, by focusing on the possible prediction biases derived from weather forecast errors, we propose a new prediction method that avoids such biases by constructing a multinomial logit model that can estimate the probability of a weather scenario based on weather forecast, and combine it with a GAM.

Next, Chapter 4 proposes hedging strategies for the prediction error loss of solar power generation, whose practical needs have emerged due to the recent expansion of renewable energies and related system changes. In this chapter, we construct a new model that applies the previous method of hedging the prediction error losses for wind power to hedging for solar power with strong periodicity. In particular, by introducing multiple weather derivatives such as solar radiation derivatives and temperature derivatives, we propose a hedging method that utilizes a tensor product spline function that effectively estimates smooth trends that exist in two different directions, such as time trends of each day and seasonal trends of each clock time.

In Chapter 5, by focusing on the simultaneous hedge for price risk and volumetric risk, we propose hedging strategies to address the fluctuation risks in the revenue of solar power generation companies trading in the Japan Electric Power Exchange (JEPX) and the risks related to the procurement costs of retail power companies trading in the PJM market in US. We propose various specific non-parametric regression models that can effectively estimate different trends on seasonality and annual change by using derivatives portfolios consisting of fuel and weather

derivatives. The proposed model is somewhat complex and contains entangled interactions. Therefore, in order to demonstrate the robustness and versatility of the models, we perform extensive empirical studies using the actual data of different market models, such as the JEPX and PJM, as well as different businesses, such as solar power companies and retail utilities.

Then, Chapter 6 describes arbitrage strategies for retail businesses under the current Japanese system, motivated by the latest system changes related to the adjustment for the gap between supply and demand, which is called "imbalance." In this chapter, we demonstrate that the system stabilization effect of arbitrage by retailers, which was shown in previous studies using European market models, can also be confirmed under the Japanese market system. Specifically, this research aims to obtain useful, practical suggestions not only in terms of effective trading strategies performed by retailers but also in terms of the market system designed by policymakers. Finally, a summary and concluding remarks are given in Chapter 7.

As described above, the handing of data and the modeling of objects are different in each chapter. However, from the viewpoint of the methodology, all works deal with the same problem of how to effectively model each time series data related to the electricity market, which has very strong non-linear trends in different directions. The specific explanations of the individual methodologies are given in each chapter, but taking the example of non-parametric regression, a variety of methods are used (e.g., univariate cubic spline function, spline with cross variables, tensor product spline function, and ANOVA decomposition). Thus, one of the central purposes of this thesis is the proposal of various methods that can effectively model a varied time series with complex interactions in different trend directions. Additionally, in order to eliminate biases that could occur from the point estimation with an average value, prediction models for probability distributions are used together (e.g., multinomial logit model in Chapter 3 and quantile regression in Chapter 6).

Another point that this research is focused on is real-world applicability. In decision-making processes that involve many people, one of the most important points in modeling analysis is the "interpretability" or the "explanatory power" (not necessarily the statistical context) of the results. The authors also realized this from the practical experiences in policy analyses and electricity risk consulting in the government agencies and the private company. In recent years, the development of various technologies such as artificial intelligence and machine learning has been remarkable,

and it goes without saying that they can be excellent tools for optimizing certain evaluation functions (e.g., minimizing prediction errors). However, as their computation processes are illustrated by words such as “black-boxes,” they might not always be favorable in terms of their construability or accountability. On the other hand, the methods discussed in this study are thought to have advantages in terms of interpretability. For each theme, we considered adding careful interpretations and various visualizations when performing empirical analysis. In fact, institutional policy design in public sectors and strategic decision-making in private sectors are both based on consensus building on repeated discussions among many stakeholders. Considering that fact, the most effective model would not necessarily be the one with the best value in its numerical evaluation but is often a “simple and clear but sufficiently effective” model that can facilitate efficient consensus building. In view of the above points, a common goal of each theme is to obtain practical suggestions, focusing on interpretability and applicability while grasping the changing needs of the social environment.

Chapter 2

Literature Survey

2.1 Introduction

In this Chapter, we conduct a comprehensive study on risk management for electricity market transactions by carrying out an extensive survey on previous studies about risk management. As mentioned in Chapter 1, this work makes new proposals for prediction methods, hedging strategies, and market trading strategies, each of which corresponds to key concepts of risk management, such as risk avoidance/mitigation (in the sense of preventing risks related to prediction errors), risk transfer (insurance), and risk diversification (portfolio optimization). With this classification as a background, Figure 2.1 illustrates the previous research to be surveyed in this work and the corresponding chapters of this thesis.

Main categories	Research to be surveyed	Corresponding chapter / section	Cap. 2	Cap. 3	Cap. 4	Cap. 5	Cap. 6
Prediction method ● Risk avoidance ● Risk reduction	Solar power	2.2.1	✓	(✓)	(✓)	(✓)	(✓)
	Demand	2.2.2					(✓)
	Electricity price	2.2.3				(✓)	(✓)
Hedging method ● Risk transfer/hedge (insurance)	Electricity derivatives	2.3.1				(✓)	
	Weather and other derivatives	2.3.2			✓	✓	
Trading Strategy ● Risk diversification (portfolio optimization)	Balancing market	2.4.1	(✓)	(✓)			✓
	Intraday market	2.4.2					(✓)

(Note) ✓: main theme, (✓): concepts or viewpoints are closely related

Figure 2.1: Previous research to be surveyed and corresponding chapters

In the following section, we review a series of these previous research works, ranging from basic to very recent research to provide an understanding of the transition of social needs and issues and comprehend the evolution of methodologies. By doing so, this chapter aims to generate suggestions that contribute to discovering and solving present and future problems.

2.2 Prediction Methods in Electricity Market

Predicting, or forecasting, is the most basic concept in the risk management of power trading. Developing hedging models and trading strategies is essentially the same as performing predictions in a broad sense in that they estimate effective decisions or obtain beneficial suggestions related to unknown future events. In fact, all the methods proposed in this thesis are based on the concept of forecast, as described in its title. Hence, this section reviews previous studies dealing with forecast methods related to solar power generation, demand, and electricity prices.

2.2.1 Solar Power Prediction

This section overviews research on prediction methods for solar power generation. When the prediction methods of solar power generation are classified according to the types of data used, it can be seen that some utilize widely published weather forecast values, while others deal with a detailed prediction of solar radiation (e.g., in a spatiotemporal manner using three-dimensional numerical weather models). We are interested in research related to the former type of prediction method since the purpose of this study is to propose a simple and clear but sufficiently effective model (as described at the end of Chapter 1). While an intensive survey is described in Chapter 3 (Section 3.2) in relation to that purpose, in the present section, we review a wide range of previous research on solar power prediction.

First, from the perspective of the prediction method of solar power (photovoltaic; PV), models can be roughly divided into three categories. The first category is PV performance models, which make predictions from solar radiation prediction based on the physical performance of PV. The second category is statistical models, which make predictions based solely on past data. The third category is hybrid models, which incorporate aspects of both models. The percentages of literature related to each of these are 11%, 72%, and 17%, respectively (Antonanzas 2016). Statistical models take a data-driven approach, which enables the extraction of relations on past data to predict the future behavior of a plant. These can be further classified as either regressive methods or artificial

intelligence techniques. Regressive methods include auto-regressive (AR) models (Bacher et al. 2009) and moving average (MA) models (Li et al. 2014), as well as ARX models (Bacher et al., 2009) and ARMAX models (Li et al. 2014), which incorporate exogenous variables. There are some adaptations, such as the vector AR or the vector ARX (Bessa et al. 2015), that can be used to deal with probabilistic analyses. As for artificial intelligence techniques, artificial neural networks are the most commonly used in solar power prediction (Antonanzas 2016). Regarding machine learning, various methods have been proposed, including k-nearest neighbors (Pedro and Coimbra, 2012), which is considered the simplest machine learning method, and support vector regression machines, which have a strong generalization capacity and applicability for non-linear problems (Rana 2015). Other than this, various optimization approaches are proposed, such as the genetic algorithm (Pedro and Coimbra 2012), firefly optimization (Haque et al. 2013), stepwise regression (Ramsami and Oree 2015), fuzzy logic (Simonov et al. 2012), and principal component analysis (Fonseca et al. 2014).

As described above, regarding the prediction method of solar power generation, there are various studies on advanced algorithms using the machine learning approach. Such methods have a high affinity with solar power prediction due to the complex interaction of multiple weather conditions and time-series fluctuations. However, relatively few studies have pursued simplicity and interpretability as our study does. Regarding past research—particularly works related to our approach—a more detailed survey will be conducted in Section 3.2.

2.2.2 Demand Prediction

Next, we describe previous research dealing with demand prediction. Although this thesis does not include research purely aimed at demand predictions (note that a simple demand prediction method for imbalance forecast is proposed in the Appendix of 0), we will perform a rough survey in this section. Since demand forecast errors have significant implications for profits (Bunn 2000), demand forecast is a very basic concept in power risk management for electricity trading. A survey of power demand forecasting is summarized by Suganthi and Samuel (2012), who classified past studies into the following 12 models: i. time series models, ii. regression models, iii. econometric models, iv. decomposition models, v. cointegration models, vi. ARIMA models, vii. artificial systems, viii. grey prediction models, ix. input-output models, x. fuzzy logic/genetic algorithm

models, xi. integrated models, and xii. bottom-up models. Many of these are also widely applied for solar power predictions as shown in the previous section, but the major difference between power demand and solar power is that power demand reflects social and economic activities.

Here, from the list above, iii. iv. and xii. are especially characteristic of power demand predictions. First, econometric models use the correlations between energy demand and other macro-economic variables, such as GNP, energy price, and population. Second, decomposition models consider the relationship between energy consumption and economic growth by decomposing industrial energy consumption into structural changes in production and changes in sectoral energy intensities (Ang 1995). Third, typical bottom-up models include market allocation models (MARKAL), which were originally developed as a least-cost linear programming model by the International Energy Agency (the equations are initially given by Fishbone and Abilock (1981)). This method is said to be particularly effective for predicting changes in demand due to policy changes. Since all the above methods deal with long-term demand forecasting, they fall outside the scope of this study but were taken as characteristic examples that show a strong correlation with economic activity.

Regarding short-term demand predictions, many previous studies are classified into the regression models, and typical ones include those carried out by Moghram (1989), Papalexopoulos and Hesterberg (1990), Haida and Muto (1994), and Charytoniuk (1998). Of these, Charytoniuk's (1998) work is a pioneering study that applied the non-parametric regression approach to demand forecasting. As for a related recent study, Yamada et al. (2018) propose a method that can effectively predict regional demand with a small sample size by estimating the spline function using the temperature prediction error as a cross variable.

2.2.3 Electricity Price Prediction

This section reviews previous studies on electricity price predictions. Although this thesis does not directly focus on electricity price prediction, Chapter 5 deals with hedging models against fluctuation risks, including price factors. These hedging models correspond to pricing methods based on trend forecasts, which are virtually equivalent to predictive models. In any case, electricity price forecasting plays a major role in energy companies' decision-making mechanisms (Bunn 2004, Weron 2007). Weron (2014) provided an organized survey study on power price prediction

methods and divided them into the following five categories:

- Multi-agent: *Nash-Cournot framework; supply function equilibrium; strategic production-cost; agent-based*
- Fundamental: *parameter rich fundamental; parsimonious structural*
- Reduced-form: *jump-diffusions; Markov regime-switching*
- Statistical: *similar-day, exponential smoothing; regression models; AR, ARX-type; threshold AR; GARCH-type*
- Computational intelligence (CI): *feed-forward neural networks; recurrent neural networks; fussy neural networks; support vector machines*

Multi-agent models have the advantage of high flexibility for the analysis of strategic behavior in electricity markets since it can incorporate many components, such as the players, their potential strategies, the ways in which they interact, and the set of payoffs. On the other hand, it also has a weakness in that it requires the assumptions embedded in the simulation to be justified, both theoretically and empirically (Weron 2014). This type of model is beyond the scope of the present work because of its suitableness for relatively long-term predictions.

The fundamental model is designed to capture the basic physical and economic relationships that are present in the production and trading of electricity. The analysis range of this model is wide, as the functional associations between fundamental drivers (loads, weather conditions, system parameters, etc.) are postulated, and the fundamental inputs are modeled and predicted independently. On the other hand, it faces challenges related to data availability (i.e., the data required to estimate the supply-demand curve is diversified, including the specification of individual power units), the sensitivity to violations of these assumptions , and the existence of significant modeling risks (Weron 2014). Note that the fundamental model is suitable for medium-term predictions rather than short-term predictions.

Reduced-form models are finance-inspired models that do not to provide accurate hourly price forecasts, but rather replicate the main characteristics of daily electricity prices. Since these models can generate future price distributions by simulating price dynamics, they are commonly used for derivative pricing and risk analysis (Benth et al. 2008, Eydeland and Wolyniec 2003). Interestingly, reduced-form models have been verified to perform reasonably well for forecasting volatility or

price spikes. However, some studies have reported that methods such as the Markov regime-switching model have poor performance for short-term predictions (Liebl 2013).

Statistical methods predict the current price by using a mathematical combination of historical prices and values of exogenous factors. These models have the advantages that some physical interpretation may be attached to their components, and their behavior is comparatively easy to understand. However, modeling non-linearities, especially price spikes, is considered difficult, and various research works have been conducted on their handling, including filtering, to build robust statistical models (Janczura et al. 2013). In terms of modeling such non-linearity, Yamada et al. (2015) propose a prediction method based on an approach that estimates a smooth yearly cyclical trend as a smoothing spline function using GAM. Also, they propose a method to derive a buy/sell bid rate curve by applying GAM to the buy/sell contract rate with respect to the price. In addition, Yamada et al. (2016) proposed a new method for estimating supply and demand functions expressed as parametric variables for the problem of estimating supply and demand functions in the power market and demonstrated the effect of improving errors when compared to the linear model.

The last model, computational intelligence, has strengths in its ability to handle complexity and non-linearity. However, like the Markov regime-switching model, some works report that spiky behaviors may not necessarily result in better point forecasts despite the ability to model highly volatile and non-linear price processes. Another challenge is that CI tools are so diverse that it is hard to find an optimal solution and to compare it with different CI methods thoroughly. Because of its flexibility and complexity, it can be difficult to evaluate.

2.3 Hedging Methods in the Electricity Market

In this section, we conduct a survey on the second approach of risk management: the hedging method. There are various electricity derivative markets in leading European and American power markets, where hedging with such derivatives is the basic procedure for electricity risk management. On the other hand, in Japan, although a forward market is listed as a means of fixing price fluctuation risks, the liquidity of it has been extremely low. However, new electricity futures market has just been listed as a trial in 2019, and it is expected that such electricity derivatives markets will be further activated in the future. Additionally, since electricity prices are strongly

linked to various external factors, such as fuel prices and weather conditions, it may be effective for them to be cross hedged with fuel derivatives and weather derivatives. In this section, we survey previous studies on electricity derivatives and then analyze weather and fuel derivatives.

2.3.1 Electricity Derivatives

In electricity market trading, the day-ahead market for trading the next day's electricity is the main exchange in many countries and is usually called the spot market. The spot market price fluctuates greatly because the outlook of supply and demand have significant uncertainties due to weather forecasts and accidental shutdowns of power plants. To hedge such price fluctuations, there are various power derivative transactions, as shown below (some studies such as Liu et al. (2006) and Deng and Oren (2006) sort out these concepts).

- Forward contracts
- Futures
- Options (call option / put option)
- Swaps (contracts for differences (CfDs))
- Special electricity contracts

The similar concepts of forwards and futures have the following differences. A forward is a contract that obligates the holder to buy/sell an asset for a predetermined delivery price at a predetermined future time, while a futures contract obligates each party to buy/sell a specific amount of a commodity at a specified price. Most futures contracts are used as financial vehicles with no intention of accepting delivery of the commodity (Liu et al. 2006). In a prior study, Blackmon (1985) first reported the development of a futures market in electrical energy. Later, Tanlapco et al. (2002) discussed the basic concepts of risk hedging using the futures contracts of an electricity market. In terms of the Japanese market, Yamada (2017) developed a forward price model using the concept of price prediction. In relation to renewable energy, which is of particular concern in this thesis, Peura and Bunn (2018) showed an interesting market mechanism such that increased wind power leads to higher forward prices. Specifically, by using a Cournot framework, they demonstrated that the intermittent availability of renewable (wind) power results in less aggressive behavior in forward trading, thereby increasing the equilibrium solution of prices.

Next, with regard to options, a wide range of products have been listed in the electricity market

based on the theories established in the financial market (Hull 2000). There are a wide range of underlying assets that handle not only prices (as is the case with plain vanilla electricity call and put options) but also other attributes like volume, delivery location and timing, quality, etc. (Deng and Oren 2006). Extended case studies and pricing methods in the electricity market are summarized in Eydeland and Wolyniec (2003) and Burger et al. (2008).

A swaps contract is an agreement between two parties to exchange a series of cash flows generated by underlying assets. For example, in the Nordic region, swaps are used to hedge the differential price between area price and system price (Kristiansen 2004). Meanwhile, in the UK, they are used for the difference between the spot price and a pre-defined reference price. While swaps allow flexible trading, they face challenges in that counterparties are exposed to higher credit risk.

Special electricity contracts are highly flexible derivatives contracts. For instance, Kaye et al. (1990) proposed an updated forward contract for which the contract prices set by the suppliers and can be regularly updated by consumers before the delivery date. Gedra (1994) proposed optional forward contracts, which include the callable/puttable forward contracts consisting of long forward contracts and short call/put options. Thus, there are various studies on electricity derivatives that are not only related to the utilization and pricing of existing products but also for combining them and proposing completely new contracts.

2.3.2 Weather Derivatives and Other Derivatives

As mentioned above, there are many derivatives in terms of electricity price and load, but they are not necessarily highly liquid, or they may have insufficient hedging effects on positions owned by individual companies. In such cases, the use of other derivatives, including weather derivatives and fuel price derivatives, may be considered.

Weather derivatives are financial instruments that use weather observations such as temperature and solar radiation as underlying assets. The application range of weather derivatives is wide, and they are used in various business fields, such as agriculture, travel and tourism, entertainment, and construction, where business risk depends on the weather (Turvey 2001). Interestingly, it has also been reported that weather derivatives can be linked to equity markets, where weather is observed to become a cognitive factor affecting trading activity (Cao and Wei 2005). Other researches

dealing with pricing include Davis (2001), Platen and West (2004), Kanamura and Ohashi (2009), and Brockett et al. (2006). In particular, hedging methods for solar power generation include Bhattacharya et al. (2015 and 2019), and Kanamura (2019). As for researches on other new-type pricing methods, Lee and Oren (2009) used equilibrium pricing models in a multi-commodity setting. Yamada (2008a) proposed weather derivatives based on prediction errors to mitigate risk in the wind power market, where the non-parametric method using GAM was applied for pricing derivatives payoffs. Yamada et al. (2006) produced pioneering research that introduced non-parametric techniques in this field that proposes a pricing method using trend prediction for futures and option contracts based on the monthly average temperature. As a related recent study, Yamada (2019) developed a hedging method for retail utilities' procurement costs (defined by the product of price and demand) with temperature derivatives. These papers' concepts are the basis of Chapter 4 in this thesis, which proposes similar but different hedging strategies related to the profit fluctuation of solar power generation companies in Japan and the procurement cost of retail utilities in the PJM market.

Like other derivatives, fuel-price-related derivatives (forwards) are sometimes utilized to cross-hedge for electricity prices, especially when the electricity derivatives/forwards markets at the generator's location are not liquidly traded (Deng and Oren 2006). Some empirical studies (e.g., Emery and Liu 2002, Woo et al. 2011) demonstrated high hedging effects of fuel futures, including the Henry Hub, which is a major natural gas index in the US.

2.4 Trading Strategies for Different Electricity Markets

According to Liu et al. (2006), measures that control risks are roughly classified as either hedging or portfolio optimization measures. The use of electricity or weather derivatives (dealt with in the previous section) corresponds to hedging, while the use of inter-market transactions (treated in this section) corresponds to portfolio optimization. In the electricity market, as well as in the day-ahead market, there is another market called the intraday market, in which electricity can be traded until just before delivery (one hour ahead in the case of JEPX). Furthermore, in the event of a supply-demand mismatch (imbalance), the imbalance volume is settled by the imbalance price published ex post facto (it is also called the real-time price or the balancing market price, among other names, depending on the country). In this section, we conduct a survey of research on these intraday and

balancing markets. Studies specific to these markets are very limited, and to the best of our knowledge, no such survey exists. However, considering that new research is increasing in the context of the relationship between the expansion of renewable energies and imbalance or intraday prices, this section provides an overview of such research trends.

2.4.1 Research on the Balancing Market (Imbalance System)

0 of this thesis deals with arbitrage transactions based on predictions of imbalance prices. Here, we first review the research that deals with the balancing market. Several studies have dealt with arbitrage and bidding strategies in the balancing market (see Section 6.2 for a more detailed description in the context of the work in 0). Krishnamurthy et al. (2018) proposed an arbitrage bidding strategy using energy storage in the day-ahead and real-time market. Boogert and Dupont (2005) analyzed statistical arbitrage between day-ahead and balancing markets. Weber and Just (2012) investigated the potential of statistical arbitrage for market participants in the German electricity balancing mechanism. Browell (2018) presented revenue-maximizing and risk-constrained strategies using logistic regression forecast. Klæboe et al. (2013) developed several forecasting models for balancing market prices. Bunn et al. (2018) predicted imbalance volumes using a stochastic latent moment model and found that the density forecast substantially increased trading profitability and reduced risk. Many of these papers show that the imbalance price is strongly related to the prediction error of renewable energies (especially wind power in many European countries). In this context, Goodarzi et al. (2019) found that renewable energy prediction error led to an increase in the amount of imbalance and concluded that improving the accuracy of renewable energy prediction is effective for system stabilization.

Veen and Hakvoort (2016) discussed the balancing market from the viewpoint of institutional design. Their work proposes a framework for a systematic and structured balancing market design and emphasizes the importance of providing appropriate incentives for market participants. Regarding empirical research from the perspective of balancing market incentives (market mechanism), Bunn and Kermer (2018) examine the system stabilization effect in trader's arbitrage transactions using the market model of the Austrian zone of the German/Austrian electricity market. This paper is described in detail in Chapter 6, in which we analyze the market mechanism of the Japanese imbalance system by expanding their methodology.

2.4.2 Research on Intraday Market

Next, we introduce past research that has focused on the intraday market. The literature focusing on the intraday market is very limited. Still, there are some studies on the price analysis or forecasting method, including analyses of the German market (Kiesel and Paraschiv 2017, Kath and Ziel 2018), the Spanish market (Monteiro 2016), and the US California market (Woo et al. 2016). These researchers' prediction approach to intraday prices is to use the prediction errors of renewable energies and the observed day-ahead prices. On the other hand, Maciejowska et al. (2019) provide a prediction method for the intraday market price before day-ahead market transactions. The work has many implications in that it verifies strategic decisions on whether renewable energies, such as wind and solar power, should be sold in the intraday market or the day-ahead market.

2.5 Conclusion

In this chapter, we conducted extensive surveys of previous research and found that they are diverse in terms of (1) matching changes in the market environment and social needs and (2) tapping into the development of modeling technology. The latter (2) refers to high-load computation technologies, such as artificial intelligence or machine learning, which are supported by recent advances in calculation technology. However, these are not the research directions pursued in this thesis as described at the end of 0. Instead, this study emphasizes research categorized into the former (1) group, considering that we are currently facing major issues, such as dealing with risks that have emerged in response to the expansion of renewable energy. In addition, when targeting the Japanese market, where full retail liberalization has arisen recently, it may be necessary to consider the insufficiency of market liquidity, system design, and the knowledge maturity of new entrants.

This study proposes various risk management methods to meet the needs arising from such transitions in social environments and research interests. Our research topics include a prediction method for solar power (0), a hedging method for prediction error loss (0), a hedging strategy for profit/cost fluctuation risk using a derivatives portfolio (Chapter 5), and a balancing system design to enhance market efficiency (0). Each of these topics is a part of a response to issues related to the recent rapid introduction of renewable energy. One of the main purposes of this research is to

provide valuable case studies and new suggestions that can be obtained by conducting empirical research, especially in the Japanese market, where the introduction of solar power is progressing rapidly. In addition, this research also aims to develop versatile and applicable modeling techniques by combining a variety of existing methods based on new perspectives.

Chapter 3

Prediction Method for Solar Power Business

3.1 Introduction

In recent years, due to the rapid introduction of solar power generation and the subsequent expanding impact on the power system, there is a growing need to predict solar power output and solar radiation. As the mass introduction of solar power generation progresses, although short-term output fluctuations caused by cloud passage are smoothed, daily output fluctuations caused by broad weather changes continue to increase significantly. For example, looking at the ratio of solar power output to national power demand from 12:00 to 13:00 for each day during April 2017, while the lowest day remained at 4% on April 11, the highest day reached 37% on April 23.[1] Under such circumstances, since electric utilities have business structures in which the output prediction error of solar power is directly linked to the risk of loss, improvements in the accuracy of predictions are an important issue.[2] In this study, we propose a practical method for predicting solar radiation and solar power output using only public information, considering the recent situation in which new entrants into the solar power generation business have increased.

Previous studies on the prediction of solar radiation and solar power output can be roughly classified into two types. The first uses widely publicized weather forecast values (Detyniecki et al. 2012, Hosoda and Namerikawa 2012, Kawasaki et al. 2015, Kim et al. 2017, Kudo et al. 2007, Nakamura and Mishima 2013, Orita et al. 1997, Sasaki et al. 2017, Shimura et al. 2011, Shimada and Kurokawa 2007, Shirakami and Kawahara 2016, Yamada et al. 2017), and the second is a

[1] Calculated using the data of OCCTO "System Information Service" (https://www.occto.or.jp/). Note that the ratio of solar power output to demand by area on April 23, 2017, reached 66% in the Shikoku area and 75% in the Kyushu area.

[2] The reason that the output prediction error is linked to the risk of loss will be described later in Section 3.2.2.

detailed prediction of solar radiation in a spatiotemporal manner using a three-dimensional numerical weather model. As a second example, some studies use a numerical forecast for each mesh, which is called a grid point value (GPV) (Fonseca 2014, Kataoka 2009, Lorenz 2007, Mellit and Pavan 2010, Shimada et al. 2013, Yamagishi et al. 2012, Yona et al. 2008), and some use direct predictions of solar radiation from numerical weather simulations based on the laws of physics (Jimenez et al. 2016, Lorenz 2009, Mathiesen et al. 2013, Tamura and Hiraguchi 2014). However, these prediction methods have practical problems, such as the charges for using data and the enormous computational complexity. Therefore, this work proposes a prediction method based on publicly available weather forecasts, which can be classified into the first category. However, methods such as neural networks, genetic algorithms, and time-series models (which have been proposed in previous research of the same type) face problems such as the need for imprinting complicated algorithms and troublesome procedures for classifying conditions. Therefore, in this study, we propose a convenient prediction method that can be constructed relatively easily based on generalized additive models (GAMs) (Hastie and Tibshirani 1990), where we use yearly cyclical dummy variables and actual weather condition values as explanatory variables and consider approaches to extract seasonal trends of solar radiation and solar power output by weather scenarios such as sunny, rainy, and cloudy. In addition, directly substituting predicted values into explanatory variables of the regression formula (constructed from the measured values) leads to bias in predicted values, but no studies have noted this. Therefore, in this study, we propose a new prediction model that separately estimates the probabilities of each weather scenario based on the weather forecast using a multinomial logit model (MNL) (McFadden 1974) and combining them with the original GAM.

The structure of this chapter is as follows. Section 3.2 reviews previous research on solar radiation and solar power output predictions and clarifies the necessity of power output forecasts for electric utilities. Section 3.3 details the proposed methods for predicting solar radiation and solar power output. Also, we verify the superiority of the proposed method in reducing prediction error by comparing it to prediction methods in previous research and the method directly substituting the forecast scenario into the regression formula constructed by measured data. Lastly, Section 3.4 provides a summary of this chapter.

3.2 Issues in Previous Researches and the Need for Power Output Prediction

3.2.1 Issues in Previous Research

Various methods have been proposed for predicting solar radiation and solar power output. Particularly, in recent years, many researches have been conducted in various countries around the world with the large-scale introduction of solar power generation, and there are also some well-organized survey studies such as Antonanzas et al. (2016), Pelland et al. (2013), and Kato (2017). Of these studies, those that propose a predicting method based on weather forecasts are shown in Table 3.1. There is a wide range of methods, from simple methods that use linear regression models or average values for each category to pattern recognition methods (e.g., neural networks), approximate solution search approaches that use genetic algorithms, and time series predictions (e.g., switching Kalman filters).

Table 3.1: Overview of previous studies of solar prediction methods using weather forecast data

Author	Prediction target and technique		Description variable
Orita et al. (1997)	Solar radiation	Multi-stage neural network	Weather conditions, average pressure, pressure difference, fine weather index, and temperature
Kudo et al. (2007)	Solar radiation and power output	Linear regression model	Weather (divided the amount of solar radiation, etc. by “extra-atmospheric solar radiation”)
Shimada and Kurokawa (2007)	Solar radiation	Average value by category (considering weather change patterns)	Weather (three categories)
Sharma et al. (2011)	Power output	Support vector machine	Temperature, dew point temperature, wind speed, etc.
Hosoda et al. (2012)	Power output	Switching Kalman filter	Weather (three categories) (*using data of last 90 days)
Detyniecki et al. (2012)	Power output	Fuzzy decision tree	Weather (48 categories)
Yamada et al. (2014)	Solar radiation and power output	Gray theory and neural network	Solar radiation and temperature (*using data from last 12 days)
Nakamura and Mishima (2013)	Power output	Average by category (considering weights within the date width)	Weather (four categories) and degree of cloudiness (categorized using 45 days of date width)
Kawasaki et al. (2015)	Solar radiation	Genetic algorithm	Weather, temperature, precipitation, and wind
Shirakami and Kawahara (2016)	Solar radiation	Pattern matching	Weather (three categories), precipitation, temperature, before and after weather, etc.
Kim et al. (2017)	Power output	Self-adaptive time series model	Weather, solar radiation, and temperature
Sasaki et al. (2017)	Power output	Average by category (considering weather change string)	Weather (five categories)
Qing and Niu (2018)	Solar radiation	LSTM network	Weather, temperature, dew point temperature, humidity, wind speed, etc.

The purpose of this study is to propose a highly convenient and practical prediction method that can be easily handled by new entrants into the solar power generation sector, the number of which has increased rapidly in recent years. Therefore, in this section, we review the previous studies shown in Table 3.1, focusing on methods that can allow for relatively easy modeling using only general weather forecasts (i.e., excluding those that require procedures such as complicated algorithms and complex conditions using multiple explanatory variables, such as Detyniecki et al. (2012), Kawasaki et al. (2015), Kim et al. (2017), Orita et al. (1997), Qing and Niu (2018), Shirakami and Kawahara (2016), and Sharma et al. (2011)). These previous techniques, when attention is focused on handling seasonal trends, can be roughly divided into three approaches. The first approach (1) involves extrapolating the trend of the last several tens of days (Hosoda et al. 2012, Yamada et al. 2014). The second (2) involves applying data to the pattern observed over a certain period of time, which is estimated by the measured values (Nakamura and Mishima 2013, Shimada and Kurokawa 2007, Sasaki et al. 2017). The third (3) involves performing linear regressions on the solar radiation (solar power output) index, which is obtained by dividing the original time series by the extra-atmospheric solar radiation (Kudo et al. 2007). However, each of these methods faces problems. First, (1) has problems with reliability due to the small sample size for the estimation period and with possible errors due to changes in the seasonal trends of solar radiation and solar power output. Regarding (2), the methods require time intervals to be set at fixed lengths in order to secure the sample size, but the changeable trend within the period is flattened according to the length, meaning that the error becomes large at the time division boundary. As for (3), although seasonal dependent errors can be reduced by using the solar radiation index normalized by the deterministic seasonal trend, there are other issues that are not easily resolved. For example, the difference in the seasonal trend for each type of weather cannot be reflected[3] (i.e., the seasonal effect of weather phenomena on the solar radiation index cannot be considered).[4] Therefore, in this study, focusing on the fact that solar radiation and solar power

[3] Differences in seasonal trends by weather are described later in Section 3.3.1.

[4] In addition to this, it is necessary to consider the seasonal and time-dependent trend correction due to the atmospheric transmittance separately when performing indexing more precisely. Moreover, in the case of solar power output, there is another correction to convert the solar radiation on the horizontal plane into the solar radiation on the inclined surface of the panel.

output have smooth seasonal trends throughout the year when divided by clock time and weather, we solve the problems mentioned above by applying a GAM with yearly cyclical dummy variables and measured weather conditions as an explanatory variable.

Furthermore, noting that the method of substituting the predicted values directly into the explanatory variables of the regression formula constructed from the measured weather conditions may create a bias in the forecast values, we separately estimate the probabilities of each scenario based on the weather forecast (using a multinomial logit model), and we propose a new prediction model that combines them. Note that the use of the logit model in a similar framework is thought to be novel because it has not been found in previous studies.

In addition, when predicting the solar power output, some methods have been proposed in which the predicted solar radiation is used to predict the solar power output (Yamada et al. 2014). However, care should be taken when the solar radiation used is not the solar radiation measured on the inclined surface of the solar panel but is the global radiation.[5] In other words, the solar power output is almost proportional to the solar radiation on the inclined surface of the panel (Kurokawa and Wakamatsu 1994), but the solar radiation on the inclined surface (which is proportional to the power output) varies depending on the altitude and azimuth of the sun (i.e., clock time and season), even if the global radiation is the same. For this reason, the prediction of solar power output based on the prediction of global solar radiation might include error caused by the difference in the incident angle at each point in time. Therefore, in the present study, predictions of solar power output are directly modeled using the weather conditions and the yearly cyclical trend described above without going through the prediction of global solar radiation. Since the prediction methods for solar radiation and solar power output proposed in this study are of the same type, matters common to both will be discussed with the representative of solar radiation in the following sections.[6]

In summary, our method has the following advantages over those described in previous related studies.

---

[5] The global solar radiation is the sum of the "direct" solar radiation and the scattered solar radiation by the atmosphere.

[6] Note that whereas the data on solar radiation can be sufficiently verified because the data is publicly released by the JMA, data for solar power generation is limited.

- Since the structure of the model is clearer and easier to interpret than previous methods that utilize complex algorithms (e.g., pattern recognition using machine learning), it is easy to handle in practical applications.
- Regarding the issue of securing an adequate sample size, by estimating the smoothing spline functions using a GAM (by imposing the smoothing condition on the trend that changes by date), we can extract seasonal trends efficiently while complementing the missing values and ensuring robustness.
- Because a GAM is applied to the original series of measured values, various seasonal trends (e.g., extra-atmospheric solar radiation, atmospheric transmittance, trend differences dependent on the incident angle to the solar panel) need not be considered separately.
- Instead of substituting the weather forecast value into the regression formula constructed from the measured values, the probabilities of the weather scenarios based on weather forecasts are estimated separately by MNL and new prediction methods that combine GAM and MNL are constructed, thereby prediction errors can be further reduced (see Section 3.3.4).
- It is comparatively easy and convenient since the only explanatory variables used are date/time and weather conditions. As such, the procedure required for data shaping is simple, and there is no need to implement complicated algorithms such as conditional branching or convergence calculations.

3.2.2 The Need for Electricity Generation Forecasts by Electric Utilities

In this section, we show that specific power generation companies or retailers that own or procure solar power generation have business structures in which their losses are incurred according to prediction errors of the solar power output. Therefore, we clarify the necessity of performing accurate predictions before the previous day. Figure 3.1 shows the flow of power producers' supply operations and retailers' power procurement at each time stage.

First, power generators that have alternative power sources, such as thermal power generators, need to predict the demand and solar power output before the previous day, determine the required number of thermal power generators to be started, and the start and stop times. Therefore, for example, if the prediction error is evaluated as being relatively large, the thermal power generator

will be operated more than necessary, resulting in additional power generation costs. Conversely, when the error is estimated to be small (i.e., if the amount of solar power generation is much lower than expected), it is not possible to supply enough power to meet consumers' demands (Yamada 2016). In other words, the prediction error of a power generation company that adjusts supply and demand with dispatchable power sources is directly linked to the risk of loss in that it causes uneconomical operation.

Retail electricity companies that do not have power sources have a similar profit structure. Retailers are obliged to formulate and submit the next day's supply and demand plan based on their predictions of the demand and power generation output on a daily basis, and they are then obliged to meet this demand. For retailers who have selected exceptional measures, the supply capacity that deviates from the supply and demand plan (imbalance amount) due to fluctuations in renewable energy at the delivery time will be settled by imbalance charges that are unforeseeable. Therefore, there is a high risk of price fluctuation as output prediction errors lead to loss risk for retailers.[7]

In this way, certain power generation and retail electricity companies that own or procure solar power have a structure in which losses are incurred according to the prediction error of the solar power output. The purpose of this chapter is to develop a practical and sufficiently accurate prediction method to avoid such risk of losses due to prediction errors.

[7] Under the current institution, it is also possible for retailers to select a special measure that does not incur the imbalance risk as described in the text. However, in this measure, the incentive to match the supply and demand balance does not function sufficiently, and there is an issue in increasing adjustment costs due to renewable energy forecast errors. At present, discussions on system design related to the review of the system are underway, including enforcing retailers to make certain adjustments as well as generators (METI 2018).

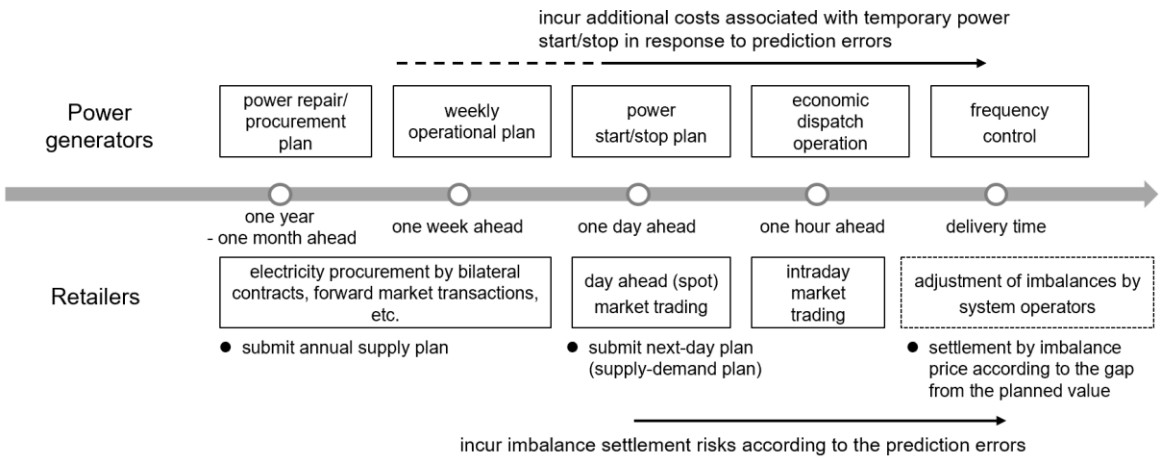

Figure 3.1: Flow of power operation/procurement by power generators/retailers

3.3 Solar Radiation and Solar Power Output Prediction Model

As stated at the beginning of this chapter, the method of directly substituting the weather forecast scenario as if the scenario were realized does not consider the possibility that the weather forecast is wrong. In this section, we first explain this fact using a concrete example. For the sake of simplicity, let us assume that the value of the solar radiation of the next day is 10 when the weather is sunny, 5 when it is cloudy, and 0 when it is rainy. At this time, if the next day's weather forecast is rainy, how is the predicted value of solar radiation estimated? If the event that the next day's weather would be rainy is deterministically realized, the predicted value of solar radiation would be 0. However, there is some chance that the prediction will be incorrect, and it could be sunny or cloudy. Here, let us assume that the probability that the forecast for the next day will be sunny despite the forecast for rain is 0.1, the probability that it will be cloudy is 0.3, and the probability that it will be rainy is 0.6. These values are the conditional probabilities of the next day's weather based on the previous day's forecast. The conditional expected value of the next day's solar radiation in this example is calculated by $10 \times 0.1 + 5 \times 0.3 + 0 \times 0.6 = 2.5$. Such a conditional expected value yields a minimum variance unbiased estimator for the next day's solar radiation prediction value based on the previous day's weather forecast and satisfies the optimal condition in the sense of minimizing variance (Takeuchi 1979).

On the other hand, in order for the prediction method treating the previous day's forecast as if it were a deterministic scenario to be an unbiased estimator, the following condition is required:

The probability that each type of weather is predicted (e.g., the probability that the weather forecast will be sunny) is equal to the probabilities that each weather is actualized (e.g., the probability that the measured weather will be sunny). As will be shown later in the empirical analysis, the forecasts released by the JMA are inclined to give forecasts in a direction that is worse than the actual weather, assuming disasters, etc. This suggests that the method of directly substituting the forecast value when calculating the solar radiation prediction value may generate bias. This point will be verified by the numerical experiment in Section 3.3.4.3.

The relationship between the model and the data used in this work is as shown in Figure 3.2, and each model is constructed by the following procedure. First, we use the GAM to estimate the seasonal trends of solar radiation and solar power output by time and observed weather (Section 3.3.1). Next, using the multinomial logit model, we estimate the conditional probability distribution of the weather scenarios when the weather forecast is given (Section 3.3.2). By combining the estimation results of these models, the prediction formula of solar radiation and solar power output from the weather forecast can be obtained (Section 3.3.3). Note that the model construction in this section is performed using measured data during the in-sample period shown in Figure 3.2. For the prediction values of solar radiation and solar power and the output used in Section 3.3.4 (verification of prediction accuracy), the calculated values obtained from the model during the out-of-sample period written in the figure shall be used.[8]

[8] The measured values of the weather conditions used in this work are obtained from the website of the JMA (http://www.data.jma.go.jp/gmd/risk/obsdl/), and the forecast values are obtained from the website that records past published weekly weather forecasts by the JMA (http://weather-transition.gger.jp/). In addition, this work uses the measured value of the solar power output of the private rooftop power generation equipment (polycrystalline type) in Hiroshima City with the permission of the owner. Note that the power generation efficiency of polycrystalline power modules is lower than that of single crystal power modules, which are the mainstream of industrial equipment.

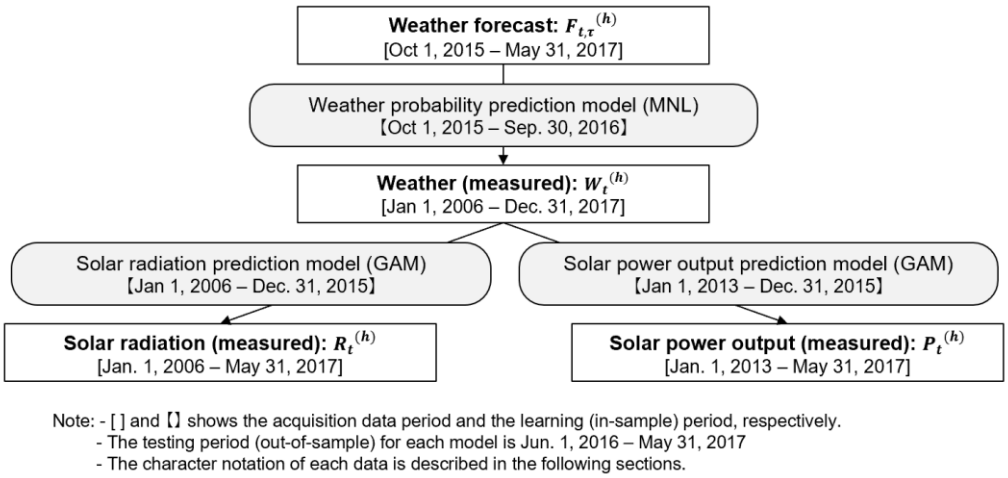

Figure 3.2: Relationship between usage data and models

3.3.1 Construction of a Prediction Model for Solar Radiation/Power Output Using GAMs

Solar radiation and solar power output are mainly affected by the solar altitude (incident angle), which is determined by the time of day and weather conditions. However, it should be considered that the effects of solar altitude and weather conditions on solar radiation are not additive relationships. For example, the effect of weather conditions on solar radiation varies with the sun's altitude, so it is assumed that it is not constant over time and across different seasons. Therefore, when we look at solar radiation and solar power output at the same clock time and under the same weather condition, it is considered that each time series has a yearly cyclical trend. Therefore, in this work, we adopt an approach to model solar radiation and power output based on time and weather conditions, and we estimate the cyclical trends by smoothing spline regression (see Section 3.5.1).[9] Specifically, we construct the following GAMs for solar radiation $R_t^{(h)}$ and power output $P_t^{(h)}$ at hour $h = 5, \dots, 19$ on date t (note that models are estimated separately by each hour)[10]:

[9] The data released by the JMA include sunshine hours and precipitation, but they are difficult to handle because the thickness of clouds is not considered and there are many time frames where the actual value is 0. Therefore, in this work, we used the actualized weather conditions as the explanatory variables for the GAM. It is also conceivable to use explanatory variables such as sunshine hours and precipitation together with weather conditions to improve explanatory power, but this work does not deal with these variables because it is intended to propose a simple prediction method using only the weather forecast that has been widely published.

[10] Hour h ranges only for the time zone when the solar radiation or power output are measured (5:00 to 19:00).

$$R_t{}^{(h)} = \sum_{j=1}^{4} f_j{}^{(h)}(Seasonal_t) I_{j,t}{}^{(h)} + \varepsilon_{r,t}{}^{(h)} \tag{3.1}$$

$$P_t{}^{(h)} = \sum_{j=1}^{4} g_j{}^{(h)}(Seasonal_t) I_{j,t}{}^{(h)} + \varepsilon_{p,t}{}^{(h)} \tag{3.2}$$

where $Seasonal_t$ is a yearly cyclical dummy variable $(= 1, \dots, 365 \text{ (or } 366))$; j is a variable representing the weather condition (sunny: 1, cloudy: 2, rainy: 3, snowy: 4); $f_j{}^{(h)}$ and $g_j{}^{(h)}$ are smoothing spline functions estimated by the GAM; $I_{j,t}{}^{(h)}$ is a dummy variable that is 1 when the measured weather condition $W_t{}^{(h)}$ at hour h on date t is j and is otherwise 0; and $\varepsilon_{r,t}{}^{(h)}$ and $\varepsilon_{p,t}{}^{(h)}$ represent the residual terms, whose means are 0. Note that the yearly cyclical dummy is sequentially allocated from 1 to 365 (366 if the allocation period includes February 29) from the starting point of the data. To cope with the problem that the spline function does not connect at the start and endpoints of the dummy variable, we adopt the yearly cyclical dummy variable's assignment method as proposed by Yamada et al. (2015) (see Section 3.5.1).

In this way, the estimated trends of solar radiation and solar power output for each measured weather condition are obtained. Figure 3.3 shows the results of estimating the amount of solar radiation for each actual weather condition (Hiroshima City, 12:00).[11] Among the curves in the figure, the solid line represents the estimation result of the yearly cyclical trend function f for the yearly cyclical dummy variable $Seasonal_t$ given by the horizontal axis. The dotted line represents the 95% confidence interval (also, the vertical axis of the figure shows the difference from the average value $\mu^{(12)}$ of the entire sample at 12:00). Note that we adopt the smoothing spline function f when the dummy variable is $1, 2, \dots, 365$ (366) (i.e., middle period) as the yearly cyclical trend used for prediction. In the extracted seasonal function, the trend of solar radiation is maximized at the end of June (around the summer solstice) during sunny and cloudy weather.[12]

[11] The statistical analysis in this chapter uses R3.3.3 (https://cran.r-project.org/), and the smoothing spline function is performed using the function "gam ()" included in the package "mgcv." The multinomial logit regression is performed using the function "glm ()" included in the package "VGAM."

[12] In rainy weather, the amount of solar radiation in summer is low compared to sunny and cloudy weather. This is perhaps because the cloud layer becomes thick due to cumulonimbus clouds in rainy weather in summer. In addition, in the case of snowy weather, there are missing values for most of the year, and the sample size observed in the limited winter period

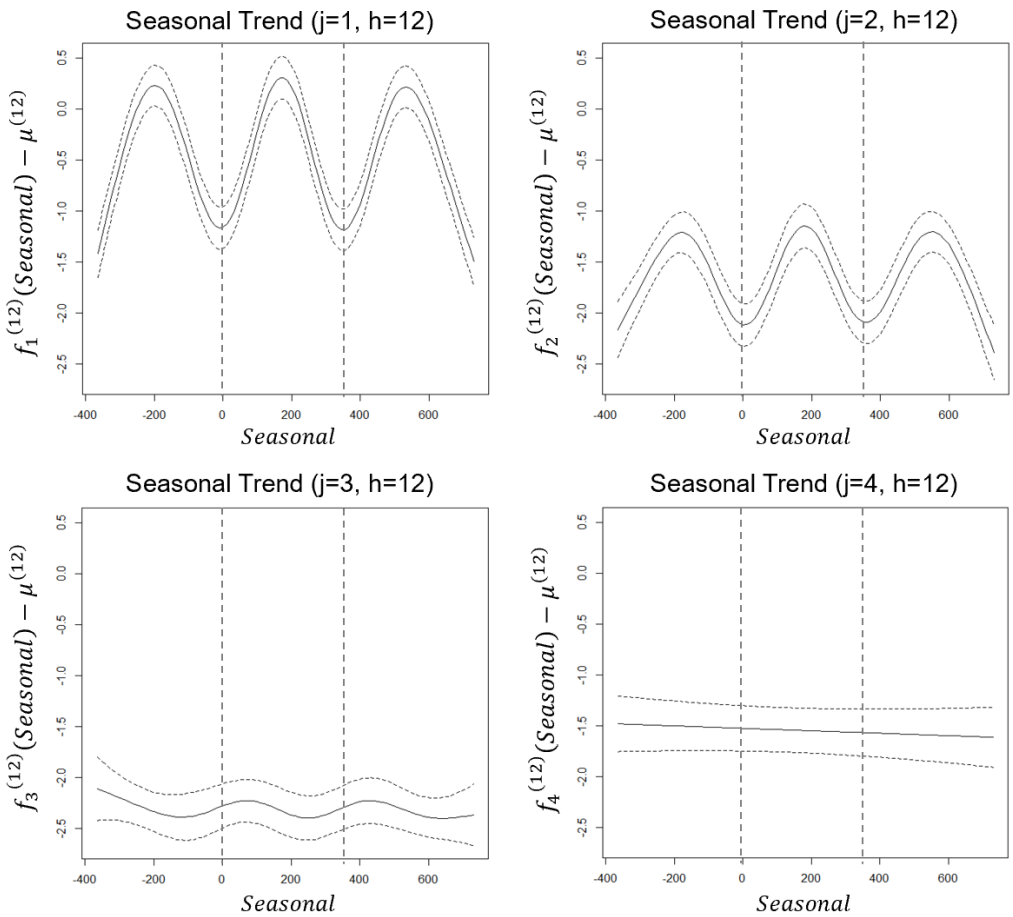

Figure 3.3: Estimation results of the cyclical trend by weather (Hiroshima City solar radiation, 12:00)

3.3.2 Construction of a Weather Probability Prediction Model Using a Multinomial Logit Model

The prediction model of weather probability consists of weather forecast data (explanatory variables) and measured weather (response variables). The measured weather conditions released by JMA have the category values specified in Table 3.2, and we reconstruct them into four categories (sunny, cloudy, rainy, and snowy) from the viewpoint of securing sample size. Since the measured value of the weather condition is published at intervals of three hours, the same weather is interpolated for one hour before and after. The weather forecast values published by JMA are given daily and are character string data such as “cloudy - rainy from noon” and “cloudy - afternoon

is extremely small. Therefore, it is confirmed that the estimated trend is almost a straight line (almost average value for all periods).

sometimes sunny." The terms related to time subdivisions are defined for each three-hour period as shown in Table 3.3. According to this, the weather forecast (daily string data) can be decomposed into hourly values.

Table 3.2: General weather condition announced by JMA and the reclassification

JMA	Item	1	2	3	4	5	6	7	8	9	10	11	12	13	14	15
	Weather Conditions	Clear	Sunny	Cloudy	Cloudy	Smoke	Dust storm	Blizzard	Fog	Fog rain	Rain	Sleet	Snow	Hail "Arare"	Hail "Hyo"	Ray
After conversion	Weather classification	Sunny			Cloudy				Rainy				Snowy			Rainy
	J	1			2				3				4			3

Table 3.3: Definition of time subdivision terms included in the weather forecast by JMA

Time	0	3	6	9	12	15	18	21
No.	1	2	3	4	5	6	7	8
Term	Early dawn	Dawn	Morning	Before noon	Afternoon	Evening	Beginning of the night	Late at night
	Morning				Afternoon			
				Daytime			Night	

All hourly forecast data are aggregated into information in the form of "A sometimes B occasionally C"; therefore, the forecast value of the weather condition $\boldsymbol{F}_{t,\tau}{}^{(h)}$ at hour h on day t announced τ days before can be expressed using dummy variable vectors corresponding to the three nominal variables $\{A, B, C\}$ as shown in the following equation:

$$\boldsymbol{F}_{t,\tau}{}^{(h)} = [A_1 \quad A_2 \quad A_3 \quad A_4 \quad B_0 \quad B_1 \quad B_2 \quad B_3 \quad B_4 \quad C_0 \quad C_3 \quad C_4]^T \tag{3.3}$$

where $A_j, B_j,$ and C_j correspond to "main weather," "sometimes weather," and "occasional weather," respectively, in the weather forecast. The dummy variable is 1 if the forecast value of the weather condition is $j \in \{0\text{: } not\ applicable, 1\text{: } sunny, 2\text{: } cloudy, 3\text{: } rainy, 4\text{: } snowy\}$ and 0 in other cases.[13] Here, for convenience, the "main weather" of the forecast (at hour h on day t announced at τ days before) $\tilde{F}_{t,\tau}{}^{(h)}$ is defined separately as category value, which returns values $j \in \{1, \dots, 4\}$ that satisfy $A_{j,t,\tau}{}^{(h)} = 1$.

In the following paragraphs, we construct a conditional probability prediction model for the

[13] "A" is classified in any of three categories $\{sunny, cloudy, rainy, snowy\}$, "$B$" is in five $\{not\ applicable, sunny, cloudy, rainy, and\ snowy\}$, and "$C$" is in three $\{not\ applicable, rainy, snowy\}$. Note that A_j, B_j, C_j in (3) are variables that depend on the date t, hour h, and predicted horizon τ, but these subscripts are omitted.

actualized weather using the multinomial logit model. The multinomial logit model is a statistical method for estimating a probability distribution when the objective variable is given as a categorical variable. It was originally developed based on the theory of utility maximization, where decision-makers make choices that maximize their utilities among multiple options. However, to date, applied research has been performed in various fields, not only for predicting choice behavior (see Section 3.5.3 for details). First, when deriving the model, we consider the following probability of weather conditions. Note that the prediction horizon τ is omitted here for simplicity.

$$Prob\left(W_t{}^{(h)} = j\right) = Prob\left(S_{jt}{}^{(h)} \geq S_{kt}{}^{(h)}, \forall k \neq j\right) \tag{3.4}$$

where $Prob\left(W_t{}^{(h)} = j\right)$ is the probability that the measured weather condition $W_t{}^{(h)}$ at hour h on date t will result in j, and $S_{jt}{}^{(h)}$ is a variable that determines the possibility that the realized weather at hour h on the date t will be j (herein, we call this the "weather possibility index").[14] In other words, the weather condition with the highest weather possibility index is determined as the measured weather condition. To estimate this probability, the weather possibility index is formulated as a linear function using the weather forecast vector $\boldsymbol{F}_t{}^{(h)}$ as follows:

$$S_{jt}{}^{(h)} = \boldsymbol{\theta}_j{}^T \boldsymbol{F}_t{}^{(h)} + \varepsilon_{jt}{}^{(h)} \tag{3.5}$$

where $\boldsymbol{\theta}_j$ is a vector of estimation parameters,[15] and $\varepsilon_{jt}{}^{(h)}$ is an unobservable element that affects the weather possibility index. Here, the term $\boldsymbol{\theta}_j{}^T \boldsymbol{F}_t{}^{(h)}$ is an observable decision term of the weather possibility index (a value determined by the weather forecast). From equations (3.4) and (3.5), the following equations can be derived:

$$Prob\left(W_t{}^{(h)} = j\right) = Prob\left(\boldsymbol{\theta}_j{}^T \boldsymbol{F}_t{}^{(h)} - \boldsymbol{\theta}_k{}^T \boldsymbol{F}_t{}^{(h)} \geq \varepsilon_{kt}{}^{(h)} - \varepsilon_{jt}{}^{(h)}, \forall k \neq j\right). \tag{3.6}$$

Here, assuming that each error term $\varepsilon_{jt}{}^{(h)}$ has independent and identical Gumbel distributions, the probability that the measured weather condition will be j is formulated using the following

[14] When used for predicting consumer choice behavior, S_{jn} is defined as the utility of individual consumers n choosing option j.

[15] It should be noted that $\boldsymbol{\theta}_j$ might be set as a parameter vector that varies based on t, but in this study, since the period during which the weather forecast data was obtained is less than two years, we use $\boldsymbol{\theta}_j$ as a value that does not depend on t, considering the viewpoint of securing the sample size and the degree of influence comprehensively.

closed equation (e.g., see McFadden 1974):

$$Prob\left(W_t^{(h)} = j\right) = \frac{exp\left(\boldsymbol{\theta}_j^T \boldsymbol{F}_t^{(h)}\right)}{\sum_{j=1}^{4} exp\left(\boldsymbol{\theta}_j^T \boldsymbol{F}_t^{(h)}\right)}. \tag{3.7}$$

By taking the natural logarithm of this equation and adding the samples, a log-likelihood function is obtained, and maximizing it for $\boldsymbol{\theta}_j$ yields the maximum likelihood estimate $\widehat{\boldsymbol{\theta}}_j$.

Figure 3.4 shows the prediction results of the probability distribution of the weather conditions that are obtained in this way. The estimated weather probability is dominated by the probability that it will be the same as the "main weather" of the weather forecast, but it is also affected to a certain extent by the weather forecast of "sometimes weather" and "occasional weather." In addition, even if the weather forecast is given only as the main weather, the probability that the actualized weather will be different is considerable (e.g., when the weather forecast is cloudy, the probability that the weather will not be cloudy is about 48%).

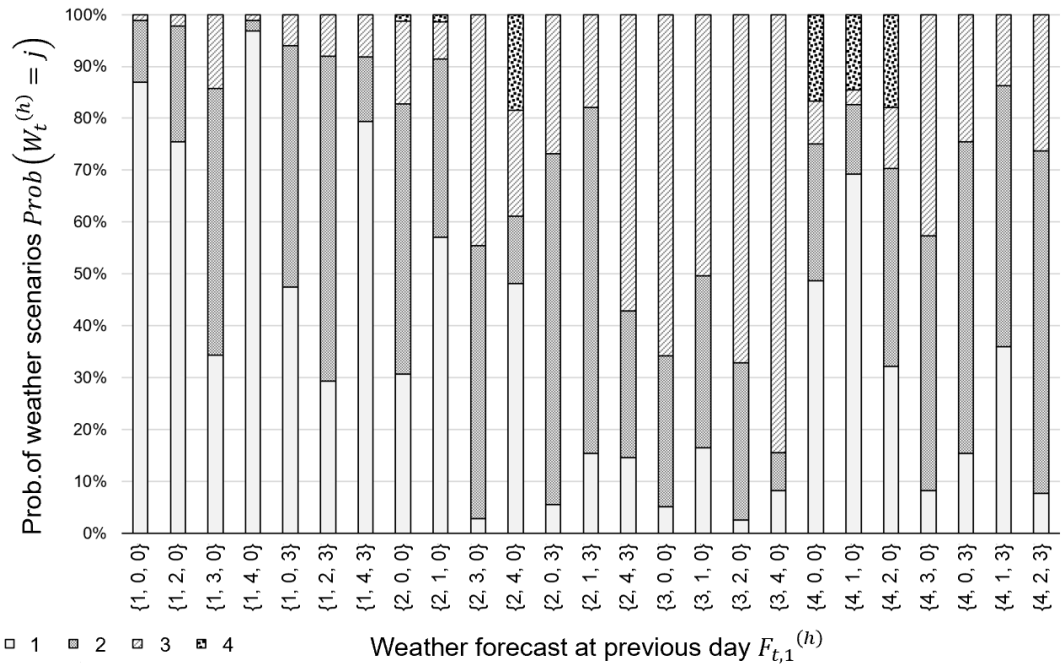

Note: The numbers of legend stand for the actualized weather conditions $j \in \{1: sunny, 2: cloudy, 3: rainy, 4: snowy\}$, and the numbers of horizontal axis in {} stand for the forecasted "main weather", "sometime weather" and "occasional weather", respectively.

Figure 3.4: Estimation results of weather probability distribution using MNL (Hiroshima City)

3.3.3 Solar Radiation and Power Output Prediction by Combining GAM and MNL

In this section, by combining the prediction model of solar radiation and power output (which was

formulated with the measured weather conditions as input values in Section 3.3.1) and the prediction model of the probability distribution of the weather scenarios (which was formulated with the weather forecast value as the input value in Section 3.3.2), we construct a formula to predict solar radiation and power output from only the weather forecast and time information. The predicted value $\widehat{R_{t,\tau}}^{(h)}$ for solar radiation $R_t{}^{(h)}$ at hour h on date t is written as follows (using the periodic trend of solar radiation $f_j{}^{(h)}(Seasonal_t)$ of each weather scenario estimated in GAM (3.1), (3.2) and the probability that the actual weather $W_t{}^{(m)}$ will become j, which is introduced in (3.7)):

$$\widehat{R_{t,\tau}}^{(h)} = \sum_{j=1}^{4} f_j{}^{(h)}(Seasonal_t) \frac{exp\left(\boldsymbol{\theta}_j{}^T \boldsymbol{F}_{t,\tau}{}^{(h)}\right)}{\sum_{j=1}^{4} exp\left(\boldsymbol{\theta}_j{}^T \boldsymbol{F}_{t,\tau}{}^{(h)}\right)} \tag{3.8}$$

$$\widehat{P_{t,\tau}}^{(h)} = \sum_{j'=1}^{4} g_{j'}{}^{(h)}(Seasonal_t) \frac{exp\left(\boldsymbol{\theta}_{j'}{}^T \boldsymbol{F}_{t,\tau}{}^{(h)}\right)}{\sum_{j'=1}^{4} exp\left(\boldsymbol{\theta}_{j'}{}^T \boldsymbol{F}_{t,\tau}{}^{(h)}\right)}. \tag{3.9}$$

To verify the effect of such stepwise prediction, a method of directly substituting the weather forecast value into the prediction formula of GAM is considered below. This is the method used to obtain a predicted value by substituting the "main" weather forecast $\widetilde{F_{t,\tau}}^{(h)}$ into the GAM (3.1), (3.2) estimated from the measured weather conditions. Through this method, the predicted solar radiation and power output $\widetilde{R_{t,\tau}}^{(h)}, \widetilde{P_{t,\tau}}^{(h)}$ are written as follows:

$$\widetilde{R_{t,\tau}}^{(h)}\left(\widetilde{F_{t,\tau}}^{(h)} = j\right) = f_j{}^{(h)}(Seasonal_t) \tag{3.10}$$

$$\widetilde{P_{t,\tau}}^{(h)}\left(\widetilde{F_{t,\tau}}^{(h)} = j\right) = g_j{}^{(h)}(Seasonal_t). \tag{3.11}$$

Hereafter, for convenience, we call the prediction obtained by the latter method (3.10), (3.11) the "forecast value substitution method" and the former prediction method (3.8), (3.9) the "probability weighted average method."

3.3.4 Validation of the Prediction Error of Each Model

In this section, we verify the prediction error of the proposed method by using measured value of solar radiation in nine cities in Japan during the out-of-sample period (from June 1, 2016, to May 31, 2017) and power outputs of the solar power system in Hiroshima City, and the forecast values

of solar radiation and solar power output calculated from weather forecasts with prediction formulas constructed in the previous section.

In the verification process, we compare the prediction errors by the two methods for different prediction horizons. Here, the "percent root mean square error: PRMSE" is calculated based on the following formula for two prediction values $\widehat{R_{t,\tau}}^{(h)}, \widetilde{R_{t,\tau}}^{(h)}$(the power output prediction is also verified in the same way)[16]:

$$PRMSE_{r,\tau} = \frac{\sqrt{\frac{1}{N}\sum_{t,h}\left(\widehat{R_{t,\tau}}^{(h)} - R_t^{(h)}\right)^2}}{\mathrm{Mean}\left(R_t^{(h)}\right)}, \widetilde{PRMSE}_{r,\tau} = \frac{\sqrt{\frac{1}{N}\sum_{t,h}\left(\widetilde{R_{t,\tau}}^{(h)} - R_t^{(h)}\right)^2}}{\mathrm{Mean}\left(R_t^{(h)}\right)} \tag{3.12}$$

$$PRMSE_{p,\tau} = \frac{\sqrt{\frac{1}{N}\sum_{t,h}\left(\widehat{P_{t,\tau}}^{(h)} - P_t^{(h)}\right)^2}}{\mathrm{Mean}\left(P_t^{(h)}\right)}, \widetilde{PRMSE}_{p,\tau} = \frac{\sqrt{\frac{1}{N}\sum_{t,h}\left(\widetilde{P_{t,\tau}}^{(h)} - P_t^{(h)}\right)^2}}{\mathrm{Mean}\left(P_t^{(h)}\right)}. \tag{3.13}$$

Note that, in the following subsection, we compare the error with other prediction methods from the previous works. However, since the prediction target point and time range are not the same, we cannot simply judge the quality of the prediction accuracy.

3.3.4.1 Verification of Error in Solar Radiation Forecasts

First, we verify the prediction error of solar radiation. In this regard, the values measured at multiple locations can be obtained from the database published by JMA, and the prediction errors are verified using data from nine locations in the cities of Sapporo, Sendai, Tokyo, Nagoya, Toyama, Osaka, Hiroshima, Takamatsu, and Fukuoka. The solid grey line in Figure 3.5 is the PRMSE of the "forecast value substitution method" $\widetilde{PRMSE}_{r,\tau}$, and the solid black line is that of the "probability weighted average method" $PRMSE_{r,\tau}$, both of which are calculated by different prediction horizon τ[17]. The dotted line is the error of the predicted value obtained by substituting the measured weather condition into the regression model. In this respect, this error can be translated into an estimation error of the model that does not depend on the error of the weather forecast. The calculation results

[16] In order to verify the effect of using the multinomial logit model from the viewpoint of minimizing the variance, the prediction error here is evaluated using the RMSE, which corresponds to the variance.

[17] The prediction horizon $\tau = 1$ indicates the forecast error as of the previous day's morning, and $\tau = 0$ indicates the forecast error as of the previous day's night.

show that the shorter the prediction horizon, the smaller the prediction error, and it approaches the dotted line (i.e., error derived from the model estimation). In addition, at each location or prediction horizon, the error of the "probability weighted average method" is smaller than that of the "forecast value substitution method."

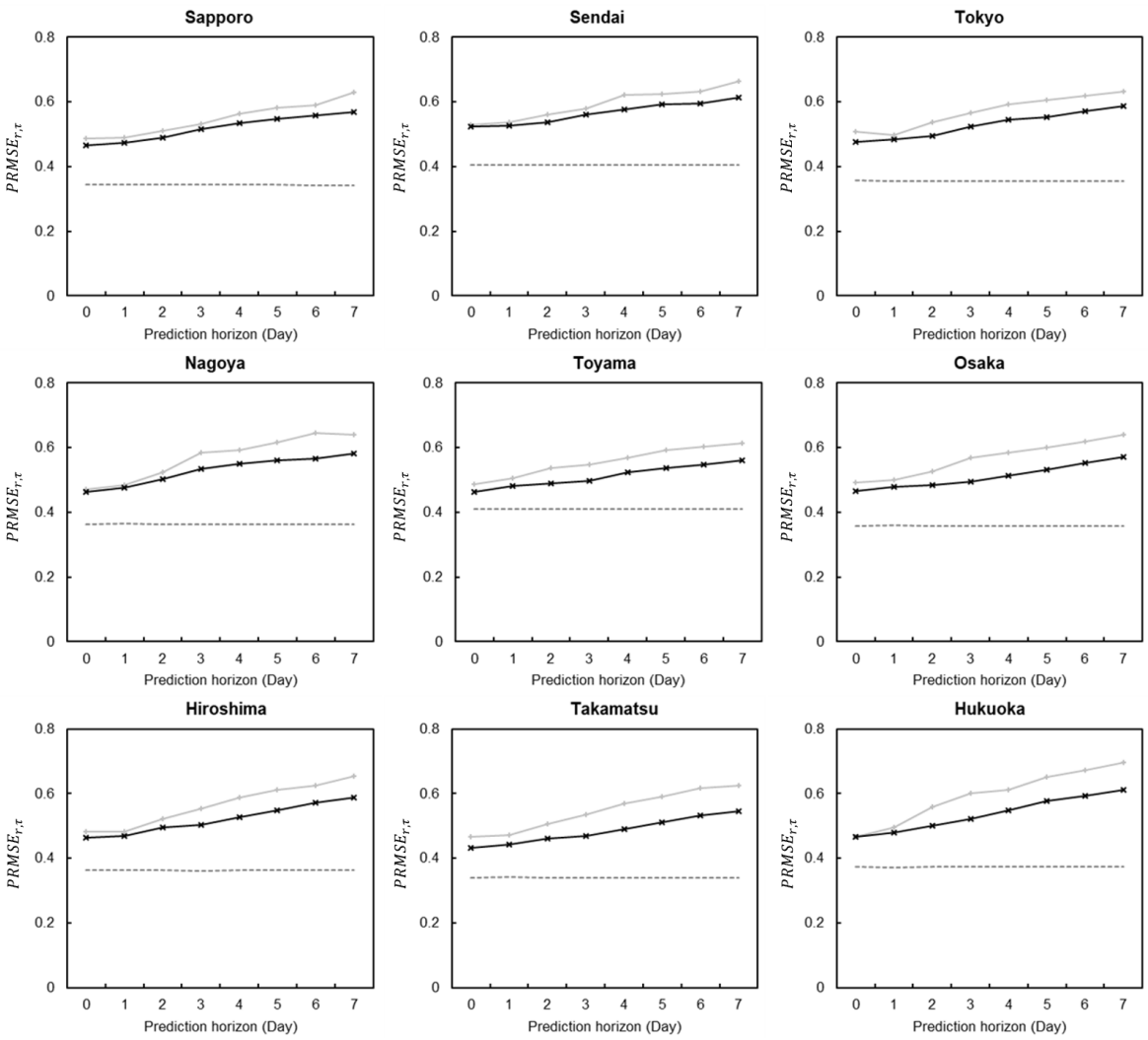

Note: Grey line: forecast value substitution method; black line: probability weighted average method; dotted line: substitution of the "measured" weather into the GAM

Figure 3.5: PRMSE of solar radiation prediction (nine locations)

In the following paragraphs, we analyze the cause of the prediction error. For example, looking at the PRMSE of the solar radiation prediction in Hiroshima City, the previous day's prediction

error of "probability weighted average method" is 43% (54% in the one week ago prediction), and that of the "forecast value substitution method" is 45% (61% in the one week ago prediction). On the other hand, since the error of 34% (when the measured value is substituted into the GAM) is due to the GAM's accuracy, the difference of 11% (45% of the "forecast value substitution method" minus 34%) is caused by the weather forecast error. Of the 11%, error derived from the weather forecast error, 2% (which is the difference between the "predicted value substitution method" and the "probability weighted average method") corresponds to the error that could be reduced by incorporating the probability when the weather forecast deviated. Similarly, in the one week ahead predictions, of the 20% error derived from the weather forecast, a relatively high portion (7%) could be reduced by the "probability weighted average method." Thus, it can be interpreted that the longer the prediction horizon, the greater the probability that the weather forecast will deviate. Therefore, in such cases, the superiority of the "probability weighted averaging method" incorporating probability distribution becomes particularly significant.

In addition, to make comparisons with the prediction accuracy of previous research, an evaluation was also performed using percent mean absolute error (PMAE).[18] The PMAE of the previous day's forecast of hourly solar radiation by the proposed forecast method is 31.4% in Hiroshima City (30.0% in Nagoya City). In previous studies, this value is 31.5% (in Fukui Prefecture) in the work of Kawasaki (2015), which proposes the prediction method from weather, temperature, precipitation, and wind power using a genetic algorithm, and 32.9% (in Fukui Prefecture) in the work of Yamagishi et al. (2012) using numerical weather forecasts. Compared to these, this work's prediction errors were equal or less, although there are differences in areas, etc.

3.3.4.2 Verification of Error in Solar Power Output Predictions

Similarly, the prediction errors for solar power output are verified using data from Hiroshima City. As in Figure 3.5 in the previous section, the solid grey line in Figure 3.6 is the PRMSE of the

[18] In a comparison with previous studies, since we could not find any studies using the PRMSE for error evaluation under the same prediction conditions as in this work, we use the PMAE. Note that the PMAE is calculated by the following equation: $\mathrm{PMAE} = (1/n)\sum_{i=1}^{n}|S_i - A_i|/\bar{A}$, where S_i is the predicted value of solar radiation at time i, A_i is the measured value of solar radiation at time i, and $\bar{A}$ is the average value of A_i.

"forecast value substitution method" $\widetilde{PRMSE}_{p,\tau}$, the solid black line represents the "probability weighted average method" $PRMSE_{p,\tau}$, and dotted line is the error of the predicted value obtained by substituting the measured weather condition into the GAM. The analysis reveals that the prediction error becomes smaller as the prediction horizon becomes shorter and approaches the prediction error with weather forecast error excluded (dotted). In addition, the prediction error of the "probability weighted averaging method" is smaller than that of the "forecast value substitution method" for each prediction horizon.

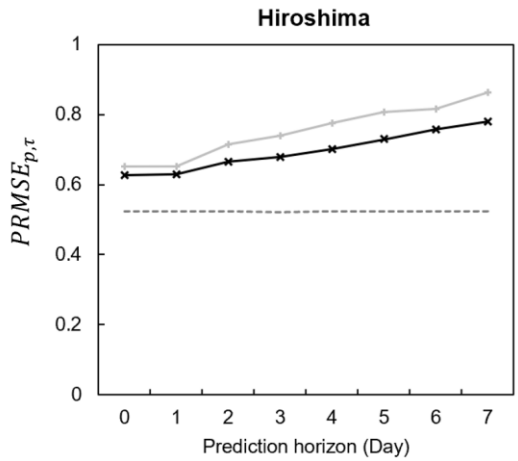

Note: Grey line: forecast value substitution method; black line: probability weighted average method; dotted line: substituting the "measured" weather into GAM

Figure 3.6: PRMSE of solar power output prediction (Hiroshima City)

The PMAE of the previous day's prediction of the daily accumulated power generation by the proposed prediction method was 25.8% (Hiroshima City). In previous studies, this value was 26-39% in the work of Kudo et al. (2007) proposing the prediction of the next day's accumulated power generation from the weather forecast (Aichi prefecture, from March to September), and "approximately 30% to 40%" in the work of Nakamura (2013) using the average values for each category created from information on weather and degree of cloudiness (from April to October in Hakodate City). Compared to these, this work's prediction errors were equal or less, although there are differences in areas, etc.[19]

[19] Since there are no papers found that used the PMAE of hourly power output, we made comparisons using daily accumulated power generation data.

3.3.4.3 Consideration of Difference in Error for Each Prediction Method

As shown in Subsections 3.3.4.1 and 3.3.4.2, the prediction error of the "probability weighted averaging method" was smaller than that of the "forecast value substitution method," both for the solar radiation and the solar power output prediction. There are several possible reasons for this outcome. In addition to the fact that the "probability weighted averaging method" makes it possible to consider detailed forecast information other than the "main weather" (i.e., "sometimes weather" and "occasional weather"), it also incorporates the probabilities when actual weather conditions may be different from forecast ones. In other words, the "forecast value substitution method" is not appropriate from the viewpoint of probability estimation because the method estimates the probability of misprediction to be 0. For example, if the next day's weather forecast is sunny, the "forecast value substitution method" calculates the expected value of the solar radiation under the condition that the probability that the weather will be sunny is 100%. However, it has an upward bias in that it does not consider the possibilities of cloudy or rainy weather. Similarly, when the weather forecast is rainy, the predicted value of solar radiation using this method has a downward bias.

The tendency of such a bias occurrence is considered using the actualized prediction error in the out-of-sample period. Here, we explain the previous day's prediction error of the solar radiation in Hiroshima City (used in Section 3.3.4.1), using the data from June, when rainy forecasts increased. The average value of the prediction error in June 2016 was -0.036 $[\mathrm{MJ/m^2}]$ for the "probability weighted average method," while it was -0.121 $[\mathrm{MJ/m^2}]$ for the "predicted value substitution method." Looking at the frequency of actual weather by main weather forecast during this period, as shown in Figure 3.7 (plotted of Hiroshima City, June 2016), the frequency of the time when the actual weather deteriorated when the forecast was sunny stayed at 10%. Meanwhile, the actual weather improved in the case of a rainy forecast reached 46% of the time. That is, in the "forecast value substitution method," the downward bias in the case of a rainy forecast had a stronger effect than the upward bias in the case of a sunny forecast. Therefore, the downward prediction error increased throughout the month.

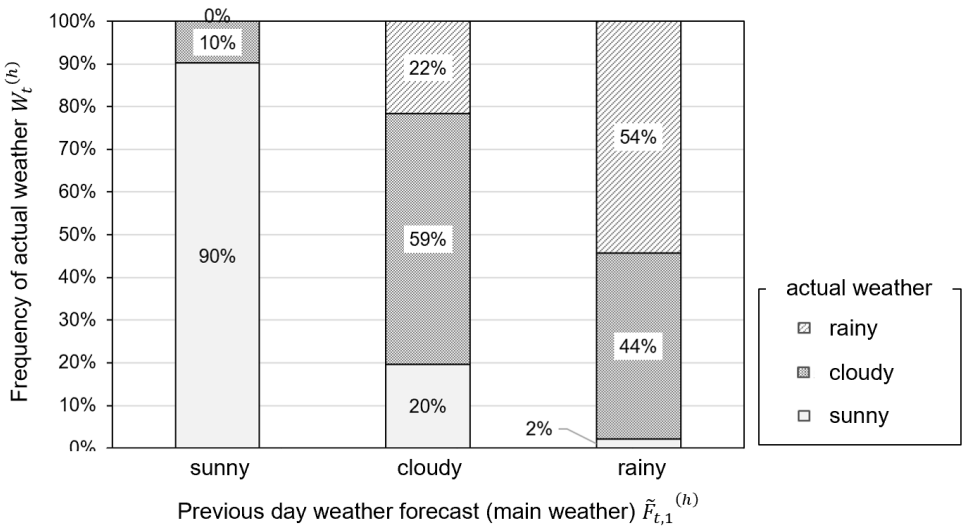

Figure 3.7: Frequency of actual weather occurrence by weather forecast

As mentioned at the beginning of Section 3.3, for the predicted value obtained by the "forecast value substitution method" to be an unbiased estimator, it is necessary that the probability of each forecasted weather scenario is equal to the probability of the actual weather. However, as shown above, if the JMA's forecast is biased in a direction that is worse than the actual weather, the prediction value of the "forecast value substitution method" will be biased. Thus, the "probability weighted average method," which incorporates the probability distribution of the explanatory variables, is superior to the "forecast value substitution method" in terms of reducing the prediction error. This finding is thought to provide useful, practical implications.

3.4 Conclusion

In this work, we proposed a new method for predicting solar radiation and solar power output using the weather forecast that is regularly announced by JMA, and we demonstrated its effectiveness. In addition, by comparing the previous prediction methods and the method with direct substitution of the prediction scenario, we verified the superiority of the "probability weighted average method" in reducing prediction errors.

The prediction approach in this study, focusing on smooth seasonal trends that come up when decomposing the time series by clock time and weather, made it possible to construct a model with simple and sufficient prediction accuracy without the need for complicated algorithms and pattern classification settings as is the case with previous methods. In addition, our method is relatively

easy to implement because it uses publicly available weather forecasts. It is also easy to handle for new entrants to the solar power business, which have increased in recent years.

This study makes additional contributions such that we particularly focused on the fact that the prediction method of directly substituting the forecast value into the regression formula estimated from the measured values may have bias. To address this issue, we separately performed the prediction of the probability distribution for the explanatory variable using a multinomial logit model and combined them to produce new prediction method with comparatively small prediction errors. Such results may provide useful suggestions in the actual practical situation.

3.5 Appendix

3.5.1 Smoothing Spline Regression Method

Smoothing spline regression is a non-parametric regression technique for estimating the shape of a regression function without specifying it based on a finite number of parameters. Now, consider the smoothing spline function h that minimizes the variance of ϵ_n when the objective variable y_n is expressed by the explanatory variables of system variation $h(x_n)$ and residual variation ϵ_n as in the following equation:

$$\begin{gathered} y_n = System\ variation\ +\ Residual\ variation = h(x_n) + \epsilon_n, \\ n = 1, \dots, N \\ \mathrm{Mean}[\epsilon_n] = 0, \mathrm{Var}[\epsilon_n] = \sigma^2. \end{gathered} \tag{3.14}$$

If h is estimated by using the ordinary least squares (OLS) method, a curve that directly complements all the data points will be obtained. Therefore, instead of the residual sum of squares, the following penalized residual sum of squares (PRSS) is considered:

$$\mathrm{PRSS} = \sum_{i=1}^{n} \{y_n - h(x_n)\}^2 + \lambda \int \{h''(x)\}^2\, dx. \tag{3.15}$$

Then, h, which minimizes PRSS and uses this as the estimation function, is found. This optimization naturally leads to a smoothing spline function. λ is called the smoothing parameter. The larger this value, the smoother the estimated spline function becomes (Hastie and Tibshirani 1990).

3.5.2 Assignment Method of Yearly Cyclical Dummy Variables

The yearly cyclical dummy (seasonal dummy) is a variable that is sequentially assigned from 1 to 365 (366 if the period includes February 29) in order from the starting point of the data. If GAM (3.1) and (3.2) are applied to estimate the smoothing spline function ${f_j}^{(h)}$ and ${g_j}^{(h)}$ on yearly cyclical dummy variables, the spline functions are not connected at the start and endpoints of the dummy variable. In addition, it is necessary to consider that the cycle is 366 days on a leap year, and strictly speaking, that one year is not the same cycle. In this work, to address these issues, we adopt the cyclical trend extraction method proposed by Yamada et al. (2015). GAM (3.1) and (3.2) are constructed so that the smoothing spline functions ${f_j}^{(h)}$ and ${g_j}^{(h)}$ are connected approximately at the start and end points of the dummy variables. The specific procedure is expressed below:

1. Let $\boldsymbol{Y}$ be the sample vector of the dependent variable, and let $\boldsymbol{S}^{(i)}$ be the sample vector of ${Seasonal_t}^{(i)}$ $(i = 1, 2, 3)$, whose yearly cyclical period is defined by the following (a), (b), and (c)

   (a) Period including February 29:

   $${Seasonal_t}^{(1)} = -365, \dots, 0;\ {Seasonal_t}^{(2)} = 1, \dots, 366;\ {Seasonal_t}^{(3)} = 366, \dots, 731$$

   (b) Subsequent period of (a):

   $${Seasonal_t}^{(1)} = -364, \dots, 0;\ {Seasonal_t}^{(2)} = 1, \dots, 365;\ {Seasonal_t}^{(3)} = 367, \dots, 731$$

   (c) Other than the above:

   $${Seasonal_t}^{(1)} = -364, \dots, 0;\ {Seasonal_t}^{(2)} = 1, \dots, 365;\ {Seasonal_t}^{(3)} = 366, \dots, 730$$

2. GAM (3.1) and (3.2) are applied to the set of the sample vectors of the dependent variable and the explanatory variable considered by the following equation:

$$\begin{bmatrix} Y \\ Y \\ Y \end{bmatrix}, \begin{bmatrix} S^{(1)} \\ S^{(2)} \\ S^{(3)} \end{bmatrix} \tag{3.16}$$

3. The spline function in the case of ${Seasonal_t}^{(2)} = 1, \dots, 365\ (366)$ is adopted as the yearly cyclical function.

3.5.3 Multinomial Logit Model

The multinomial logit model is originally based on the theory of utility maximization, in which a

decision-maker makes a choice of multiple discrete and exhaustive choices that maximizes their utility. Relevant applied researches have been conducted in various fields such as marketing, psychology, economics, and transportation planning. At present, it is used not only for predicting consumer choice behavior but also for predicting a company's credit risk and natural phenomena. For example, there are works that have estimated the probability of a company's loan status and classified statuses into normal payment, delinquency, bankruptcy, etc. (Smith 1995 and 1996); the probability of serious injury due to a motorcycle accident because of environmental factors, road conditions, driving attitude, etc. (Shankar and Mannering 1996); future vegetation distribution from climatic conditions of temperature and precipitation (Omasa et al. 1999); the probability of the form of snow cover damage in forests using meteorological and topographical factors (Kamo et al. 2013); and the probability distribution of river flow by class based on the measured temperature and precipitation (Augustin et al. 2008).

As a similar probabilistic multinomial selection model, there is a "multinomial probit model," which assumes a normal distribution for the error term distribution in (3.6). It makes natural assumptions, but since it leaves the integral form in the selection probability, the parameter estimation becomes complicated. On the other hand, the multinomial logit model has a closed distribution form without an integral form, making it easy to handle and having an advantage in interpretation, which is why it is widely used today (e.g., Greene 1993).

Chapter 4

Prediction Error Weather Derivatives for Loss of Solar Output Prediction Errors

4.1 Introduction

Predicting future solar conditions is important for electricity industries with solar power generators to quote a next-day sales contract (i.e., day-ahead sales contract) in the electricity market. If a prediction error exists, the market-monitoring agent has to prepare another power generation resource to immediately compensate for the shortage, resulting in an additional cost. In this context, a penalty may be required depending on the size of the prediction error, which may lead to a significant loss for solar power generation industries. Because the main source of such losses is from prediction errors of solar conditions (Ministry of Economy, Trade and Industry; METI 2017), they can instead effectively utilize an insurance contract (or a derivative contract) based on solar prediction errors to hedge against loss caused by prediction errors of solar power output. The objective of this work is to provide such a derivative contract, namely, a prediction error weather derivative.

In this study, we propose multiple hedging methods for prediction error losses in solar power generation using derivatives of weather prediction errors, and then measure the hedge effect under a certain loss function. Weather derivatives are widely used mainly for methods using the temperature index (PricewaterhouseCoopers 2011), and previous studies applied weather derivatives to the electricity industry as follows. Yamada et al. (2006) proposes a pricing method using trend prediction for futures and option contracts based on the monthly average temperature. Yamada (2008a and 2008b) propose weather derivatives for effectively hedging the loss risk of power prediction errors for wind power. Yamada (2018) propose a hedging method using

temperature prediction error derivatives against the loss associated with the electricity retailers' imbalance. Another related study, Bhattacharya et al. (2015), verified the cross-hedging effect for a solar power producer in the US when using standard temperature derivatives. This study proposes a derivative to hedge the loss due to solar power prediction errors and relies on the design method proposed in Yamada (2008a, 2008b, and 2018). Specifically, we not only design the solar radiation derivatives on prediction error and measure its hedge effect, but also introduce the temperature derivatives on absolute prediction error and validate the cross-hedging effect when using them together. To price temperature derivatives and construct the hedging model, we propose a method using a tensor product spline function that simultaneously incorporates smoothing conditions for both, the direction of time and seasonal trend, to ensure the robustness of estimation while using small sample size data.

This study is structured as follows. Section 4.2 introduces the minimum variance hedging method using prediction errors, especially focusing on the tensor product spline function. Section 4.3 outlines the data we work with in this study and proposes the prediction method for hourly temperature (pricing method for the temperature derivative). In Section 4.4, we construct several hedging models using derivatives of solar radiation and temperature, measure the hedge effects, and add a consideration. Section 4.5 summarizes this study.

4.2 Minimum Variance Hedging Problem Using Prediction Errors

As previously mentioned, the prediction errors of solar power outputs lead to losses in the form of a penalty for electricity industries with solar power generators. In this section, we introduce hedging methods for such losses using derivatives on weather prediction errors. Here, using a simple market model shown in Figure 4.1, we explain the concept of derivatives introduced in this study and the related transactions, intended for a solar power producer who sells all the produced power on the spot market (i.e., day-ahead market where next day's power output is exchanged).

First, the power producer prepares weather derivatives contracts with an insurance company in advance (and pays a premium on the derivatives if needed)[20]. Then, as part of daily operations, the

[20] Regarding the weather derivative contract, we will introduce two types of derivatives: solar radiation derivative, which is directly contracted between a solar power producer and an insurance company (introduced in Section 4.2.1.2 and the

power producer predicts next-day solar power outputs (the output prediction at time n is denoted as $\widehat{P_n}$) and sells them at spot price S_n; hence, it gets profit $S_n\widehat{P_n}$ on the spot market. Subsequently, on the delivery day, if the realized output P_n deviates from the prediction $\widehat{P_n}$ (i.e., sales contract volume on the spot market), the deviated output, which is corresponding to the output prediction error $\varepsilon_{P,n} := P_n - \widehat{P_n}$, is procured (sold) by the system operator under the supervision of the monitoring agent and settled by the imbalance price I_n that is determined by adding the penalty unit price (corresponding to the prediction error loss) to the spot-market-based price. Concurrently, the payoffs of the contracted derivatives are also determined as the function of weather prediction errors. The aim of hedging method proposed in this study is to minimize the variance of a portfolio comprising the solar output prediction error loss and the derivatives payoffs[21].

4.2.1 Definition of Loss and Payoff Functions of Derivatives

4.2.1.1 Loss Function

Here, we will outline the prediction error loss dealt with in this study. For simplicity, we define the imbalance price I_n at time n as the price obtained by adding the penalty term δ (k in the case of shortage, or $-l$ in the case of surplus, both of which are time constant values) to the spot price S_n as follows[22]:

$$I_n = S_n + \delta \text{ s.t. } \delta = \begin{cases} k \text{ if } \varepsilon_{P,n} < 0 \\ -l \text{ if } \varepsilon_{P,n} > 0 \end{cases}, k \text{ and } l > 0. \tag{4.1}$$

Here, the power producer's total profit π_{total}, which is comprising the profit π_S due to the spot market transaction and the profit (loss) π_I by the imbalance price settlement, is obtained from the following equation:

$$\pi_{total} = \pi_S + \pi_I = S_n\widehat{P_n} + I_n\left(P_n - \widehat{P_n}\right) = S_nP_n + \delta\varepsilon_{P,n}. \tag{4.2}$$

---

optimal hedging problem is set in Section 4.2.2.2), and temperature derivative, which may be traded liquidly (introduced in Section 4.2.1.3 and the optimal hedging problem is set in Section 4.2.3.2). The specific concepts for both derivatives are described in each section.

[21] Under Japan's current institution, most of the renewable power producers are not subject to the application of imbalance price since all the output is purchased at a fixed price determined in advance under the feed-in tariff (FIT) law. Instead, imbalance risk is borne by retailers or system operators. In the future, however, it is assumed that the scheme will be shifted to one where renewable power producers themselves make predictions and bear the imbalance risk.

[22] In Japan, this penalty term was included in the imbalance price applied from April 2019.

Since the first term $S_n P_n$ of the right side in equation (4.2) means the profit when the prediction was accurate and the total amounts of realized output were sold out on the spot market (at the spot price), the flipped value of the second term $-\delta\varepsilon_{P,n}$ ($-k\varepsilon_{P,n}$ in the case of shortage, or $l\varepsilon_{P,n}$ in the case of surplus, both of which are positive values) corresponds to the opportunity loss compared to the case where no prediction error occurs. In this study, we refer to such opportunity loss as prediction error loss. This loss function ($-\delta\varepsilon_{P,n}$) is described in Figure 4.2.

Here, we define a loss function assuming that the penalties have the same unit price for both the shortage and surplus; that is, we define the loss function proportional to the absolute value of the output prediction error $\varepsilon_{P,n}$ at the time $n(=1,\dots,N)$ as follows[23]:

$$L_n := c\left|\varepsilon_{P,n}\right|. \tag{4.3}$$

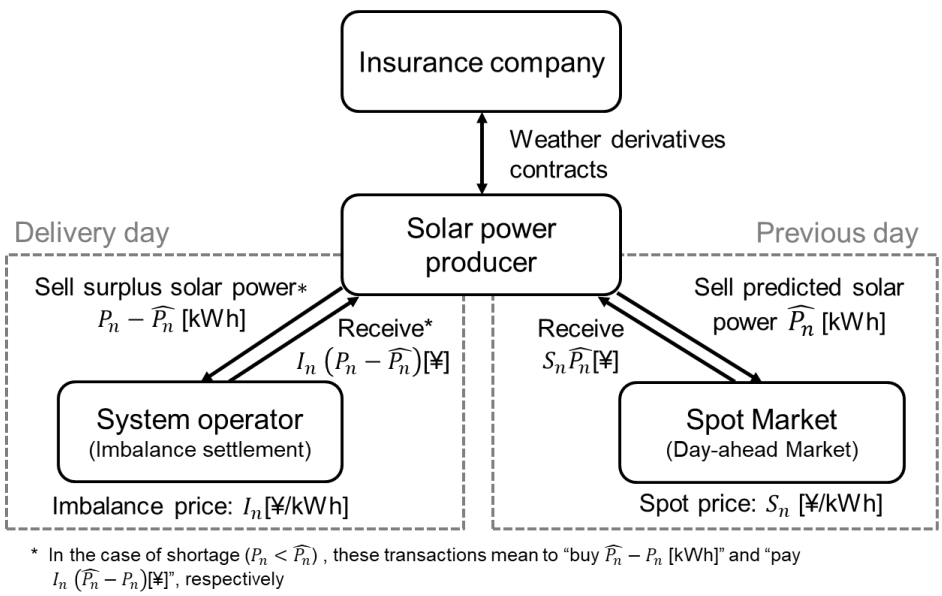

Figure 4.1: Simple market model for a solar power producer

[23] The method proposed in this study can also be applied in the case of $k = l$. If such an asymmetric loss function is assumed, the optimal payoff function of the solar radiation derivative calculated correspondingly (in the empirical analysis described in Section 4.4.2) may change such that the asymmetry becomes stronger (or weaker).

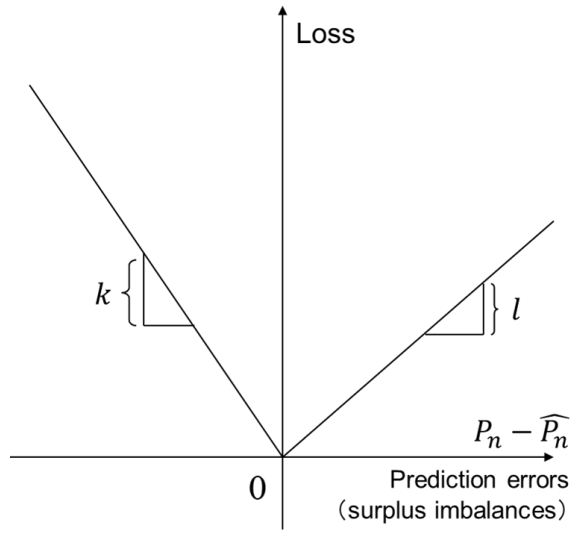

Figure 4.2: An example of loss function

4.2.1.2 Solar Radiation Derivatives on Prediction Errors

Next, we consider the solar radiation derivatives based on prediction error. This payoff function is denoted by $\psi(\varepsilon_{R,n})$, as a function of solar radiation prediction error $\varepsilon_{R,n} := R_n - \widehat{R_n}$ (the actual solar radiation minus its prediction)[24]. This derivative may play an insurance roll and is assumed to be contracted between a solar power generation company and an insurance company directly. For this, we set a problem of finding the optimal payoff function given the solar power producer's loss function (formulated in Section 4.2.2.2).

4.2.1.3 Temperature Derivatives on Absolute Prediction Errors

Then, we introduce the temperature derivatives on absolute prediction error. The payoff of the derivative is defined as $|\varepsilon_{T,n}|$ (i.e., the absolute value of the temperature prediction error $\varepsilon_{T,n} := T_n - \widehat{T_n}$, the actual temperature minus its prediction). Unlike the solar radiation derivative, the temperature derivative has a specific payoff function and may be traded more liquidly. Hence, in this research, the problem we deal with in relation to the temperature derivative is to solving the optimal contract volume (formulated in Section 4.2.3.2).

[24] The solar radiation derivative is assumed to be contracted without transaction costs. That is, it satisfies the equation $\mathrm{Mean}[\psi(\varepsilon_{R,n})] = 0$. Note that we assume the same condition for the solar radiation derivative on absolute prediction errors $\psi(|\varepsilon_{R,n}|)$, which will be introduced later.

4.2.2 Minimum Variance Hedging Using Smoothing Spline Functions

4.2.2.1 Estimation of the Smoothing Spline Functions

In this study, we use the generalized additive model (GAM; see e.g., Hastie and Tibshirani 1990) for estimating the payoff function or the optimal contract volume of prediction error derivatives, in line with the ideas proposed in Yamada (2008b and 2018). A univariate smoothing spline function is estimated as a function $h(\cdot)$ that minimizes a penalized residual sum of squares (PRSS) as follows (y_n and x_n are the dependent and independent variables, respectively):

$$\mathrm{PRSS} = \sum_{n=1}^{N} \{y_n - h(x_n)\}^2 + \lambda \int \{h''(x)\}^2 \, dx. \tag{4.4}$$

In equation (4.4), the first term measures closeness to the data while the second term penalizes curvature in the function (penalty term). Estimation of the spline function using GAM corresponds to solving the minimum variance problem under smoothing constraints, and in this context, GAM here can be rephrased as hedge model (Yamada 2008b and 2018)[25].

4.2.2.2 Minimum Variance Hedging Using Solar Radiation Derivatives on Prediction Errors

The method of estimating the univariate smoothing spline described above is applied to the calculation of how to solve the optimal payoff function of solar radiation derivatives. That is, the minimum variance hedging problem to solve the optimal payoff function of solar radiation derivatives is given as follows:

$$\min_{\psi(\cdot)\in \boldsymbol{S}_\lambda} \mathrm{Var}\left[L_n - \psi\left(\varepsilon_{R,n}\right)\right] \text{ s.t. } \mathrm{Mean}\left[\psi\left(\varepsilon_{R,n}\right)\right] = 0. \tag{4.5}$$

where $\boldsymbol{S}_\lambda$ is set of smoothing spline function with smoothing parameter λ. This corresponds to solving the problem of minimizing $\mathrm{Var}\left[L_n - \psi\left(\varepsilon_{R,n}\right)\right]$, the variance of the portfolio constituted by loss L_n and optimal derivatives payoff $\psi^*\left(\varepsilon_{R,n}\right)$ under the smoothing conditions.

As this derivative is assumed to be contracted with the insurance company directly (as mentioned in Section 4.2.1.2), if the solar power generation company knows an optimal payoff

[25] In this study, we construct GAM using the function gam () in the R 3.5.1 package "mgcv" (https://cran.r-project.org), where gam () adopts general cross-validation criterion to calculate the smoothing parameter λ (Wood 2017).

structure by solving with the optimization problem in (4.5), then it may try to find an insurance company to offer such an optimal payoff function. This is the reason why the power generation company needs to solve the optimization problem in (4.5) over ψ.

Note that since this derivative is designed to make its average payoff equal to 0, the buyer does not have to pay premium at the contracting time, as long as it is a fair derivative.

4.2.3 Minimum Variance Hedging Using a Bivariate Spline Function (Tensor-Product Spline Function)

4.2.3.1 Estimation of the Tensor Product Spline Function

In this study, we estimate the tensor-product spline function for the pricing of temperature derivatives and calculating its optimal contract volume. Tensor product spline is a type of multivariate spline function whose basis functions are given as tensor products, and in the PRSS to be minimized, penalty terms are added for each explanatory variable. For example, the penalty term $J_{te}(h)$ of a bivariate cubic tensor product spline is given by the following equation (Wood 2017):

$$J_{te}(h) = \int_{x,z} \lambda_x \left(\frac{\partial^2 h}{\partial x^2}\right)^2 + \lambda_z \left(\frac{\partial^2 h}{\partial z^2}\right)^2 dxdz. \tag{4.6}$$

A typical multivariate spline function other than tensor product spline is a thin plate spline function. An example of a penalty term $J_{tp}(h)$ of a bivariate thin plate spline function is shown in the following equation (Wood 2017):

$$J_{tp}(h) = \lambda \int_{x,z} \left(\frac{\partial^2 h}{\partial x^2}\right)^2 + \left(\frac{\partial^2 h}{\partial x \partial z}\right)^2 + \left(\frac{\partial^2 h}{\partial z^2}\right)^2 dxdz. \tag{4.7}$$

Comparing equations (4.6) and (4.7), it is found that the term related to $\partial^2 h/\partial x \partial z$ is added to the penalty term of the thin plate spline. As can be observed, "thin plate spline" is called so because it is similar to the bent shape of a thin elastic plate, having a feature that the smoothing penalties are isotopically incorporated.[26]

[26] For example, Wood (2013) modeled the density of mackerel eggs in the ocean using a thin plate spline using latitude and longitude as explanatory variables, which can be said to be an intuitive case using the isotropic nature of the function.

We adopt the tensor product spline considering that it is appropriate for the time series data handled in this study to be given both the smoothing conditions of time and seasonal trend independently.

4.2.3.2 Minimum Variance Cross-Hedging Using Temperature Derivatives on Absolute Prediction Errors

The method of estimating the tensor-product spline function is applied to the problem of calculating the optimal contract volume of temperature derivatives on prediction error. We work with a different model compared to solar radiation for the following reason. Since the solar power output prediction error is assumed to have an almost constant correlation (for any time) with the solar radiation prediction error, hedging by univariate derivatives such as in equation (4.5) is effective; on the other hand, as the temperature prediction error has different sensitivities depending on the time (e.g., at the time in which solar radiation is originally small, such as early mornings or late evenings, the output error's sensitivity to the temperature error is significantly small), the same hedging method as solar radiation is not effective. Therefore, for hedging using temperature derivatives, we apply a method to change the contract volume depending on time. In other words, this hedging model is a problem of estimating the time dependent sensitivity of the absolute temperature prediction error with respect to the loss function (absolute output prediction error). To estimate this sensitivity trend, we use the tensor product spline function. Specifically, we solve the following minimum variance hedging problem:

$$\min_{\Delta(\cdot)\in\boldsymbol{S}_{\lambda}} \mathrm{Var}\left[L_n - \Delta(Seasonal_t, h)\left|\varepsilon_{T,n}\right|\right] \tag{4.8}$$

where t and h represent the date and hour corresponding to the hour h, $\Delta(\cdot)$ represents the contract volume of the derivative, and $Seasonal_t$ is the periodicity dummy variable ($= 1, \ldots, 365(or\ 366)$)[27]. Equation (4.8) minimizes the variance of the portfolio consisting of losses L_n and $\Delta(\cdot)$ units of temperature derivative whose payoff is $\left|\varepsilon_{T,n}\right|$.

The average payoff of this derivative, $\mathrm{Mean}\left(\left|\varepsilon_{T,n}\right|\right)$, clearly does not equal to 0; hence, unlike solar radiation derivatives introduced in the previous section, the temperature derivative requires

[27] For allocating periodic dummy variables, we use the method proposed in Yamada et al. (2015) (the same applies hereafter in this chapter).

buyers to pay a premium at the contracting time (time 0). Note that the premium can be calculated as the present discounted value of unconditional expected value of the payoff $\mathrm{E}(|\varepsilon_{T,n}|)$.

4.3 Preliminary

4.3.1 Data Description

To design the prediction error derivatives proposed in this study, actual measured values of solar power output, solar radiation, and temperature, and their respective predicted values on the previous day are required. Since each predicted value is hard to acquire, we obtain it to separately construct the prediction model by using the next-day weather forecast of the past, which is announced by JMA every day. Specific data to be used and its sources are shown below (all of the data pertains to Hiroshima City):

(a) Solar power output P_n: Measured value of household's solar power system[28]

(b) Solar radiation R_n, temperature T_n, and weather condition W_n: Measured value by JMA[29]
Prediction of weather F_n, daily maximum temperature $Temp\_max_t$, and minimum temperature $Temp\_min_t$: Weather forecast announced by JMA on the previous morning[30]

(c) Prediction of solar power output $\widehat{P_n}$: Calculated value by prediction model using P_n, F_n, and W_n

(d) Prediction of solar radiation $\widehat{R_n}$: Calculated value by prediction model using R_n, F_n, and W_n

(e) Prediction of temperature $\widehat{T_n}$: Calculated value by prediction model using T_n, $Temp\_max_t$, and $Temp\_min_t$

Among the above, (a)-(c) are historical data, and (d)-(f) are values calculated by separately constructed prediction models. Of these, (d) and (e) are obtained using the prediction method (calculated value) proposed in Matsumoto and Yamada (2018a), and the prediction model of (f) is explained in the next section.

We now pay attention to the relationship between R_n and P_n. Figure 4.3 shows this in a scatter diagram, and Figure 4.4 shows a spline regression fitted to it (dotted lines denote the 95%

[28] With the permission of the owner, we use the data of the private roof-mounted power system in Hiroshima City.

[29] Downloaded from https://www.data.jma.go.jp/gmd/risk/obsdl.

[30] Downloaded from http://weather-transition.gger.jp.

confidence intervals, and they also apply to subsequent graphs of the same type)[31]. As shown in Figure 4.4, the solar radiation and solar power output have the following tendencies: the power output increases proportionally until the solar radiation reaches around 2.0 $[\mathrm{J/m^2}]$, but beyond that, the slope of the power output decreases with respect to the solar radiation. Originally, the solar power system has technical characteristics such that the power-generating efficiency decreases due to the rise in temperature of the power generation module (Yukawa et al. 1996); hence, this characteristic seems to be reflected.

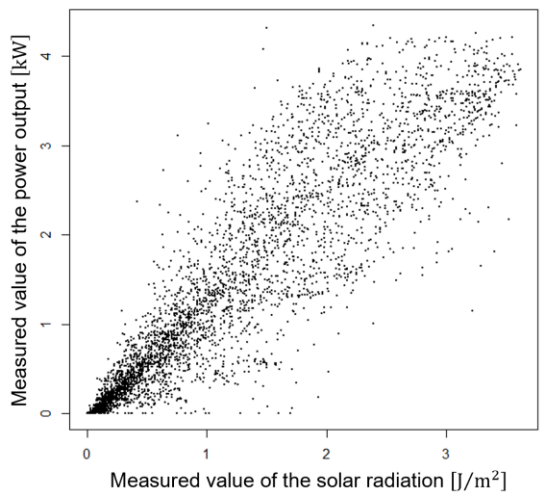

Figure 4.3: Solar radiation vs. power output

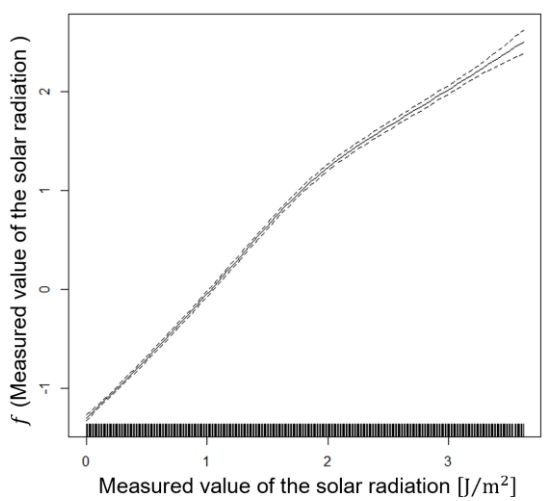

Figure 4.4: Spline regression curve for Figure 4.3

[31] We use the data from June 1, 2016, to May 31, 2017.

4.3.2 Prediction Model of Hourly Temperature (Pricing Method for Temperature Derivatives)

In this section, we build a model that obtains hourly predicted values of temperature using the daily maximum or minimum temperature as announced by JMA on the previous morning and the hourly actual temperature. Note that this is also interpreted as a pricing method for temperature derivatives on the absolute prediction error defined in Sec. 4.2.1, as it determines the hourly payoffs for the derivative. [32]

Here, we build the prediction model by applying GAM using the tensor product spline regression to the hourly measured temperature $T_{t,h}$ at hour h on date t as follows:

$$T_{t,h} = \gamma(Seasonal_t, h) + s_1(Temp\_max_t) + s_2(Temp\_min_t) + \varepsilon_{T,t,h} \tag{4.9}$$

where $\gamma(\cdot)$ is a tensor product spline function, and $s_1(\cdot)$ or $s_2(\cdot)$ is a univariate spline function.

Each spline function estimated by the above equation is shown in Figure 4.5[33]. The estimated value of the term $\gamma(Seasonal_t, h)$, which refers to the time series trend of the temperature, has two directions of smooth trends such as the intraday time trend (e.g., low in the morning and high in the early afternoon) and the seasonal trend of the same hour (e.g., low in the winter and high in the summer), and it is confirmed that these trends are effectively extracted. As in this case, even when the sample size of available data is small, the tensor-product spline allows for a relatively robust trend estimation by incorporating the smoothing conditions in two different directions.

The spline functions related to the predicted values of the maximum and minimum temperatures are confirmed to be monotonically increasing functions.

[32] In the weather forecast publicly announced by the JMA, we cannot obtain the hourly predicted temperature values for the next day, so we introduce this new pricing method.

[33] We use the data from June 1, 2016, to May 31, 2017, during which it was possible to obtain past weather forecasts.

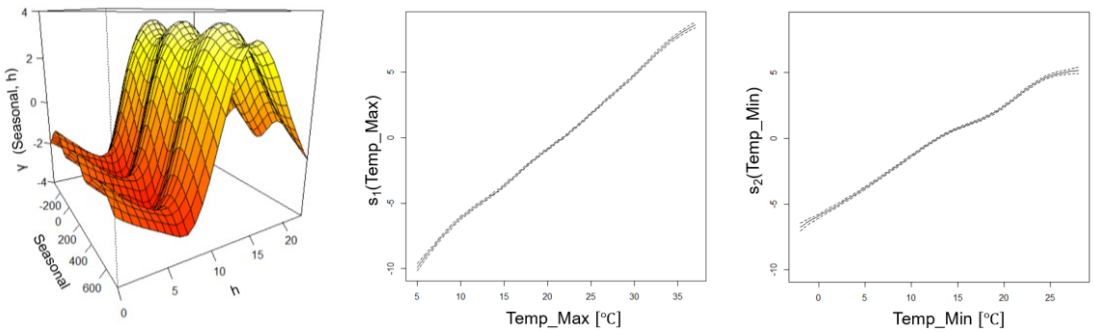

Figure 4.5: Estimation results for each term in the temperature prediction model

4.4 Construction of Hedging Models of Prediction Error Loss and Empirical Analysis

In this section, we construct various hedging models using derivatives on the prediction error of solar radiation and temperature against the prediction error loss of solar power output, and verify their hedge effects. We construct hedging models using the prediction errors of solar power output, solar radiation, and temperature ($\varepsilon_{P,n}$, $\varepsilon_{R,n}$ and $\varepsilon_{T,n}$) during the period from June 1, 2016 to May 31, 2017. We also measure the hedge effect of models and add a consideration. Upon measurement, the variance reduction rate (VRR) is determined by the following equation as in Yamada (2008a, 2008b and 2018), and 1-VRR is hereinafter referred to as the hedge effect.

$$\text{VRR}:=\frac{\text{Var[Portfolio after hedging]}}{\text{Var[Prediction error loss]}}=\frac{\text{Var}(\varepsilon_n)}{\text{Var}(L_n)} \tag{4.10}$$

where ε_n indicates the residual term of each hedging model defined in the following sections.

4.4.1 Hedging Using Solar Radiation Derivatives on Absolute Prediction Errors

First, we consider the problem of hedging the loss function L_n with a solar radiation derivative on absolute prediction error. In line with the concept stated in Section 4.2.2, solving the payoff corresponds to estimating the spline function $\psi(\cdot)$ in the following way:

$$L_n-\text{Mean}(L_n)=\psi\left(\left|\varepsilon_{R,n}\right|\right)+\varepsilon_n. \tag{4.11}$$

Figure 4.6 shows the scatter diagram of $\left|\varepsilon_{R,n}\right|$ and $\left|\varepsilon_{P,n}\right|$, and Figure 4.7 shows the optimal payoff function of the derivative obtained by the hedging model (4.11).

The horizontal axis is the solar radiation prediction error, and the vertical axis is the payoff[34]. In this case, the 1-VRR is calculated as 0.523, which shows that the variance of the prediction error loss risk is reduced by about 52% of the original value.

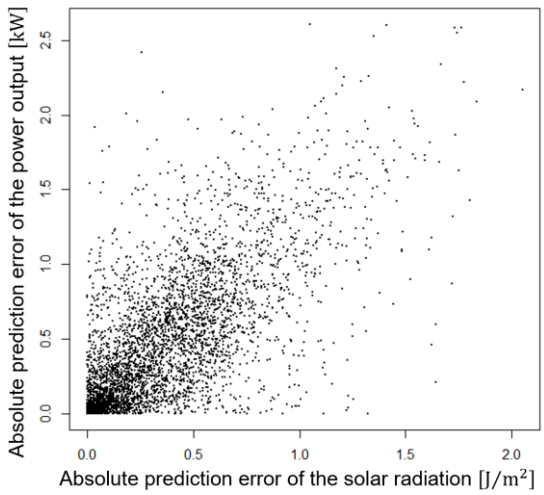

Figure 4.6: Absolute prediction error of the solar radiation vs. absolute prediction error of the solar power output

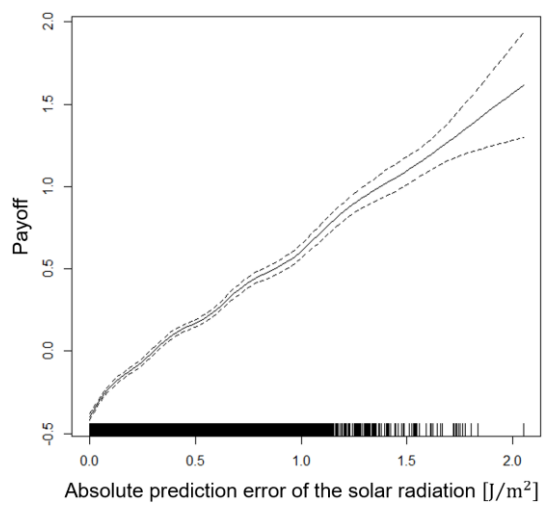

Figure 4.7: Payoff of solar radiation derivative in model (4.11)

4.4.2 Hedging Using Solar Radiation Derivatives on Prediction Errors

Next, we consider the following hedging model. It differs from the previous one as the underlying

[34] Since the coefficient of the loss on the absolute output prediction error is set to 1, the value obtained by multiplying the vertical axis by c is equivalent to the actual payoff (same applies to the subsequent sections).

asset of the derivative is not the absolute value but the pure value of the solar radiation prediction errors:

$$L_n - \mathrm{Mean}(L_n) = \psi(\varepsilon_{R,n}) + \varepsilon_n. \tag{4.12}$$

Figure 4.8 shows the scatter diagram of $\varepsilon_{R,n}$ and $|\varepsilon_{P,n}|$, and Figure 4.9 shows the payoff function of the derivative on model (4.12). The 1-VRR of this model is calculated as 0.536, and the hedge effect is slightly improved over model (4.11). The estimated payoff function shows that the absolute slope when $\varepsilon_{R,n}$ is positive is smaller than when it is in the negative range. As mentioned above, this is because when the $\varepsilon_{R,n}$ is positive, the influence of output reduction due to temperature tends to increase, which causes the output error to decrease. It is considered that since model (4.12) can accommodate such asymmetry, the hedge effect is higher than model (4.11) in the previous section.

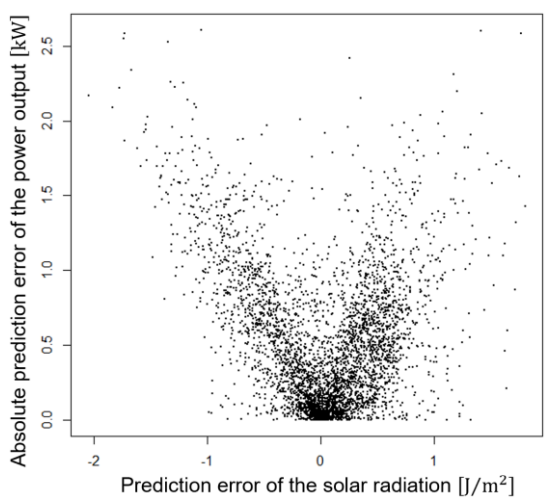

Figure 4.8: Prediction error of the solar radiation vs. absolute prediction error of the solar power output

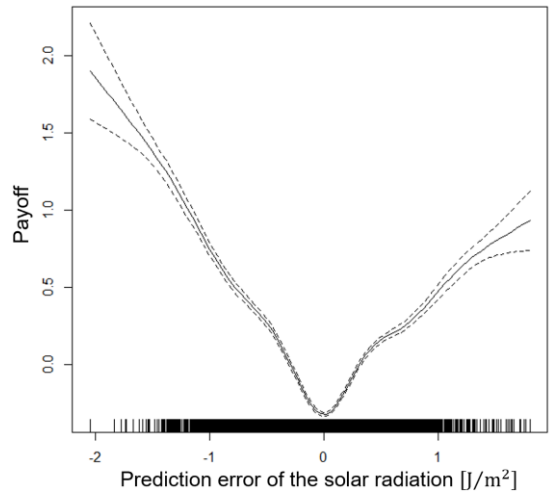

Figure 4.9: Payoff of solar radiation derivative in model (4.12)

4.4.3 Cross Hedging Using Solar Radiation and Temperature Derivatives

Next, we consider the following model using the solar radiation derivative on prediction error and the temperature derivative on absolute prediction error in combination[35]:

$$L_n - \mathrm{Mean}(L_n) = \Delta(Seasonal_t, h)\left|\varepsilon_{T,n}\right| + \psi\left(\varepsilon_{R,n}\right) + \varepsilon_n. \tag{4.13}$$

The estimated value of the tensor product spline $\Delta^*(Seasonal_t, h)$, which is the coefficient of the first term on the right side, is the optimal contract volume of the temperature derivative determined by the delivery time. Figure 4.10 shows $\Delta^*(Seasonal_t, h)$ and Figure 4.11 shows $\psi^*\left(\varepsilon_{R,n}\right)$. The 1-VRR of this model was calculated to be 0.622 and it was confirmed that the variance was further reduced compared to hedging models (4.11) and (4.12). In Figure 4.10, it is considered that the sensitivity of the temperature prediction error which changes depending on the time can be effectively estimated by using the spline model with the intersection variable.

[35] Equation (4.13) has a term with crossing variables attached to the tensor product spline, but since the intersection term replaces only the new function by multiplying the basis function of the tensor product spline by the crossing variable, it can be estimated by the same procedure using normal GAM, as described in Yamada (2018).

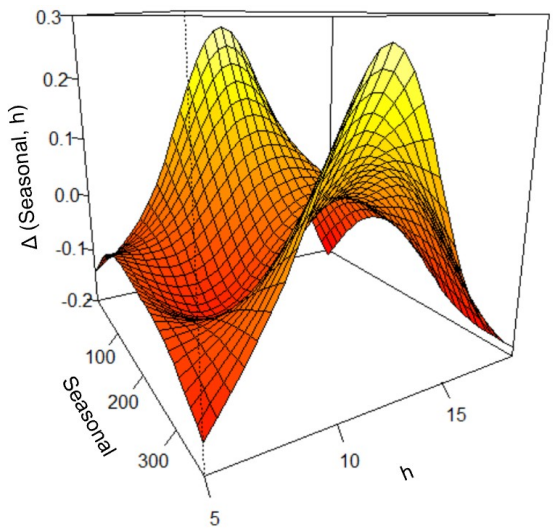

Figure 4.10: Optimal contract volume of temperature derivative in model (4.13)

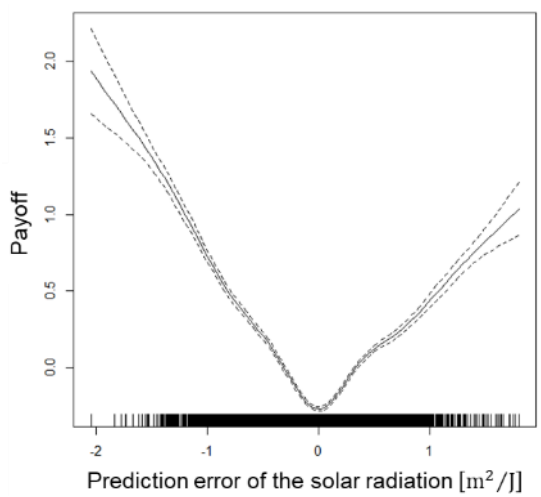

Figure 4.11: Payoff of solar radiation derivative in model (4.13)

4.4.4 Cross Hedging Using Temperature Derivatives

In this section, we measure the hedge effect when using only temperature derivatives on the absolute prediction error without using solar radiation derivatives. Here, we consider the following hedging model:

$$L_n - \text{Mean}(L_n) = \Delta(Seasonal_t, h)\left|\varepsilon_{T,n}\right| + \varepsilon_n. \tag{4.14}$$

Model (4.14) differs from model (4.13) in that there is no term for solar radiation. The optimal contract volume $\Delta^*(Seasonal_t, h)$ of the temperature derivative in this model is shown in Figure 4.12:

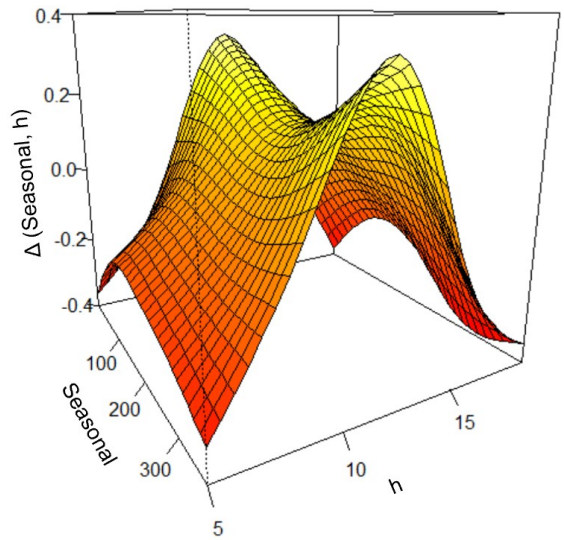

Figure 4.12: Optimal contract volume of temperature derivative in model (4.14)

The 1-VRR of this model is 0.310. This result is interesting because even with the hedging model using only the temperature derivative on the absolute prediction error, the variance of loss decreases by about 31%. This hedge effect can be explained as follows: since there is a positive correlation between the temperature and solar radiation (e.g., high temperature is usually due to large solar radiation) and a strong positive correlation between solar radiation and power output, there is a similar positive correlation between temperature and solar power output even when viewed with the prediction error.

The correlation between solar power output and temperature is a bit complicated: the characteristics of solar power output are such that power-generating efficiency decreases as temperature rises, but this can also be interpreted from the shape of Figure 4.12, which stands for the sensitivity of the output prediction error to the temperature prediction error. For example, if we look at the value around noon, it can be confirmed that the value in summer (near the saddle point) is lower than that in winter. A possible interpretation of this is, during daytime in summer, the output reduction due to the rise in temperature is remarkable enough for the sensitivity of the output prediction error to become smaller than during winter with respect to the temperature prediction error.

4.5 Conclusion

In this study, we proposed hedging methods based on derivatives on prediction errors of solar

radiation and temperature for the prediction error loss in solar power generation, and measured the resultant hedge effects.

Our proposed method is based on the previously examined research concept of prediction error derivatives in wind power, but it is new in the following points:

- It showed that the previous method can be applied to solar power generation with periodic trends
- It demonstrated the hedge effect using plural weather derivatives such as solar radiation and temperature
- It introduced hedging modeling with a tensor-product spline function and showed its effectiveness

It was found that the variance of prediction error loss in solar power generation can be reduced by about 54% by using solar radiation derivatives on prediction errors, and by about 31% even when only using the temperature derivative on the absolute prediction error. Furthermore, it was demonstrated that the hedge effect was improved by up to 62% by using the solar radiation derivative and temperature derivative together.

The temperature derivative on the absolute prediction error designed from publicly available forecasts and measured values are thought to be effective for hedging the prediction error loss of power demand, which has a strong correlation with temperature; therefore, further application and versatility may be expected. In addition, it is considered that the demonstrated cross-hedging effect obtained when using only the temperature derivative suggests practical recommendations in the case of product development and application.

Chapter 5

Simultaneous hedging strategy for price and volume risks using derivatives portfolio

5.1 Introduction

Fluctuation risks of revenue or cost in electricity businesses can be roughly divided into two factors: price risk and the volumetric risk. In mature electricity markets, different derivative instruments are liquidly traded to hedge against each type of risk. For example, in the PJM market in the US, which is the world's largest regional transmission organization (RTO), derivatives or futures are listed both for electricity price and demand. These derivatives are expected to have significant hedging effects if one of the two fluctuation risks does not fluctuate. However, since the revenue/cost of an electricity business usually takes the form of the product of price and volume (sales amount or demand), both of which fluctuate with time, it is impossible to be completely hedged by combining existing derivatives. On the other hand, considering that both the price and volume of electricity greatly depend on weather conditions, the use of weather derivatives is expected to have a significant hedging effect on these variables. Naturally, it does not provide a complete hedge, but considering that weather derivatives are effective in hedging risks in many businesses other than the electricity industries, they are expected to have liquidity in transactions. Because electricity price risks are also linked to fuel prices, in this study, we propose hedging strategies for fluctuation risks of revenue/cost within the electricity business by constructing a portfolio of fuel derivatives and weather derivatives. In particular, by using empirical data in two different market models—such as the revenue fluctuation risk of a solar power company that sells generated electricity at the JEPX market and the cost fluctuation risk of a retail company that procures electricity at the PJM market—we demonstrate the effects of the hedging strategies

proposed in the research.

Previous studies that have applied weather derivatives to the electricity volume risks have proposed a pricing method using trend predictions for futures and options based on the monthly average temperature (Yamada et al. 2006) and weather derivatives for hedging the loss of power prediction errors either for wind power (Yamada 2008b) or solar power (Matsumoto and Yamada 2019b). Although these studies propose methods for hedging volume risk, such as demand and power output, Yamada (2019) also considers price fluctuation risk and proposes hedge methods for the retailer's procurement cost (as defined by the product of electricity market price and demand volume) by using temperature derivatives. Another related study by Bhattacharya et al. (2015) verified the cross-hedging effect for a solar power producer in the US when using standard temperature derivatives. In addition, as a previous study on cross-hedging by fuel price, Woo et al. (2011) demonstrated the hedging effect of Henry Hub (HH) natural gas futures for electricity spot prices in Mid-Columbia. In other recent related research, Meier et al. (2019), constructed a model in which a tensor product spline function is applied to the prediction of electricity prices. This model shows the significant advantage of its prediction accuracy, computational load, and interpretability with visualization in comparison with conventional time series models such as ARIMAX.

This study has the same objective as Yamada (2019) in that the hedging target is defined by the product of electricity price and volume, and the modeling method based on non-parametric regression is applied; however, this work is characteristic in terms of the following points: (1) To estimate the derivatives' payoff function that changes with date, we use a tensor-product spline function that can incorporate the two-dimensional smoothing conditions of the underlying asset price and expiration date with yearly cyclical trends; (2) We show that the applied method of ANOVA decomposition can separate deterministic time trends from the original multivariate payoff functions, and hence, a simultaneous estimation of multiple derivatives payoff functions is achieved; (3) By assuming that revenues have a yearly cyclical trend even when viewed at the rate of annual change, we also introduce a spline function with cross variables to consider such mixed effects. Furthermore, (4) we propose new standardized derivatives with the square of temperature prediction error as the underlying asset.

This work is organized as follows: First, Section 5.2 gives an overview of the JEPX and the PJM market, focusing on the relationship between electricity and fuel prices, and recent changes in power supply configuration. Second, Section 5.3 introduces the theoretical background of the hedging models, showing that they are equivalent to the prediction models; third, Section 5.4 formulates specific hedging models treated in this work; fourth, Section 5.5 examines the hedging effects of derivatives using empirical data; and lastly, Section 5.6 provides a summary.

5.2 Recent Electricity Market Overview of JEPX and PJM

Intended for effective hedge modeling, this section provides an overview of the determinants and features of electricity prices, describing recent environmental changes of the JEPX and PJM.

5.2.1 Market Overview in JEPX

Generally, in many mature electricity markets, such as in the US and European countries, there are liquid products of forwards or futures to hedge the risks of spot market transactions. On the other hand, in Japan, JEPX lists a forward market, but it has extremely low liquidity, so there are virtually no flexible hedging instruments on electricity derivatives. Therefore, as a means of hedging the price risk of JEPX, it is conceivable to use energy derivatives, which are liquidity traded in world commodity markets. In fact, the JEPX price is distinguished by its strong link to crude oil prices in the international oil market. For example, WTI, a typical crude oil price, has a substantial correlation with the JEPX spot price, with a time lag of approximately one month, as shown in Figure 5.1.[36]

Due to an increase in the supply capacity of nuclear (subsequent restart after all unit suspension because of the Fukushima nuclear accident) and of solar power generation, the JEPX price has been declining in recent years. In particular, solar power generation has continued to increase rapidly since 2012 when a feed-in tariff (FIT) scheme was implemented. In 2018, the percentage of solar power in the total national power generation reached 6.5%, as shown in Figure 5.2.

[36] The marginal generation cost, which determines the JEPX spot price, depends on the price of LNG, which is the marginal plant in most of the time. The supply of LNG is usually financed by long-term contracts that employ pricing formulas that are linked to the arrival price of the imported oil. For this reason, there is a market mechanism whereby crude oil market prices such as WTI affect JEPX spot price with time lags until they are reflected in Japan arrival prices and LNG long-term contract prices.

Next, for an overview of the electricity price fluctuation pattern, Figure 5.3 shows the daily maximum electricity demand and the daily average JEPX spot price in 2018, where seasonal characteristics can be seen, such as a remarkable price increase when the power demand increases during summer (July–August) and winter (January–February). From a longer-term perspective, as the left graph of Figure 5.1 shows, the fluctuation range of the monthly average price is expanding year by year. The remarkable recent price drop during the low demand period is thought to be due to the increase in the supply capacity of nuclear power and solar power, while the increasing price rise during the high-demand period may be due to intensified market competition resulting from the progress of liberalization. In this context, it is important for new small-scale solar power producers to hedge revenue fluctuations caused by daily changes in weather conditions.[37]

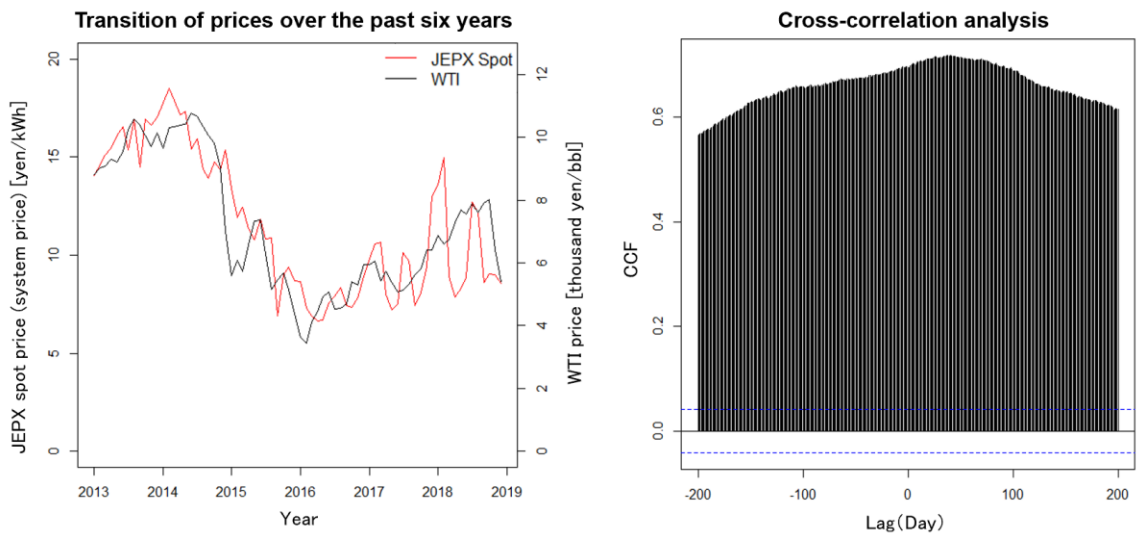

Source: JEPX (http://www.jepx.org/) and EIA (https://www.eia.gov/).

Figure 5.1: Relationship between JEPX spot price (system price) and WTI (JPY base)

[37] The purchase period of Japan's FIT has been gradually coming to an end since 2019, and it is expected that these hedging needs will further expand in the future.

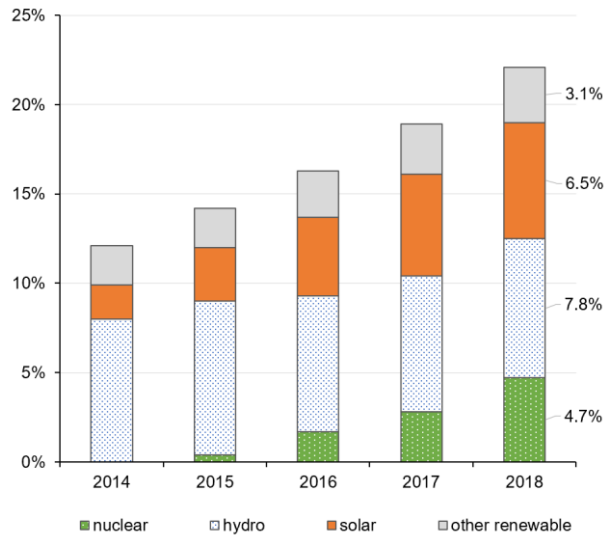

Source: METI (https://www.meti.go.jp/).

Figure 5.2: Recent change in power generation ratio in Japan (excluding thermal power)

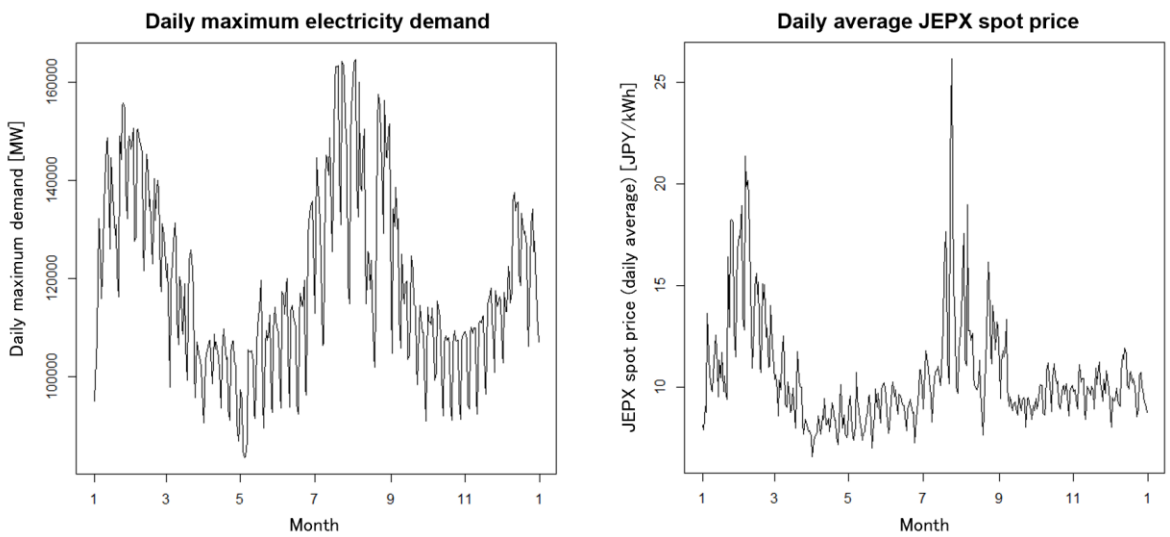

Source: JEPX (http://www.jepx.org/) and OCCTO (http://occtonet.occto.or.jp/).

Figure 5.3: Daily maximum demand in Japan (left) and daily average JEPX spot price (right) in 2018

5.2.2 Market Overview in PJM

In this subsection, we provide a simple overview of the PJM market. To hedge electricity risks in the PJM market, various electricity derivatives with different maturities are available at the Intercontinental Exchange (ICE) and NYMEX, but only monthly products are traded liquidly, and daily products are illiquid (Mahoney 2016). Futures products with demand (load) are also listed in

the ICE; however, the daily fluctuation risk of procurement costs consisting of demands and prices cannot be hedged completely only with the existing products. Thus, alternative means such as the cross-hedging approach combining weather and fuel derivatives would be effective in the PJM market.

The following provides an overview of recent trends in the PJM market. First, Figure 5.4 shows the transition of the yearly power generation amount by generation type in the PJM area. Notable features in recent years are the significant decreasing trend in the power generation of coal and an increasing trend in that of natural gas. Renewable energy has a solid increasing trend, but not as much as the rapid change of coal and gas. Next, Figure 5.5 demonstrates the daily price of PJM, natural gas (HH), and coal (Central Appalachia; CAPP). The PJM price has a trend close to both HH and CAPP; however, focusing on price spike timings, it is confirmed that PJM prices tend to be more strongly correlated to HH than CAPP. In view of the above, this study uses only HH futures as fuel derivatives and constructs hedge models reflecting the recent situation in which the power source composition ratio is dramatically changing, as Figure 5.4 shows.

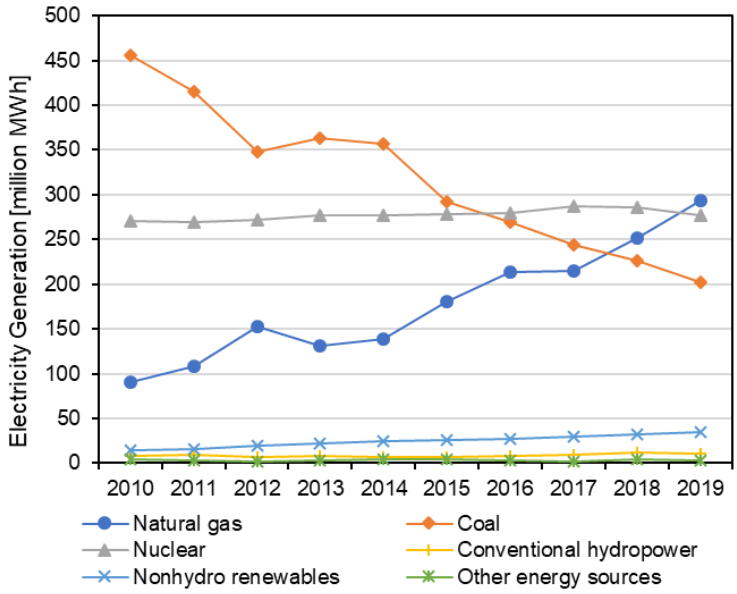

Source: EIA (https://www.eia.gov/outlooks/steo/)

Figure 5.4: Trends in power generation by generation type in the PJM area

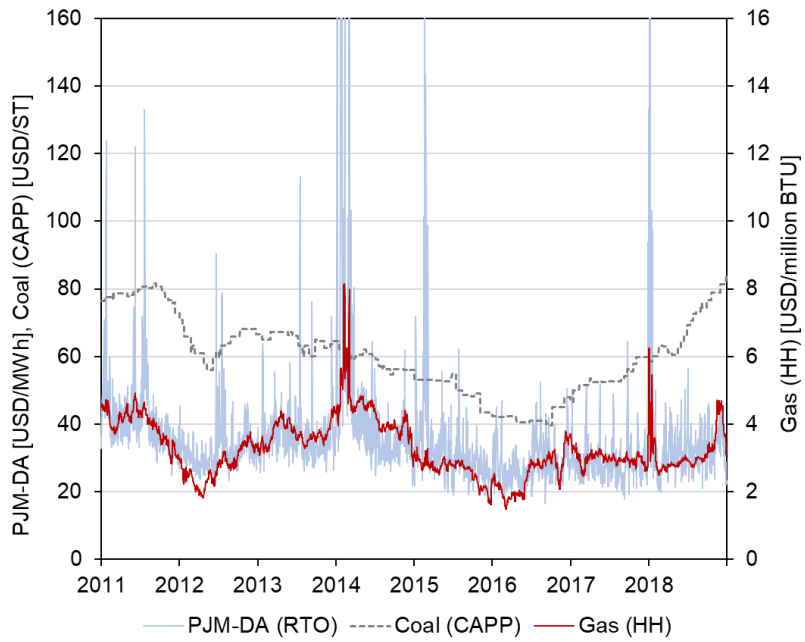

Source: PJM (http://dataminer2.pjm.com/) and EIA (https://www.eia.gov/)

Figure 5.5: Daily time series data of PJM (electricity, coal and gas prices)

5.3 Construction of Prediction Model and Interpretation as a Hedge Model

In this section, we introduce prediction models for the profit/loss value (i.e., solar power producer's profit or retailer's procurement cost) given by the product of electricity price and volume (solar power output or demand), and show that they are equivalent to the hedging models for the profit/loss in our problem setting.

Before introducing concrete equations for such prediction-based hedging models, the basic concept of weather derivatives used in this study is briefly explained using the retailer's simple market model shown in Figure 5.6 (note that in the case of a solar power producer, the procurement of power output is simply replaced by the sale of power output, so the explanation is omitted). First, a retailer procures all the power output to meet the demand $D_{t,h}$ at date t hour h from the spot market at the spot price $S_{t,h}$, and pays the procurement cost $\pi_{t,h} := S_{t,h} \times D_{t,h}$ as the consideration. In order to hedge the fluctuation of the cost, the retailer enters into a weather derivative contract with an insurance company in advance (it also procures fuel futures from the energy market although omitted here), where some kind of payoff function on measured weather values such as temperature is specified. If this derivative contract is bilateral, it can be traded with an arbitrary

payoff function, so we consider the problem of finding the optimal payoff function depending on the particular buyer's cost function (the temperature derivative introduced in Section 5.3.2 and 5.3.3 corresponds to this type of derivatives). Derivatives with fixed payoff functions (standardized derivatives), on the other hand, may be traded more liquidly, and for such products, we address the problem of optimizing the contract amount (the solar radiation futures introduced in Section 5.3.1 and the temperature squared error derivatives proposed in Section 5.4.4 correspond to this type of derivatives).[38]

In the following subsections, specific formulae of the prediction-based hedging models based on this market model are constructed using two examples: one is to hedge the sales revenue of a solar power producer using solar radiation futures, and the other is to hedge the procurement cost of a retailer using temperature derivatives (see Yamada 2019 for an example of hedging retailers' procurement costs with temperature futures).

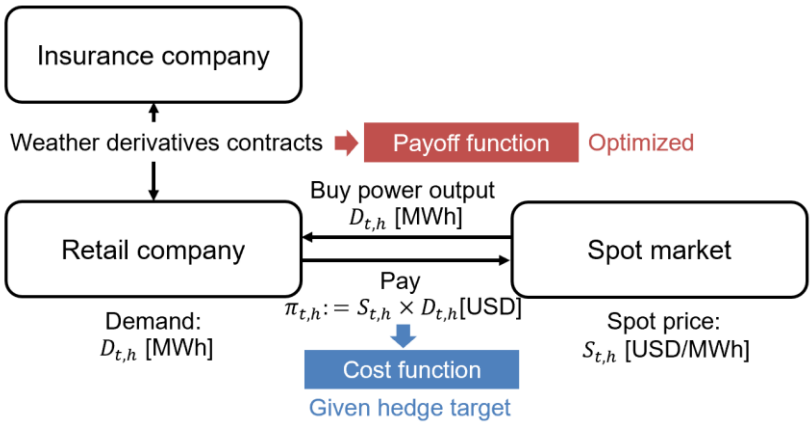

Figure 5.6: Simple market model for a retail company

5.3.1 Model Using Solar Radiation Futures

For the sales revenue of a solar power producer, we consider a prediction model using solar radiation (correlated to both electricity price and solar power output) and fuel price (linked to electricity price) as explanatory variables. Here, defining the wholesale electricity price hour h on

[38] Even non-standardized derivatives such as the former can be replicated with standardized derivatives with four payoff functions, such as European type call and put options, discount bonds, and underlying assets (if its payoff function is twice continuously differentiable) (Carr and Madan 2001). An approach to use only these products that can be liquidly traded is also conceivable, but such expansion is a future issue.

day t as $S_{t,h}$, the power output as $V_{t,h}$, the fuel price on date t as F_t, and the solar radiation prediction error[39] on date t obtained by subtracting the expected value (trend) from the measured value as $\varepsilon_{R,t} \coloneqq R_t - f_R(t)$, we consider expressing the solar power sales revenue $\pi_t := \sum_h S_{t,h} \times V_{t,h}$ as follows:

$$\pi_t = f(t) + \beta(t)F_t + \gamma(t)\varepsilon_{R,t} + \eta_t \tag{5.1}$$

where, $f(t), \beta(t)$, and $\gamma(t)$ are deterministic functions with respect to t, and η_t is the residual term with mean 0.

In this study, we estimate $f(t)$, $\beta(t)$, and $\gamma(t)$ as smoothing spline functions by applying a generalized additive model (GAM; Hastie and Tibshirani 1990) to (5.1); this corresponds to solving an optimization problem that minimizes the residual sum of squares $\sum_{t=1}^{N}\{\eta_t\}^2$ (i.e., sum of squared prediction error of π_t), subject to constraints on the smoothness of each spline function. Note that $\beta(t)$ and $\gamma(t)$ are given as forms of the product with F_t or $\varepsilon_{R,t}$, but can be obtained as a spline function with cross variables, and estimated by the same means as normal GAM.

If we consider GAM (5.1) as a hedge model, it can be interpreted as follows. First, F_t and $\varepsilon_{R,t}$ can be regarded as a payoff for fuel futures and solar radiation futures with expiration date t (note that as the unconditional expected value of $\varepsilon_{R,t}$ is 0, solar radiation futures can be treated as derivatives that do not require premium payment at the contract time), and the coefficients $\beta(t)$ and $\gamma(t)$ can be regarded as contract units of fuel futures and solar radiation futures, respectively. The point here is that solving GAM (5.1) corresponds to solving the following hedging problem (estimating the optimal functions) that minimizes the sample variance of the cash flow difference between the sales revenue and the derivatives (futures) payoff portfolios under the smoothing conditions of each spline function. That is, the residual term η_t in GAM (5.1) can be reinterpreted as the hedge error when the solar power producer hedges the sales revenue π_t using the above derivatives. Note that $f(t)$, which is a function that depends only on t, can be regarded as a payoff of discount bonds with date t as the expiration date.

[39] It is also conceivable to use the original series of solar radiation (instead of the prediction error) as an explanatory variable in the prediction equation. However, by using the prediction error, the trend term that depends only on t in the prediction equation is unified into the first term $f(t)$, which makes it easy to interpret the equation structure and handle it as the hedge model described later.

$$\min_{f(\cdot),\beta(\cdot),\gamma(\cdot)\in \boldsymbol{S}_\lambda} \mathrm{Var}\left[\pi_t - f(t) - \beta(t)F_t - \gamma(t)\varepsilon_{R,t}\right]. \tag{5.2}$$

where $\boldsymbol{S}_\lambda$ is set of smoothing spline function with smoothing parameter λ (see Section 4.2.2 for λ).

5.3.2 Model Using Temperature Derivatives

Next, we consider a prediction model for the retailer's procurement costs using fuel prices and temperatures as explanatory variables. For the model in the previous section since it was assumed that the solar power revenue had a roughly linear relationship with the amount of solar radiation, thus a linear model was constructed for the solar radiation prediction error. On the other hand, a non-linear relationship is assumed between the retailer's procurement costs, expressed as the product of electricity price and demand, and the temperature prediction error, as temperature has a very strong correlation to both electricity price and demand. Therefore, to estimate the procurement cost using the temperature prediction error $\varepsilon_{T,t} \coloneqq T_t - f_T(t)$ obtained by subtracting the time trend from the measured temperature, we can construct the following GAM by introducing a nonlinear function for $\varepsilon_{T,t}$ (note that in this paper, the hedged value such as the solar power revenue and the retailer's procurement cost are expressed as π_t without distinction):

$$\pi_t = f(t) + \beta(t)F_t + \psi\left(\varepsilon_{T,t}\right) + \eta_t \tag{5.3}$$

where $\psi\left(\varepsilon_{T,t}\right)$ is a spline function estimated by GAM, as with $f(t)$ and $\beta(t)$.

Here, as in the previous section, if the prediction model (5.3) is regarded as a hedge model, the estimated function $\psi\left(\varepsilon_{T,t}\right)$ can be rephrased as the optimal payoff function for the derivative with the temperature prediction error as the underlying asset. In addition, to estimate GAM (5.3) corresponds to solving the hedging problem that minimizes the sample variance of the cash flow difference between the procurement cost and the derivative portfolio payoff consisting of discounted bonds, fuel futures, and temperature derivatives under the smoothing conditions of each payoff function.

$$\min_{f(\cdot),\beta(\cdot),\psi(\cdot)\in \boldsymbol{S}_\lambda} \mathrm{Var}\left[\pi_t - f(t) - \beta(t)F_t - \psi\left(\varepsilon_{T,t}\right)\right] \text{ s.t. } \textstyle\sum_t \psi\left(\varepsilon_{T,t}\right) = 0. \tag{5.4}$$

Note that as this temperature derivative is assumed to be contracted with the insurance company directly (as mentioned in Section 5.3), if the retailer knows an optimal payoff structure by solving with the above optimization problem, then it may try to find an insurance company to offer such

an optimal payoff function. This is the reason why the retailer needs to solve the optimization problem over ψ (this concept is also applied to the temperature derivatives introduced in Section 5.3.3).

5.3.3 Extension of Derivatives Payoff to Bivariate Function

Tensor Product Spline Function

In the following, assuming that the derivatives payoff function $\psi(\varepsilon_{T,t})$ in (5.4) is not constant throughout the year but changes smoothly according to seasons, we set up the following optimal payoff function calculation problem:

$$\min_{f(\cdot),\beta(\cdot),\psi(\cdot)\in\mathcal{S}_\lambda} \mathrm{Var}\left[\pi_t - f(t) - \beta(t)F_t - \psi(t,\varepsilon_{T,t})\right] \text{ s.t. } \sum_t \psi(t,\varepsilon_{T,t}) = 0 \tag{5.5}$$

where the bivariate derivatives payoff function $\psi(t,\varepsilon_{T,t})$ is estimated as a tensor-product spline function that incorporates the different two-way smoothing conditions of the underlying asset price and seasonal direction simultaneously (e.g., see Matsumoto and Yamada (2019) for a more specific explanation in the context of applying the tensor-product spline function to hedging problems).

ANOVA Decomposition

As the function $\psi(t,\varepsilon_{T,t})$ mentioned above contains a trend related to the date t, and has overlapping degrees of freedom with $f(t)$, there is a problem in that it is difficult to grasp the structure as a hedging model. Therefore, in the following, we consider a method of separating the deterministic trend on t from the term $\psi(t,\varepsilon_{T,t})$ by applying ANOVA decomposition (Efron and Stein 1981). When ANOVA decomposition is applied to the function $\psi(t,\varepsilon_{T,t})$, the following equation is obtained:

$$\psi(t,\varepsilon_{T,t}) = \psi_t(t) + \psi_\epsilon(\varepsilon_{T,t}) + \psi_{t\epsilon}(t,\varepsilon_{T,t}). \tag{5.6}$$

Here, each term on the right side of (5.6) can be found as a function with zero mean. The univariate spline functions $\psi_t(t)$ and $\psi_\epsilon(\varepsilon_{T,t})$ are called "main effects," and correspond to the trends in which the date or weather index contributes independently to the original tensor-product spline functions. Alternatively, the bivariate spline function $\psi_{t\epsilon}(t,\varepsilon_{T,t})$ is called the "interactions effect" and corresponds to the interaction trend of date and weather index, which is obtained by removing

the main effects from the original tensor product spline function. At this time, the function $\tilde{\psi}(t, \varepsilon_{T,t}) := \psi_{\epsilon}(\varepsilon_{T,t}) + \psi_{t\epsilon}(t, \varepsilon_{T,t})$ is obtained as a derivative payoff function in which the yearly cyclical deterministic trend is removed from the original tensor-product spline function. When this derivative is used, the objective function part of (5.5) is corrected to the following minimum variance problem:[40]

$$\min_{\tilde{f}(\cdot),\beta(\cdot),\tilde{\psi}(\cdot)\in\mathcal{S}_{\lambda}} \mathrm{Var}\left[\pi_t - \tilde{f}(t) - \beta(t)F_t - \tilde{\psi}(t, \varepsilon_{T,t})\right] \tag{5.7}$$

where, $\tilde{f}(t)$, $\beta(t)$ and $\tilde{\psi}(t, \varepsilon_{T,t})$ are the contract unit of discount bonds, fuel futures, and temperature derivatives payoff, respectively.

By using ANOVA decomposition, it is possible to estimate multiple different tensor-product spline functions with the same explanatory variables (date t in this case) uniquely and simultaneously (detailed in Section 5.4.3). Furthermore, owing to the property of the ANOVA decomposition, the temperature derivative payoff in (5.7) is calculated such that its expected value is zero for each t. In other words, such as futures, the derivatives here also can be treated as that which does not require a premium payment at the contract time. Note that a series of properties of the ANOVA decomposition is based on the precondition that the explanatory variables (of tensor product function) are independent of each other. Regarding this point, the prediction errors $\varepsilon_{T,t}$ for each t can be considered to have approximately the same probability distributions with a mean of 0 (i.e., as independent trials on each t); therefore, the assumption of the independence condition has a certain rationality.

5.4 Construction of Hedging Models

In this section, based on the background theory explained in Section 5.3, we build several specific hedging models to deal with the empirical analysis in Section 5.5.

5.4.1 Hedging Model Consisting of Fuel Price and Calendar Trend

First, considering only that electricity prices are linked to fuel prices and calendar trends, we

[40] In the R package "mgcv," such ANOVA decompositions can be calculated by using the "ti" term in the function "gam ()" (Wood 2019). In the calculation using the "ti" term, the estimation can be performed as in the case of a linear model by imposing a constraint that does not include the main effect term in the interaction effect of the tensor product spline function (Wood 2017).

construct the following GAM and call it "base model":

$$\pi_t = f(t) + \beta(t)F_t + \eta_t$$
$$\text{s.t.} \begin{cases} \beta(t) := \beta_O(t) + \beta_P(t)Period_t \\ f(t) := f_O(t) + f_H(t)I_{H,t} + f_P(t)Period_t \end{cases} \tag{5.8}$$

where π_t is sales revenue (in this case we especially write it as $\pi_{1,t}$) or procurement cost ($\pi_{2,t}$) at date t,: $= \sum_h S_{t,h} \times \beta(t)$ is the variable coefficient of fuel futures F_t, $f(t)$ is a calendar trend (the contract unit of discount bonds), and η_t is the residual term with an average of 0. f and β are yearly cyclical trends estimated as spline functions by the GAM (as univariate functions $f(Seasonal_t)$ and $\beta(Seasonal_t)$ with yearly cyclical dummy variables $Seasonal_t$ $(= 1, \dots, 365(or\ 366))$ proposed by Yamada et al. (2015), but denote them as $f(t)$ and $\beta(t)$ for concise notation), $I_{H,t}$ is a dummy variable that is 1 if the day is Saturday, Sunday, or holiday, and 0 otherwise; $Period_t$ is the number of days elapsed (annualized) from the beginning of the data starting year. Of these, the terms $\beta_P(t)Period_t$ and $f_P(t)Period_t$ are introduced assuming that the calendar trend and the sensitivity of π_t to F_t have yearly cyclical trends even when viewed at the rate of annual change (detailed in the Appendix section 5.7.1). $f_P(t)$ and $\beta_P(t)$, which refer to the cyclical trend of the annual change rate, can be obtained as a spline function with cross variables.

5.4.2 Hedging Model Using Solar Radiation Futures

Next, assuming the case where solar radiation futures can be used to hedge the fluctuation risk of the solar power business in JEPX, we consider the following hedging model:

$$\pi_{1,t} = f(t) + \beta(t)F_t + \gamma_1(t)\varepsilon_{R,t} + \eta_t \tag{5.9}$$

where $\varepsilon_{R,t}$ is the solar futures payoff (solar prediction error) on date t, and $\gamma_1(t)$ is the yearly cyclical trend of the solar futures' contract volume (note that this equation corresponds to the reused of (5.1), but γ_1 is used instead of γ to distinguish it from the term introduced in the next equation).

In addition, as shown in Section 5.2.1, due to an increase in solar power generation, the sensitivity of power sales revenue to the solar radiation prediction error (i.e., contract volume of solar futures) is assumed to have a yearly cyclical annual change rate. Considering this point, the following model can be constructed:

$$\pi_{1,t} = f(t) + \beta(t)F_t + \gamma_1(t)\varepsilon_{R,t} + \gamma_2(t)l(Period_t)\varepsilon_{R,t} + \eta_t \tag{5.10}$$

where $\gamma_2(t)$ is the yearly cyclical trend, and $\gamma_1(t) + \gamma_2(t)l(Period_t)$ corresponds to the solar futures contract volume. Here, among the fourth term, we define $l(Period_t)$ in advance as $1 - exp[-Period_t]$ a nonlinear annual change trend function (a monotonically increasing decay function).[41]

5.4.3 Hedging Model Using Temperature Derivatives

Similarly, a hedging model using temperature derivatives is as follows[42]:

$$\pi_{2,t} = f(t) + \beta(t)F_t + \tilde{\psi}(t, \varepsilon_{T,t}) + \eta_t \tag{5.11}$$

where $\varepsilon_{T,t}$ is the temperature prediction error on date t and $\tilde{\psi}(t, \varepsilon_{T,t})$ is the payoff function of a temperature derivative estimated as a tensor-product spline function from which a deterministic yearly cyclical trend has been removed by ANOVA decomposition as described in Section 5.3.3.

When multiple derivatives such as the maximum and minimum temperatures are used together, the following model can be considered:

$$\pi_{2,t} = f(t) + \beta(t)F_t + \widetilde{\psi_1}(t, \varepsilon_{Tmin,t}) + \widetilde{\psi_2}(t, \varepsilon_{Tmax,t}) + \eta_t. \tag{5.12}$$

The point here is that each payoff function can be uniquely estimated because the trend dependent on t the existing in the model is unified into the identical term $f(t)$.

5.4.4 Hedging Model Using Temperature Derivatives on Squared Prediction Error

The temperature derivatives payoff in equation (5.11) are differently estimated by each hedger (i.e., depending on each hedger's profit/loss), but in the following, we consider introducing a standardized temperature derivatives that can be commonly used by multiple hedgers (i.e., independent of individual hedgers profit/loss). Here, the payoff $\tilde{\psi}(t, \varepsilon_{T,t})$ is a smooth nonlinear function of $\varepsilon_{T,t}$ when viewed on a specific date; therefore, from the idea of approximating it with

[41] As a possible trend function that attenuates with such a monotonic increase, the logarithmic function or power function can also be considered. However, in this work, we do not go into the method of selecting or estimating such function type, and we use $1 - exp[-Period_t]$ as a representative and simple equation that converges to 1 and passes through 0.

[42] Although temperature derivatives are also used for hedging solar power revenue $\pi_{1,t}$, the hedged target here is denoted as retailer's procurement costs $\pi_{2,t}$ for convenience.

a quadratic function, we introduce a derivative on the temperature squared prediction error and consider the following model:

$$\pi_{2,t} = f(t) + \beta(t)F_t + k(t)\varepsilon_{T,t} + \tau(t)\left({\varepsilon_{T,t}}^2 - \overline{{\varepsilon_{T,t}}^2}\right) + \eta_t \tag{5.13}$$

where ${\varepsilon_{T,t}}^2 - \overline{{\varepsilon_{T,t}}^2}$ is the payoff of the squared prediction error derivative of temperature ($\overline{{\varepsilon_{T,t}}^2}$ is the predicted value (expected value) of ${\varepsilon_{T,t}}^2$), and $k(t)$ and $\tau(t)$ are contract volumes of temperature futures and squared prediction error derivatives, respectively, both of which are estimated as the smoothing spline functions (contract amount of the derivatives) by GAM (5.13). This temperature squared error derivative also has zero expected payoff for each t, and does not require a premium payment like other derivatives or futures already introduced. Note that because the seasonality is not assumed to exist for the squared prediction error ${\varepsilon_{T,t}}^2$, the expected value $\overline{{\varepsilon_{T,t}}^2}$ can be calculated as being equal to the average value of the entire sample.

5.5 Empirical Analysis

In this section, using two different markets models, such as the revenue fluctuation risk of a solar power company that sells generated power at the JEPX market ("JEPX model") and cost fluctuation risk of a retailer that procures electricity at the PJM market ("PJM model"), we estimate the trends of the derivative payoff functions (or derivatives contract amounts) and measure the hedge effects. Here, we define the variance reduction rate (VRR) as follows and call 1-VRR the "hedge effect":

$$\text{VRR:} = \frac{\text{Var[hedge error of the target model]}}{\text{Var[hedge error of the base model]}}. \tag{5.14}$$

5.5.1 Empirical Analysis of the JEPX Model

In this section, we conduct an empirical analysis on the JEPX model using actual data as follows:

(a) Electricity spot price $S_{t,h}$ [JPY/kWh]: JEPX area price of Chugoku, where Hiroshima City is located[43]

(b) Solar power output volume $V_{t,h}$ [kWh]: measured value of the household's solar power

[43] Downloaded from http://www.jepx.org/market/index.html.

system in Hiroshima City[44]

(c) Daily integrated solar radiation $R_t[\mathrm{J/m^2}]$, Daily maximum temperature $Tmax_t$ [℃]: realized value of Hiroshima City published by the Japan Meteorological Agency[45]

(d) WTI crude oil price WTI_t [thousand JPY/bbl]: historical monthly WTI spot price FOB[46]

Note that for the hedge models constructed in Section 5.4, sales revenue $\pi_{1,t}$ is calculated as $\pi_{1,t} := \sum_h S_{t,h} \times V_{t,h}$, F_t corresponds to WTI_t, and $\beta(t)$ is set as a constant value (i.e., $\beta(t) := \beta$) to ensure robustness. The model parameters and functions are estimated from the data of the in-sample period (Jan. 1, 2013–Dec. 31, 2017), and the hedge effect of derivatives is calculated by the data using the out-of-sample period (Jan. 1, 2018–Dec. 31, 2018).

5.5.1.1 Trend Estimation of the JEPX Model

Solar radiation futures

First, we consider the estimation results of model (5.10) on solar radiation futures. The left side of Figure 5.7 shows a composite (weekday) calendar trend $f_O(t) + f_P(t)Period_t$ (displayed range of $seasonal$ axis is from January 1 to December 31). In 2013, the peak power sales revenue was around May; however, the peak in 2017 has moved to around August because an increase in solar power facilities has led the JEPX price to decline, particularly in May, when the amount of solar radiation increased in the year. Next, the estimation result of the solar radiation future contract amount $\gamma_1(t) + \gamma_2(t)l(Period_t)$ is illustrated on the right side of Figure 5.7. This trend corresponds to the sensitivity of power sales revenue to the solar radiation prediction error. As this estimated result shows, the rate of annual change varies greatly depending on the season.

---

[44] With the permission of the owner, we use the data of the private roof-mounted power system in Hiroshima City.

[45] Downloaded from https://www.data.jma.go.jp/gmd/risk/obsdl. Note that considering the correlation with the JEPX Chugoku area price, the maximum temperature data is created by averaging the temperatures in Nagoya City, Osaka City, and Hiroshima City by weighting the total prefecture population in which each city is located.

[46] Downloaded from https://www.eia.gov/dnav/pet/hist/RWTCD.htm. Note that it is converted into JPY using the past exchange rate published by the Bank of Japan (downloaded from https://www.stat-search.boj.or.jp/). Yen-denominated WTI futures are not traded, but they can be replicated in conjunction with foreign exchange futures. Also, we use WTI_t as the WTI spot price in the month previous to the month to which the date t belongs, considering the one-month lag as confirmed in Section 5.2.1.

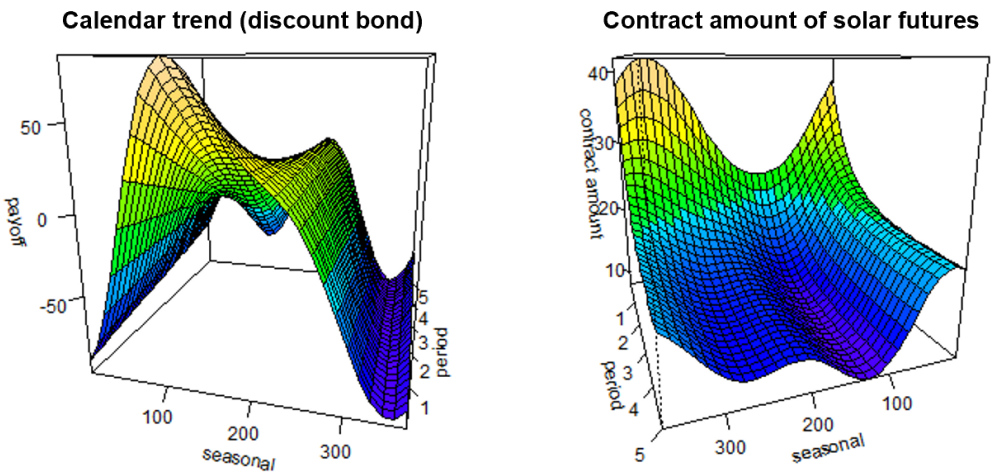

Figure 5.7: Estimated calendar trend (left) and contract amount of solar futures (right) in (5.10)

Temperature derivatives

Figure 5.8 shows the estimated result of the temperature derivative payoff function $\tilde{\tau}(t, \varepsilon_{Tmax,t})$, which is defined as a tensor-product spline function using ANOVA decomposition in the model (5.11). It has been confirmed that the sensitivity (slope) of solar power revenue to the temperature prediction error significantly increases in summer. The reason is thought to be because the rise in temperature in summer affects both the increases in power output and price (due to an increase in power demand). On the other hand, in winter, the sensitivity of the temperature prediction error is an inverse U-shaped curve, indicating that the power sales revenue decreases if the temperature rises or falls from the normal value level. It can be interpreted that as the temperature in winter has a negative (linear) relationship with electricity price and a positive (linear) relationship with solar power output, the sales price, which is expressed as the product of price and power output, would have a parabolic-like shape that is convex upward. In addition, looking at the contour graph together with the perspective graph, it can be seen that the payoff when the temperature prediction error is 0 becomes positive in the winter season (when the payoff is convex upward) and is a negative value in the summer season (when the payoff is convex downward); this reflects the deterministic seasonal trend, which has been removed by the ANOVA decomposition method.

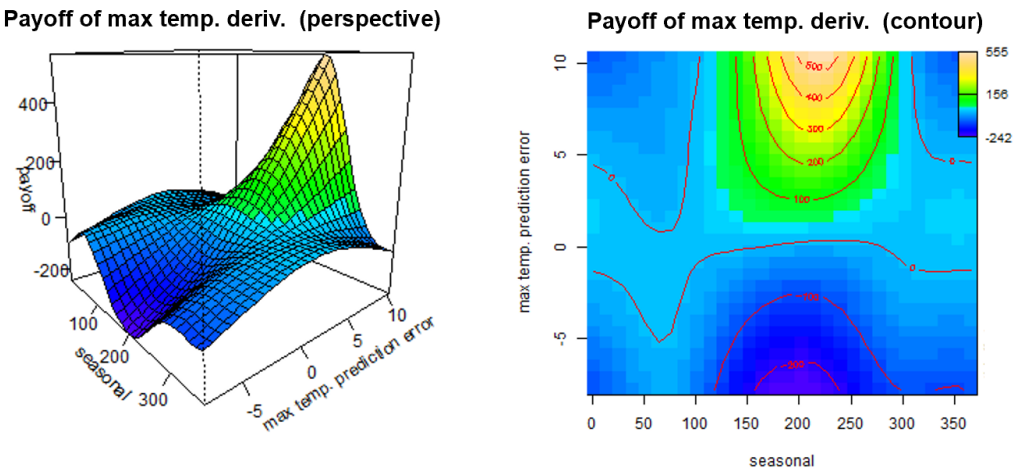

Figure 5.8: Payoff function for temperature derivatives in model (5.11)

Model using solar futures and temperature derivatives

Here, we show the estimation results of a model using both solar radiation futures and temperature derivatives in combination[47]. The estimation result of the contract amount of solar radiation futures is demonstrated in the left side of Figure 5.9, and the estimation result of the payoff of temperature derivatives is provided on the right side. First, the solar futures contract in this model (left side of Figure 5.9) is lower in summer than in the case using only solar futures (the right side of Figure 5.7). On the other hand, the payoff level for temperature derivatives (right side of Figure 5.9) is closer to 0 in summer (especially where the temperature prediction error is around 0) compared with the case using only temperature derivatives (Figure 5.8). The reasons are as follows: As both prediction errors on solar radiation and temperature are incorporated in the model, their contributions to sales revenue are shared, especially in the summer when both have strong positive correlations with sales revenue, which led to a decrease in the sensitivity of each variable compared to the single-use case.

[47] The model formula is the combination of (5.10) and (5.11) and is written as follows: $\pi_t = f(t) + \beta(t)F_t + \gamma_1(t)\varepsilon_{R,t} + \gamma_2(t)l(Period_t)\varepsilon_{R,t} + \tilde{\psi}(t, \varepsilon_{T,t}) + \eta_t$.

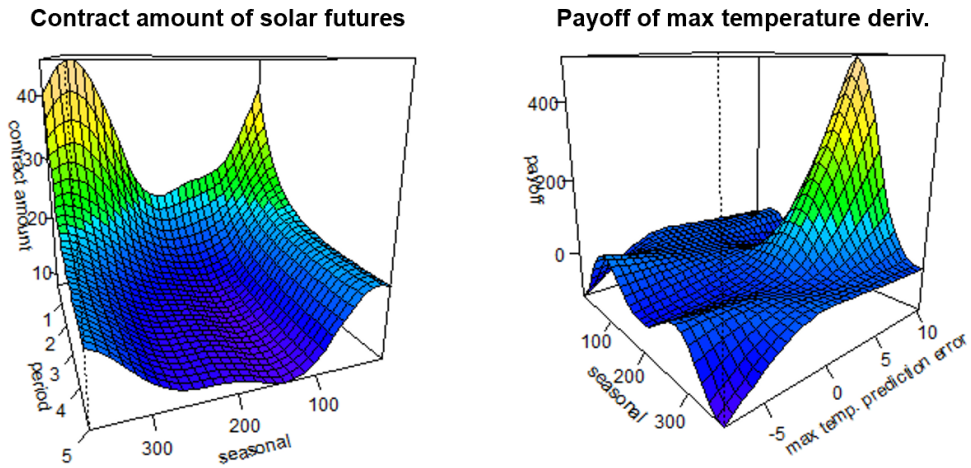

Figure 5.9: Estimated contract amount of solar futures and payoff of temperature derivatives when used together

5.5.1.2 Measurement of Hedge Effects on the JEPX Model

Next, using the parameters and functions estimated from the in-sample period data, we calculate the hedge effect during the out-of-sample period (from January 1, 2018 to December 31, 2018).

Cumulative hedge effect

Here, we analyze changes in hedge effects when each derivative (hedge model term) is combined cumulatively. Figure 5.10 shows the contribution ratio[48] when each derivative is used alone (bar graph), the cumulative contribution ratio when the terms are combined in order from the left (blue line graph), and the cumulative hedging effect of the weather derivatives compared to the base model (red line graph). The corresponding derivatives (terms) are provided in Table 5.1.

First, it was confirmed that the highest two contribution ratios are solar derivatives and temperature derivatives. The contribution ratio of solar derivatives is highest in both the in-sample period and the out-of-sample period because fluctuations in solar radiation directly correlate with fluctuations in solar power output. The reason that the contribution ratio of the temperature derivative improved significantly during the out-of-sample period, although it was low during the in-sample period is considered as follows. That is, during the out-of-sample period (2018), the JEPX price fluctuated greatly because of the severe cold winter and intense heat summer, but temperature derivatives were able to effectively follow these changes. Note that the reason why the

[48] The contribution ratio here is defined as follows: "contribution ratio": $= 1 - \frac{\mathrm{Var[hedge\ error\ of\ the\ target\ model\ ]}}{\mathrm{Var[hedge\ target;}\ \pi_{1,t}\ \mathrm{or}\ \pi_{2,t}]}$.

contribution ratio of WTI is small in the out-of-sample period is because the crude oil price did not fluctuate in the period. Next, looking at the cumulative contribution ratio, a significant improvement was observed by adding yearly cyclical trends of annual change to the calendar trend or the solar radiation future contract amount. The former is improved by 7% (from 0.130 to 0.204) and the latter by 4% (from 0.587 to 0.631). In addition, the cumulative contribution ratio increased monotonously with the inclusion of each term (even for the out-of-sample period) and reached 0.687 when all were combined.

Finally, the cumulative hedging effect of the solar radiation derivatives was 0.517, which improved to 0.588 when combined with the temperature derivatives. Although not shown in the figure, even when using only temperature derivatives, a sufficient cross-hedging effect of 0.300 was obtained. As for the hedging related to temperature, it is interesting that the hedging effect is greatly improved by using derivatives given by nonlinear payoff functions instead of using futures with a linear payoff function. Compared to the hedging effect when using only solar radiation derivatives (0.517), there was an improvement of 3% when combined with temperature futures (0.546) and an improvement of 7% when combined with temperature derivatives (0.588).

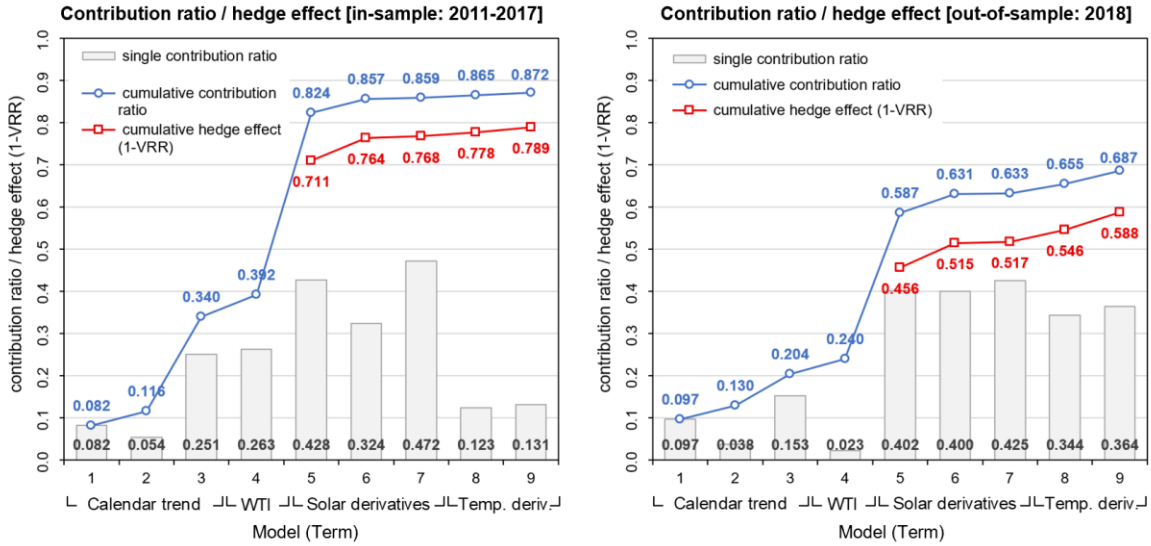

Figure 5.10: Cumulative contribution ratio and hedging effect of derivatives in JEPX model

Table 5.1: Correspondence of terms included in each model in Figure 5.10

Model No.	Term			Included terms of cumulative model								
				1	2	3	4	5	6	7	8	9
1	Calendar trend (discount bond)	Yearly cyclical trend (base trend)	$f_O(t)$	●	○	○	○	○	○	○	○	○
2		Yearly cyclical holiday effect	$f_H(t)I_{H,t}$		●	○	○	○	○	○	○	○
3		Yearly cyclical annual change	$f_P(t)Period_t$			●	○	○	○	○	○	○
4	WTI	WTI	$\beta \cdot WTI_t$				●	○	○	○	○	○
5	Solar Derivatives	Solar futures	$\gamma_1(t)\varepsilon_{R,t}$					●	○			
6		Solar futures (annual change)	$\gamma_2(t)l(Period_t)\varepsilon_{R,t}$						●	○	○	○
7		Solar derivatives	$\tilde{\varphi}(t, \varepsilon_{R,t})$							●	○	○
8	Temp. Derivatives	Max temp. futures	$k(t)\varepsilon_{Tmax,t}$								●	
9		Max temp. derivatives	$\tilde{\psi}(t, \varepsilon_{Tmax,t})$									●

* The bar graph on Figure 5.10 shows the individual contribution ratio of the hedge model using only the black circled term. The line graph shows the cumulative contribution ratio / hedge effect of the hedging model with all black and white circle terms included.

Monthly hedge effect

Next, the hedging effects of solar radiation and temperature derivatives are calculated by month. Figure 5.11 shows monthly 1-VRRs when using solar derivatives, temperature derivatives, and both solar and temperature derivatives.[49]

For solar derivatives, a high hedging effect is confirmed throughout the year for both the in-sample period and the out-of-sample period. In particular, there is a tendency for the hedging effect to be higher in spring and autumn when demand fluctuations are mild and extreme price spikes are unlikely to occur. For the out-of-sample period, the hedging effect in January, February, and July and August is significantly lower than that of the in-sample period, indicating that solar derivatives are not very effective against price spikes in severe winter and intense heat summer in the out-of-sample period.

Regarding the temperature derivative, it is confirmed that the hedge effect is higher (and further improved when combined with the solar derivative) around July and August, and the reason for this is as follows. In summer, when the temperature rises, both the electricity price and the power generation output increase, and the correlation between power sales revenue and temperature increases synergistically. On the other hand, the reason for the low hedge effect in other seasons is that the rise in temperature leads to not only increasing power output but also lowering electricity prices; thus, it has little effect on the power sales revenue by offsetting both effects. Based on this,

[49] For each case, 1-VRR is calculated by constructing a hedge model that combines the following items (numbers are shown in Table 5.1) with the base model: the solar derivatives model include No. 6-7, the temperature derivatives model include No. 9, and the combination model include No. 6-7 and 9.

a strategy for using temperature derivatives only in July and August is effective for solar power producers.

In addition, Figure 5.12 compares the realized value of electricity sales revenue (black line) and the predicted value, that is, the estimated derivatives payoff (red line) when solar radiation and temperature derivatives are used together. Except during the period when prices fluctuate, it can be confirmed that they can follow relatively daily fluctuations.

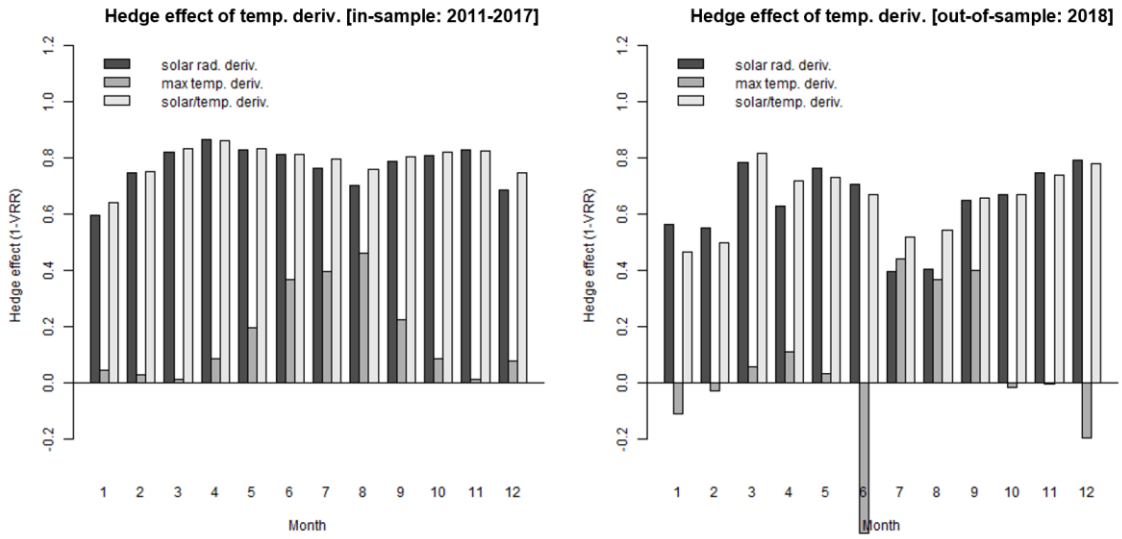

Figure 5.11: Monthly hedging effect of solar radiation and temperature derivatives in JEPX model

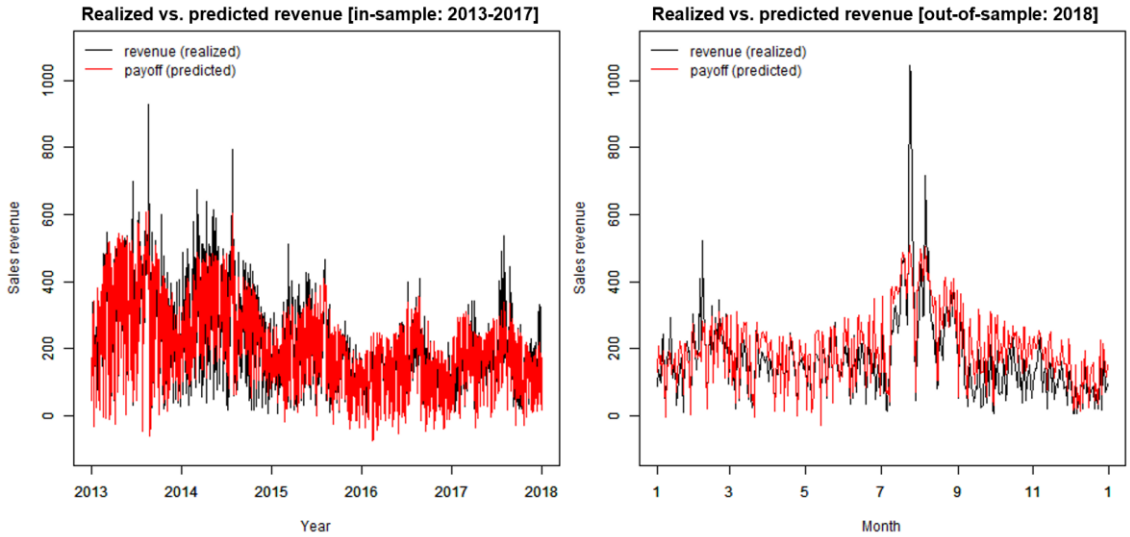

Figure 5.12: Comparison of realized and predicted sales revenue in JEPX model

5.5.2 Empirical Analysis of the PJM Model

In this section, we perform an empirical analysis on the PJM model using the following data:

(a) Demand $D_{t,h}$ [MWh]: entire PJM-RTO hourly load[50]

(b) Electricity spot price $S_{t,h}$[USD/MWh]: day-ahead hourly price of PJM-RTO[51]

(c) Maximum and minimum temperature $Tmax_t, Tmin_t$: Population weighted average of four main cities (Philadelphia, Pittsburgh, Baltimore, and Newark) published by the National Oceanic and Atmospheric Administration (NOAA)[52]

(d) Henry Hub natural gas price HH_t [USD/Million Btu]: Historical daily HH spot price FOB[53]

Note that for the hedge model constructed in Section 5.4, the procurement cost $\pi_{2,t}$ is calculated as $\pi_{2,t} := \sum_h S_{t,h} \times D_{t,h}$, F_t corresponding to HH_t. The model parameters and functions are estimated from the data of the in-sample period (Jan. 1, 2011–Dec. 31, 2017), and the hedge effect of derivatives is calculated by the data using the out-of-sample period (Jan. 1, 2018–Dec. 31, 2018).

5.5.2.1 Trend Estimation of the PJM Model

Calendar trend and contract amount of Henry Hub

First, we review the estimated results of the calendar trend and contract amount of HH. The left side of Figure 5.13 shows a composite calendar trend $f_O(t) + f_P(t)Period_t$, and the right side demonstrates HH's contract amount $\beta(t)$ of model (5.12). The contract amount of HH futures $\beta(t)$, which indicates the sensitivity of the HH price to the retailer's procurement cost and corresponds to (the product of demand and) the "market heat rate"[54] of the natural gas, is getting significantly higher in winter year by year. It is thought that the recent decline (abolition) of coal power, as shown in Figure 5.4 results in an increased heat rate in the winter when demand becomes particularly high. On the other hand, the calendar trend, which means the hedge residual of HH,

[50] Downloaded from http://dataminer2.pjm.com/feed/hrl_load_metered.

[51] Downloaded from http://dataminer2.pjm.com/feed/da_hrl_lmps.

[52] Downloaded from https://www.ncdc.noaa.gov/cdo-web/search.

[53] Downloaded from https://www.eia.gov/dnav/ng/hist/rngwhhdd.htm.

[54] Market heat rate is obtained as electricity price divided by fuel price and corresponds to the inverse efficiency of the thermal plant.

has a trend opposite to that of the HH contract trend, which can be interpreted by imaging the simple linear regression for HH, where the intercept becomes smaller as the slope (HH's sensitivity) becomes larger.

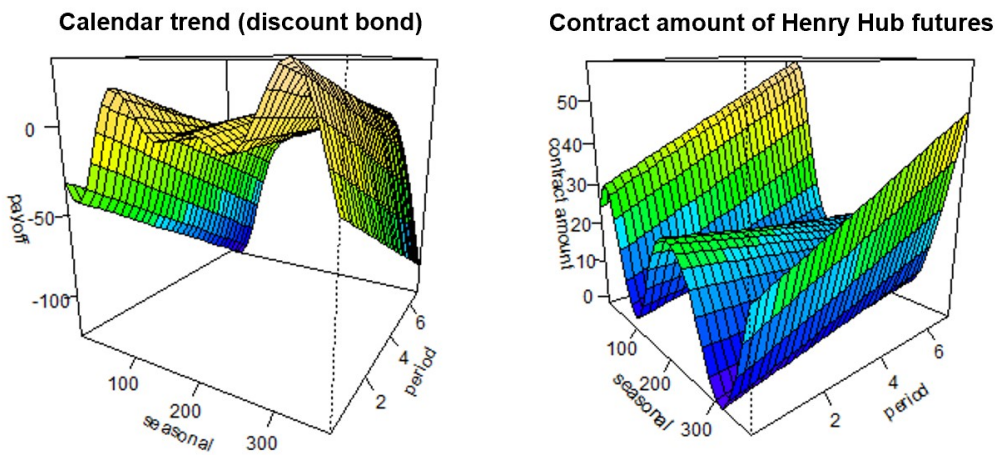

Figure 5.13: Estimated calendar trend (left) and contract amount of HH futures (right) in model (5.12)

Temperature derivatives

Figure 5.14 shows the min/max temperature derivative payoff functions $\widetilde{\psi_1}(t, \varepsilon_{Tmin,t})$, $\widetilde{\psi_2}(t, \varepsilon_{Tmax,t})$ which are simultaneously estimated as a tensor-product spline function using ANOVA decomposition in model (5.12). In both, it can be confirmed that the trends in the seasonal direction are removed from them (having such shapes with zero means at each time t) by using the ANOVA decomposition. In addition, the derivative payoff (whose slope corresponds to the sensitivity of the temperature prediction error to the procurement cost) of the minimum temperature is specifically increased as the temperature drops in winter, whereas that of maximum temperature increases as the temperature rises in summer; this reflects that both distinctive effects complement each other.

Figure 5.15 illustrates the estimated results of the contract amount trends of the squared prediction error derivatives of the min/max temperatures (note that they are corresponding to $\tau(t)$ in (5.13), and dotted lines denote the 95% confidence intervals). They can be rephrased as seasonal trends that reflect the magnitude of the downward convexities of derivative payoff functions at each date. Both trends rise in summer and winter, but they also reflect the difference that the nonlinearity of the minimum temperature's sensitivity to procurement cost increases, particularly

in winter, compared to that of the maximum temperature, which particularly rises in summer.

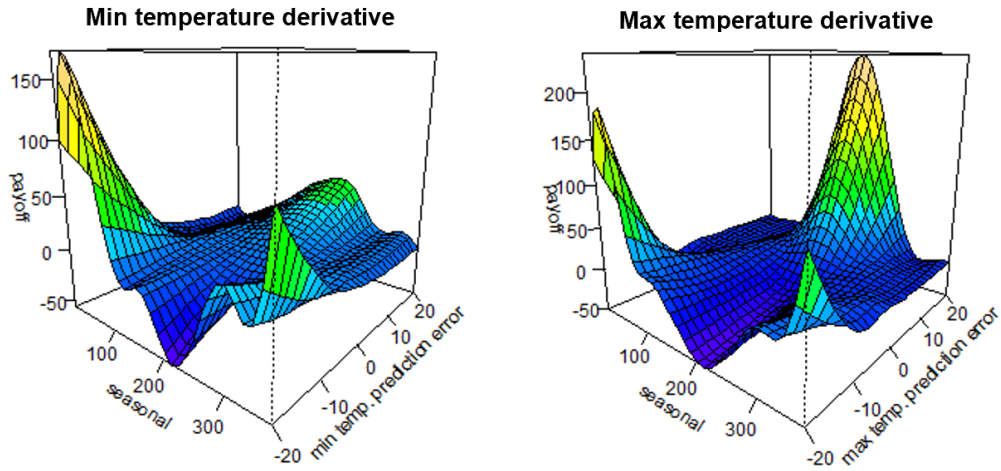

Figure 5.14: Estimated payoff of minimum (left) and maximum (right) temperature derivatives in model (5.12)

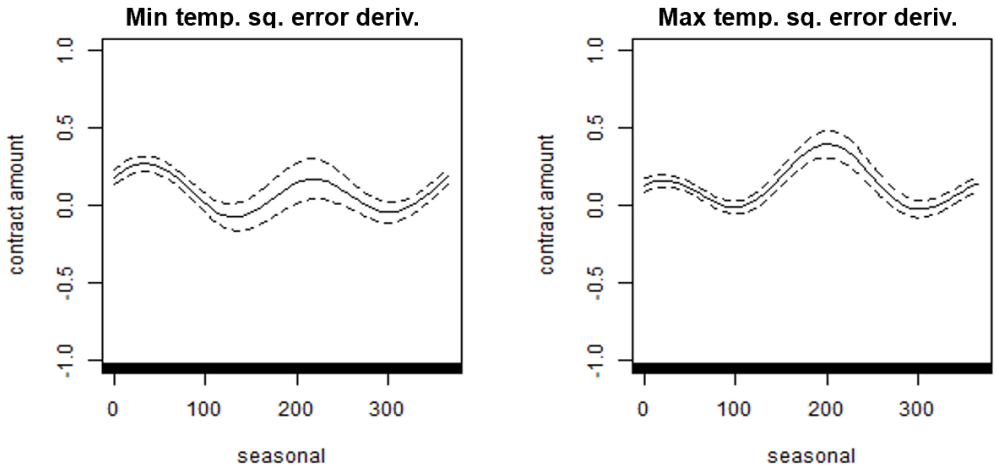

Figure 5.15: Estimated contract amount of minimum (left) and maximum (right) temperature squared error derivatives in model (5.13)

5.5.2.2 Measurement of Hedging Effects on the PJM Model

Cumulative hedge effect

Next, we analyze the cumulative contribution ratio and hedge effects expressed in Figure 5.16 and Table 5.2. First, the single contribution ratios are high in the order of the temperature derivatives, the HH futures, and the calendar trend. It is noteworthy that the temperature derivative alone has a significant contribution ratio of more than 62% in the out-of-sample period. The cumulative

contribution ratio increases monotonously with the inclusion of each term, even in the out-of-sample case, and reached approximately 76% when all derivatives were combined. It can also be confirmed that both the calendar trend and HH have improved the contribution ratio, albeit slightly, by incorporating the cyclical annual change trend. Finally, with regard to the cumulative hedge effect, it is remarkable that the effect is further improved by about 4.3%, when the maximum temperature derivative is used in combination with the minimum temperature derivative alone (from 0.238 to 0.281). Furthermore, compared to the case using only temperature futures, the combined use of squared error temperature derivatives further improved the hedging effect by approximately 27% (almost twice from 0.281 to 0.555), and about 6.6% more improvements when using derivatives of tensor-product spline functions. This result reflects the strong non-linear correlation between temperatures and procurement costs (i.e., the product of electricity price and demand) in the PJM market. Note that the reason why the out-of-sample has a higher cumulative contribution ratio and hedging effect than the in-sample period is that in-sample data include an extreme price spikes in January 2014, when "PJM experienced tight operational conditions and a significantly higher number of forced generator outages due to the extreme weather" (PJM 2014), which is also shown in the daily cost fluctuation graph provided in Figure 5.18.

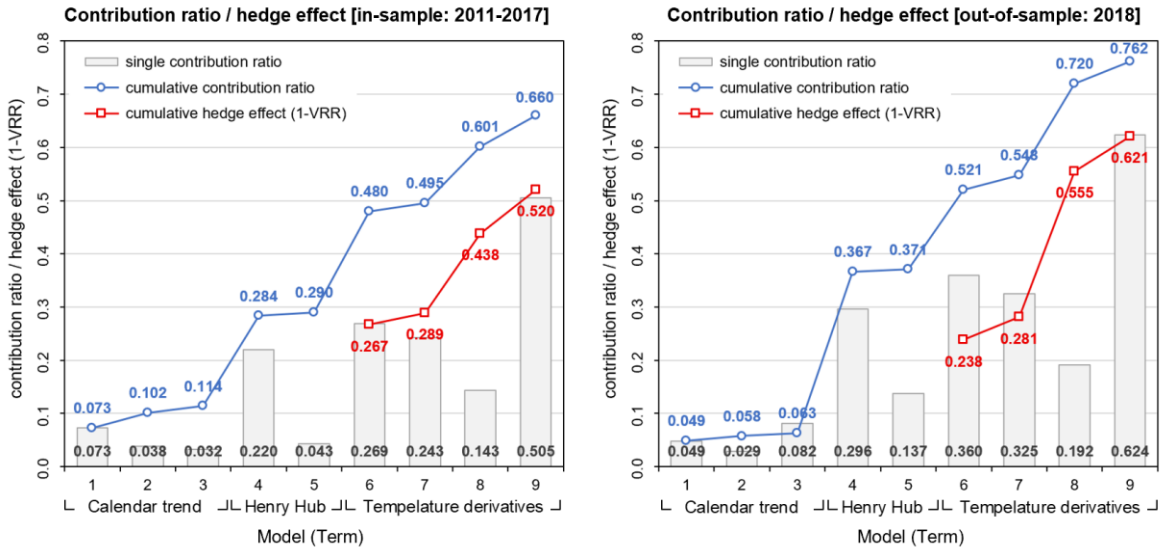

Figure 5.16: Cumulative contribution ratio and hedging effect of derivatives in PJM model

Table 5.2: Correspondence of terms included in each model in Figure 5.16

Model No.	Term			Included terms of cumulative model								
				1	2	3	4	5	6	7	8	9
1	Calendar trend (discount bond)	Yearly cyclical trend (base trend)	$f_O(t)$	●	○	○	○	○	○	○	○	○
2		Yearly cyclical holiday effect	$f_H(t)I_{H,t}$		●	○	○	○	○	○	○	○
3		Yearly cyclical annual change	$f_P(t)Period_t$			●	○	○	○	○	○	○
4	Henry Hub	Henry Hub	$\beta_O(t)HH_t$				●	○	○	○	○	○
5		Henry Hub (annual change)	$\beta_P(t)Period_tHH_t$					●	○	○	○	○
6	Temp. Derivatives	Min temp. futures	$\gamma_1(t)\varepsilon_{Tmin,t}$						●	○	○	
7		Max temp. futures	$\gamma_2(t)\varepsilon_{Tmax,t}$							●	○	
8		Min & Max temp. derivatives (squared prediction error)	$\tau_1(t)\left({\varepsilon_{Tmin,t}}^2 - \overline{{\varepsilon_{Tmin,t}}^2}\right) + \tau_2(t)\left({\varepsilon_{Tmax,t}}^2 - \overline{{\varepsilon_{Tmax,t}}^2}\right)$								●	
9		Min & Max temp. derivatives (tensor product spline)	$\widetilde{\psi_1}(t, \varepsilon_{Tmin,t}) + \widetilde{\psi_2}(t, \varepsilon_{Tmax,t})$									●

* See the note below Table 5.1 for the meaning of symbols.

Monthly hedge effect

Next, Figure 5.17 shows the monthly hedging effect (1-VRR) by the minimum and maximum temperature derivatives (estimated by the tensor-product spline function) displayed by month. For both in-sample and out-of-sample cases, the hedging effect is, for many months, highest when the two derivatives are used together. Particularly in summer (around June–August), the hedge effect of the maximum temperature derivatives is higher than that of the minimum ones, and the opposite tendency is seen in late winter (around March), which can be understood that each payoff function has an extremely large slope, Figure 5.14 shows. On the other hand, the hedging effect tends to decrease in spring and autumn (around April and November), when the demand for cooling and heating is decreased and the sensitivities of temperatures to electricity demand and price become low, which is also consistent with the small slope of the payoff functions in these seasons, as seen in Figure 5.14. However, overall, the two different temperatures complement each other's effects throughout the seasons.

Finally, Figure 5.18 compares the observed procurement cost (black line) and the estimated payoff of the derivative portfolio (red line) when using all derivatives. It can be confirmed that the derivatives' payoffs largely follow daily fluctuations, even during periods when significant price fluctuations occur, such as summer and winter.

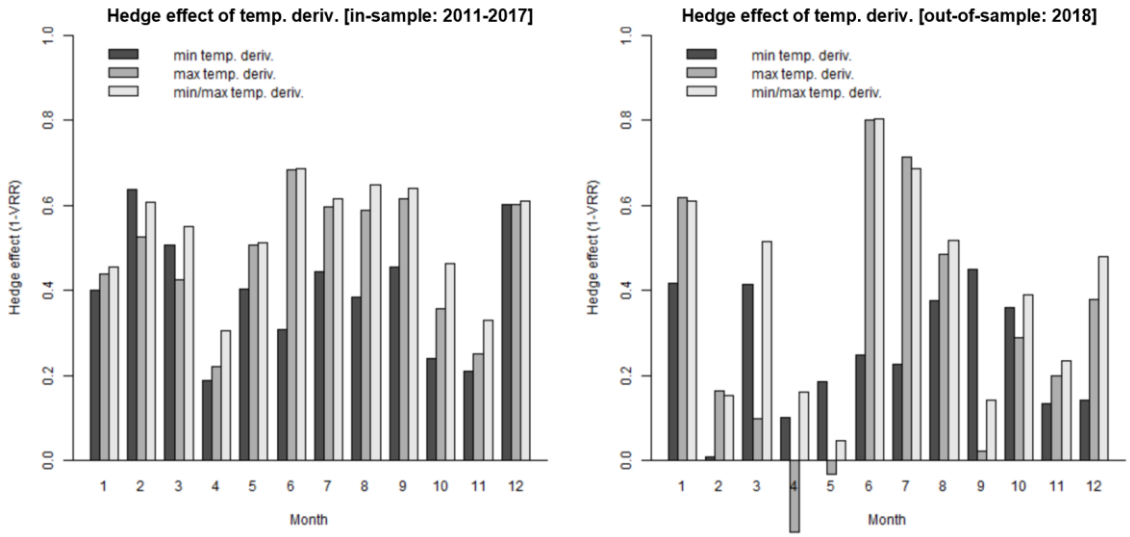

Figure 5.17: Monthly hedging effect min/max temperature derivatives in PJM model

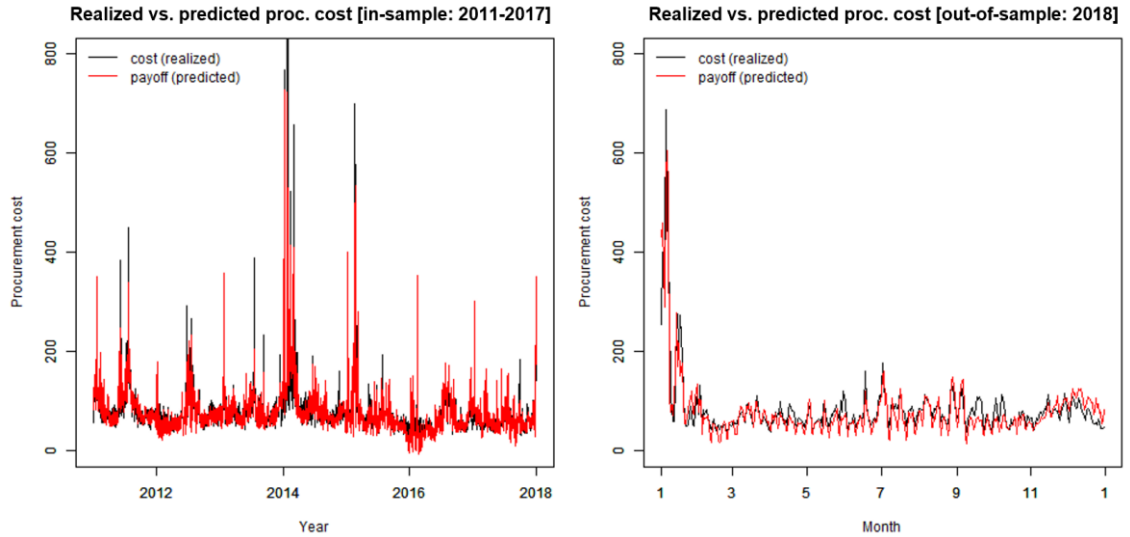

Figure 5.18: Comparison of realized and predicted procurement cost in PJM model

5.6 Conclusion

In this work, we proposed a hedging method using derivative portfolios related to energy and weather derivatives against the fluctuation of the solar power producer's sales revenue or retailer's procurement cost and measured the hedge effects using empirical data from JEPX and PJM. Our modeling approach is based on the concept of the non-parametric modeling methods proposed in previous studies, but includes the following new points:

- We set up a problem of finding the payoff function of nonlinear derivatives that change

with the season and apply the tensor-product spline function to estimate it.

- By using ANOVA decomposition, we made it easier to capture the structure of the hedge model and showed that multiple different payoff functions such as minimum and maximum temperatures can be estimated simultaneously and effectively.
- Assuming that the solar power sales revenue and the retailer's procurement cost have seasonality even when viewed at the rate of annual change, we use a spline function with cross variables to estimate this mixed trend
- We proposed new standardized derivatives with squared temperature prediction errors as underlying assets and demonstrated their significant hedging effect for hedging risks in the PJM market, which has particularly strong non-linearity.

For solar power sales revenues in JEPX, the solar radiation derivatives provide a hedging effect that reduces the original variance by approximately 52%, and the combined use of temperature derivatives enables an improvement of approximately 59%. Furthermore, there was a cross-hedging effect of approximately 30% even when temperature derivatives alone were used. As for the retailer's procurement cost in PJM, the set of minimum and maximum temperatures futures whose payoffs are given by linear functions demonstrates a hedging effect of 28%, and the nonlinear pricing method using tensor product splines enables an improvement of approximately 62%. Furthermore, a combination of the squared error derivatives and futures, both of which can be designed as standardized derivatives independent of company-specific costs, showed a 56% hedging effect.

Trading the squared prediction error may seem strange, but it is thought to be suggestive that such derivative products can be significantly effective if the hedged target has a strong non-linearity with respect to the underlying asset, such as the retailer's procurement cost in the PJM market. With the diversification of power sources and traders in recent years, it is expected that such hedging strategies and products of high granularity or variety will have room for further development, aiming at practical use in the future.

5.7 Appendix

5.7.1 Estimation of the Yearly Cyclical Trend of Annual Change

It is assumed that the various time series data in this work have yearly cyclical trends. This section details the method of estimating the periodicity function that reflects such a trend by using the example of solar power sales revenue. First, we consider constructing the following GAM for sale revenue $\pi_t, t = 1, \dots N$ on the date t.

$$\pi_t = f(Seasonal_t) + \epsilon_t \tag{5.15}$$

where f is the smoothing spline function, ϵ_t is the residual term with mean 0, and $Seasonal_t$ is defined as a yearly cyclical dummy variable $\big(= 1, \dots, 365 \text{ (or } 366)\big)$. To assign periodic dummy variables and estimate the periodicity function f, those in Yamada et al. (2015) are used.

In the following, we propose a method for estimating the yearly cyclical trend of the annual change rate, which exists in the sales revenue of solar power generation. Consider constructing the following GAM by adding the term of the yearly cyclical trend of annual change to (5.15):

$$\pi_t = f(Seasonal_t) + g(Seasonal_t)Period_t + \epsilon_t \tag{5.16}$$

where $Period_t$ is defined as a dummy variable calculated by the following equation:

$$Period_t := Year_t - Year_1 + \frac{Seasonal_t}{Days_t} \tag{5.17}$$

where $Year_t$ represents the year to which date t belongs ($Year_1$ is the year to which the starting point of sample data ($t = 1$) belongs), and $Days_t$ represents the total number of days to which date t belongs (i.e., 365 or 366). That is, $Period_t$ means the annualized elapsed day from the beginning day of the data starting year.

The second term $g(Seasonal_t)Period_t \coloneqq \theta(t)$ in (5.16) is obtained by estimating g as a smoothing spline function with cross variables, which is defined as a function of two-dimensional coordinates, $(Seasonal_t, Period_t)$ as shown in Figure 5.19. The data sample used for the estimation is on the diagonal line shown on the coordinate plane (the data sample of the year n is on the bold line in the figure, and the start and end points are indicated by A_n and B_n). The smoothing spline function $g(Seasonal_t)$ means the amount of change per year on each date, and

is estimated as a smoothly connected curve in the domain $Seasonal_t \in [-365, 731]$; therefore, $\theta(t)$ is also obtained as a smoothly connected "surface" in the domain of the two-dimensional coordinates in Figure 5.19. Considering the fact that the start point A_n of $Seasonal_t{}^{(2)}$ in year n is connected to the end point B_{n-1} of $Seasonal_t{}^{(1)}$ in year $n-1$, the end point B_n of $Seasonal_t{}^{(2)}$ in year n is connected to the start point A_{n+1} of $Seasonal_t{}^{(3)}$ in year $n + 1$, and that the data sample of the starting cross section of $Seasonal_t{}^{(2)}$ for each $Period_t$ is the same as that of its ending cross section, the annual changing rate $g\left(Seasonal_t{}^{(2)}\right)$ estimated by GAM (as well as the "surface" $\theta(t)$) is approximately connected at the start and end points.

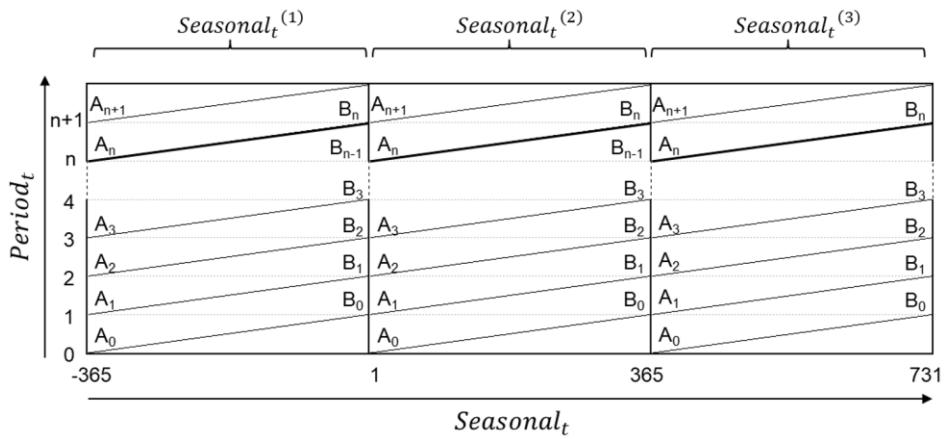

Figure 5.19: Location of data sample in two-dimensional coordinates consisting of yearly cyclical dummy and annual changing trend dummy

Chapter 6

Statistical Arbitrage in Imbalance System

6.1 Introduction

In Japan, where the electric power market has been gradually liberalized since 2000, various institutional revisions have been made according to changes in the market environment, particularly regarding the settlement system for the supply-demand gap ("imbalance"). Under such changing circumstances, a new rule was incorporated from 2019 regarding the "imbalance penalty." This is a formula revision for the imbalance settlement price applied to power generators and retailers, such that if the imbalance volume they have generated is deficient, they are compensated with a price higher than the price of the spot market (which is the main power exchange held the day before), and if they have a surplus, it is withdrawn at a lower price. The trigger for this system revision is the recent situation that the amount of imbalance in the entire system has increased due to the prediction error of rapidly expanding renewable energies, including solar power generation. The imbalances that occur in the power system are adjusted by system operators in each broad area, which incurs social costs. That is, the imbalance penalty has a policy intent to incentivize each individual operator to adjust their supply and demand, thereby reducing the system imbalance volume as an integrated value and suppress the total adjustment cost (METI 2017).

The transition of the imbalance system was also experienced in the UK, which has a long history of a liberalized market. However, in the UK's new imbalance system (introduced in 2015), the "dual price" system, which determines the imbalance price by the deficit or surplus status of individual operators (i.e., that corresponds to the penalty introduced in Japan in 2019) was abolished, and alternatively, the "single price" system was adopted, which determines the price

only depending on the imbalance status of the entire system. This revision was made based on the idea that dual pricing '*drives inefficiency in balancing by over-incentivising parties to balance'* and that *'under a single price parties with reducing imbalances benefit from the cost saving their reducing imbalances deliver for the System Operator.'* (OFGEM, 2014) Motivated by such a system change in the UK, Bunn and Kermer (2018) simulated market transactions using the Austrian zone of the German/Austrian electricity market model, which adopts a single-price system. This led to the result that permitting arbitrage to market participants contributes both to the arbitrager's profit acquisition and system stabilization. In other words, the study demonstrated that the single price system (in a fully liquid/mature market environment) has an efficient market mechanism in which traders' arbitrage behavior driven by profit pursuit also helps system operators to adjust the supply-demand balance.

On the other hand, in Japan, where full retail liberalization was finally achieved in 2016 and where the market is not yet fully mature, the system was just changed in 2019 from the single price to the dual price system with a penalty, as mentioned above, which is the opposite of the UK system. In this study, in addition to verifying the imbalance penalty newly introduced in the Japanese market, we will demonstrate whether the arbitrager's effect shown by Bunn and Kermer (2018) can be confirmed under the current Japanese market system. In doing so, this research aims to provide useful suggestions not only in terms of effective trading strategies performed by retailers but also regarding aspects of the market system designed by policymakers. In particular, when applying a previous analysis method to the Japanese market, we consider uncertainties that exist both in the imbalance volume and the imbalance price. We also model two probability distributions linked to each other using two-step quantile regression. In addition, we expand the existing method by formulating an optimization problem in which the player's transaction volume (decision variable) is treated as a continuous variable and derive an effective approximate solution for it. In the empirical analysis, we quantitatively evaluate the impact of the disclosure time lag on imbalance-related information and that of the imbalance penalties on trader's profits and imbalance volumes.

Additionally, in constructing a prediction model for imbalance volume (where prediction error values are required as explanatory variables), this study incorporates renewable energy (solar power generation) and demand prediction error at the same time, considering their statistical

significance. Also, since the forecast values for demand and solar power generation in the Japanese market are not currently published, we separately propose a practical modeling method that can predict these parameters easily (and robustly with a small sample size) using widely available previous-day weather forecasts.

This chapter is structured as follows. In the next section, we briefly review the related research. Then, in Section 6.3, we provide a Japanese market overview. In Section 6.4, we formulate an effective arbitrage strategy, the results of which are provided in Section 6.5. Lastly, Section 6.6 offers conclusions.

6.2 Background Research

Imbalance issues have been receiving increasing attention among researchers, especially when it comes to looking at strategic behavior and optimal positions. Ding et al. (2017) proposed a two-stage stochastic model for an integrated strategy of day-ahead offering and real-time operation policies, considering the uncertainty of wind power generation. Krishnamurthy et al. (2018) proposed an arbitrage bidding strategy using energy storage in the day-ahead and real-time market. Boogert and Dupont (2005) analyzed statistical arbitrage between day-ahead and balancing markets. Weber and Just (2012) investigated the potential of statistical arbitrage for market participants in the German electricity balancing mechanism. Browell (2018) presented revenue-maximizing and risk-constrained strategies using logistic regression forecasts in electricity markets with a single price balancing mechanism. Klæboe et al. (2013) developed several forecasting models for balancing market prices and confirmed their unpredictability before the closure of the day-ahead market. Bunn et al. (2018) applied a stochastic latent moment model to predicting the imbalance volumes and found that the use of the density forecast substantially increased trading profitability and reduced risk when compared to conventional methods.

Thus, there are various studies on optimal imbalance positions that have been analyzed from the viewpoint of earning profits for market participants, but Bunn and Kermer (2018) examine this matter also from the perspective of a system stabilization effect. Their paper, however, developed the discussion using the model of the Austrian zone of the German/Austrian electricity market, where there is a deterministic imbalance price calculation formula on imbalance volume. Therefore, it is debatable whether the same effect can be empirically verified in other markets where such a

deterministic formula does not exist. In other words, even if no such deterministic formula is institutionally given, if we could obtain only valid observed values in the market and construct a prediction formula for the imbalance price based on the imbalance volume (which can be increased or decreased by players' transaction volumes), similar simulations may be possible in market models of various countries. Furthermore, whereas the previous work dealt with the trader's decision variable as a discrete action of spillage or shortage, the present study performs an empirical analysis by using a model that can also optimize the "volume" of transactions. Such refinement of analytical methods is considered to add value in terms of improving the reliability of the simulation. Thus, this study is not only aimed at applying the analysis method proposed by Bunn and Kermer (2018) to the Japanese market to obtain local policy suggestions, but it also aims to expand the method's applicability to other markets through evolving methodologies.

6.3 Japanese Market Overview

In Japan, wholesale electricity transactions are generally conducted on the Japan Electric Power Exchange (JEPX), which is a privately-owned organization that was established in 2003. Although there is no obligation to participate, many companies, including power generation and retailers, take part in the JEPX, as it is the only electricity market exchange in Japan. The JEPX started market trading in 2005, and as of the end of 2019, it was conducted in three markets: the "forward market" for trading relatively long-term electricity that is delivered within one year, the "day-ahead market" where 30 minutes unit of electricity for next-day delivery is traded by bidding by up to 10:00 on the previous day, and the "intraday market" where each unit of electricity is traded through continuous sessions up to one hour before delivery. Table 6.1 summarizes the day-ahead and intraday arrangements. In principle, all power generators and retailers are required to submit a supply and demand plan by noon on the previous day ("next day plan"), and, if necessary, an updated "current-day plan" one hour before delivery (i.e., the "gate closure" deadline). The imbalance caused by deviating from the submitted plan after the gate closure is adjusted (compensated or withdrawn) by the system operators and settled by the separately determined imbalance price (detailed in Section 6.3.2).

Table 6.1: The day-ahead and intraday markets in JEPX

	Day-ahead market (spot market)	Intraday market
Commodity	48 products dividing a day into 30-minute delivery periods	
Deadline for trading	10:00 on the day before the delivery date	One hour before delivery (for trading from 17:00 on the day before the delivery date)
Trading method	Blind single price auction	Continuous session
	The price is determined by the intersection of all the cumulated buy/sell curves.	Match buy and sell orders
Opening	Apr. 2005	Apr. 2016

The following is an overview of actual transaction data in JEPX. Figure 6.1 shows the average hourly prices of each market in 2018 (the imbalance price does not include the area correction factor or imbalance penalties, which are described later). It is confirmed that prices become high in the summer (Jul-Aug) and winter (Jan-Feb) when the electricity demand increases. Three market prices (day-ahead, intraday, and imbalance) have almost the same average level. However, intraday price tends to deviate somewhat (e.g., slightly high in Feb and low in Sep 2018). The JEPX sets the lower limit of the bid price as 0.01 [JPY/kWh], so no price can ever be a negative value.

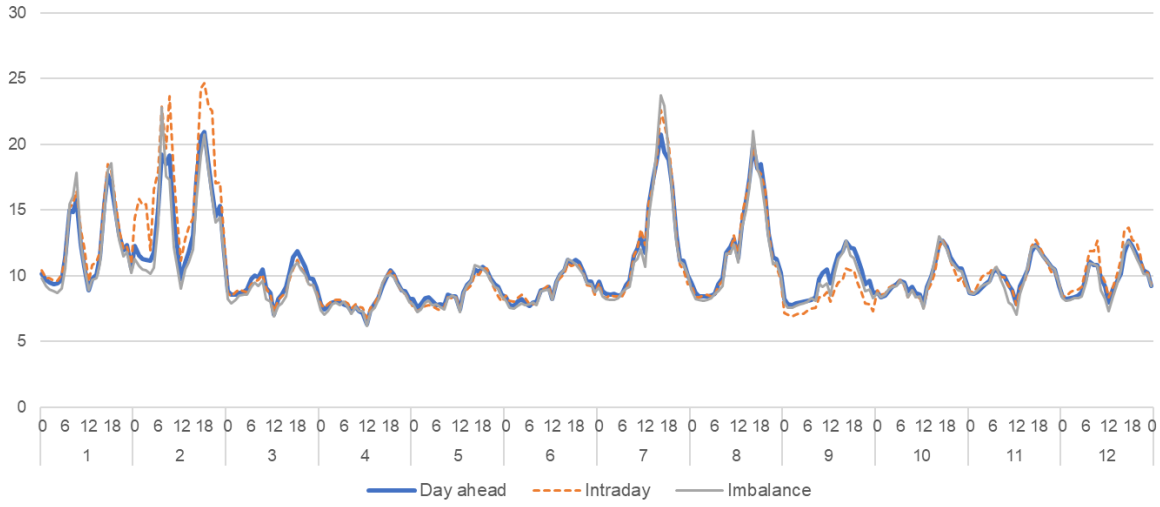

Data source: JEPX (http://www.jepx.org/)

Figure 6.1: Monthly average prices in 2018

Figure 6.2 shows changes in the transaction volume of the day-ahead market and the intraday market. The contract amount of the day-ahead market has dramatically increased in recent years,

while that of the intraday market has remained very low. Such low liquidity in the intraday market is thought to be one of the factors that cause price divergence from the day-ahead/imbalance price.

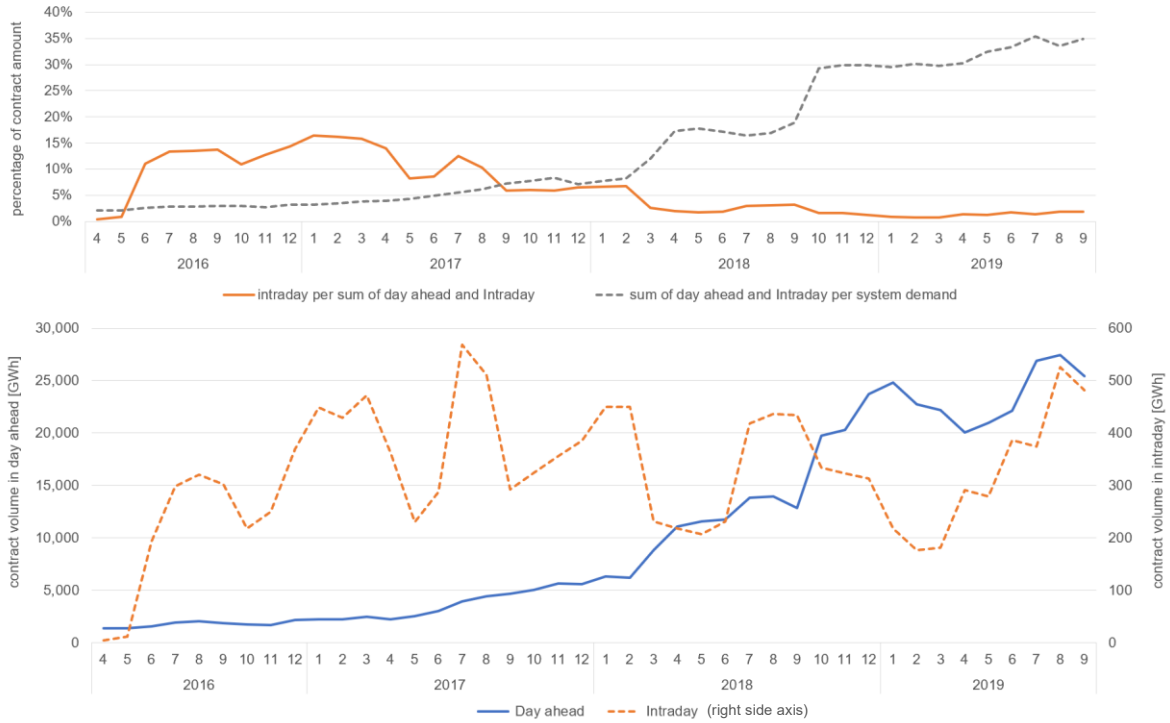

Data source: JEPX (http://www.jepx.org/) and Organization for Cross-regional Coordination of Transmission Operators (OCCTO) (http://occtonet.occto.or.jp/)

Figure 6.2: Changes in transaction volume of the day-ahead and the intraday market

6.3.1 Transition in the Imbalance System

In this section, before detailing the current imbalance system mechanism used in this study, we will review the transition in the Japanese imbalance system. Table 6.2 shows the main change phases. At first, when the system was established in 2000 (i.e., the start of liberalization), it was a mechanism that imposed a relatively large penalty on a company when its imbalance volume exceeded 3% of their demand. However, in 2016, with the full liberalization of retail, a single imbalance price formula was set regardless of the imbalance position of individual businesses to reduce the burden on new market entrants. Thus, by linking the single price to the entire net system imbalance, there was an incentive to promote the supply-demand balance of the entire system in a matching direction ("macro adjustment"). At the same time, by publishing imbalance prices after enough time had passed (i.e., reducing predictability), the policy was intended to suppress the

imbalance of individual operators. Yet, within this system, the function of ensuring that companies comply with their plans (i.e., the effort to make an appropriate forecast for demand and renewable power outputs and match the supply and demand) was not fully demonstrated, especially regarding small businesses. Accordingly, there is an issue in that the imbalance volume has been increasing with the expansion of renewable energies (METI 2017b). Therefore, since 2019, in addition to the conventional incentives for macro adjustment, a new incentive (penalty) was introduced to promote individual operators to maintain their supply-demand balance and not to speculate against the direction of the market ("micro adjustment"). Incidentally, another policy discussion for long-term review on imbalance system has recently begun in parallel with the current system update; the new policy direction is expected to "promote system users to appropriately forecast imbalance prices ... to ensure the supply-demand balance of the entire system" by "publishing information on imbalance status and prices in a timely manner" (EMSC 2019). In this way, Japan's imbalance system has been reviewed continuously to adapt to changes in the market environment.

In this study, the validity of the current enforced imbalance system is examined from the viewpoint of the arbitrage effect. However, the current Japanese market system does not give a favorable response to intentional imbalance production for the purpose of arbitrage (although it is not legally prohibited, it is announced to be in the scope of "government order for business improvement" (METI 2017b)). In this respect, it is possible that the potential punishment under the ambiguous rule will impede the market's efficiency. This study assumes there is no such implicit incentive for imbalance avoidance. In other words, we perform the simulation while assuming that market participants freely conduct transactions only in accordance with an explicitly institutionalized formulation.

Table 6.2: Transition of the Japanese imbalance system

Year	Related event	Summary of imbalance system	Price	Policy intent
2000-	Start of market liberalization	When shortage (surplus) exceeds 3% of demand, compensated at a high price (withdrawn for free).	Dual price	Secured incentives for grid users to comply with their plans.
2016-	Full liberalization for retailers	A single market price calculated by the adjustment factor α based on the system imbalance (note that the area correction term β was also added).	Single price	Considering the burden for new entrants, only the incentive of "macro adjustment" for the entire system was granted.
2019-	Review of imbalance system (Current system)	The fixed penalty term of k, l (as determined by the imbalance position of individual company) was added to the existing formula.	Dual price	Triggered by imbalance expansion due to renewable energy, the incentive of "micro adjustment," which urged appropriate planning (forecast), was added.

.*Source:* METI 2017b

Note: α, β, k, and l are detailed below.

6.3.2 Imbalance System Mechanism

This section details the current imbalance system in the Japanese market. Since 2019, the imbalance price has been determined by the following equation:

$$RT_t = \alpha_t DI_t + \beta + \begin{cases} k\ (if\ player's\ position\ is\ deficit) \\ -l\ (if\ player's\ position\ is\ surplus\ ) \end{cases},\ k\ and\ l > 0 \tag{6.1}$$

where RT_t is an imbalance price (it is not called the real-time price in Japan but is still written as RT_t to avoid confusion with imbalance volume). DI_t is the weighted average price by transaction-amounts of the day-ahead market price DA_t and the intraday price ID_t (since the day-ahead market transaction volume predominates, DI_t is close to DA_t). α_t is a variable factor that depends on the supply-demand balance of the entire system, β is constant term for area-specific correction, and, k and l are penalty values that are determined by the player's imbalance position and location.

6.3.2.1 Imbalance Price Related Parameter

Table 6.3 summarizes each imbalance price related parameter mentioned in (6.1) describes each parameter's meaning, update frequency, publication time, and specific values.

Table 6.3: Imbalance price related parameter overview

			α	β	k	l
Meaning			adjustment based on system imbalance	area price correction	deficit imbalance penalty	surplus imbalance penalty
Granularity (Update frequency)			half hourly	constant (monthly)	constant (unscheduled)	
Publication time			post (within 5 days)	pre	pre	
Example value	Applicable period		-	Apr. 2019	from Apr.2019	
	Area	Hokkaido	variable value common to each area	2.28	2.98	1.49
		Tohoku		1.07	0.59	0.20
		Tokyo		1.10	0.64	0.17
		Chubu		-0.95	0.27	0.68
		Hokuriku		-0.95	0.28	0.68
		Kansai		-0.95	0.28	0.69
		Chugoku		-0.95	0.28	0.68
		Shikoku		-0.95	0.28	0.68
		Kyushu		-1.09	0.43	0.83

Data source: METI (https://www.meti.go.jp/)

α is the ratio of the intersection price of the actual selling bid curve in the day-ahead market and the virtual buy bidding curve, which is shifted by the realized imbalance volume, against the realized day-ahead price. In this way, the imbalance price reflects the actual supply-demand balance (adjustment cost) of the entire system (METI 2017b). However, since this bidding curve is not disclosed, even if the imbalance volume is known, that alone is insufficient to identify α, although there is a significant correlation between α and imbalance volume (see Appendix section 6.7.1). In order to display the image of the time series fluctuation of α calculated in this way, the hourly shape of α (Feb. 2018 and Aug. 2018) is shown in Figure 6.4. It is evident that α is distributed randomly around 1.

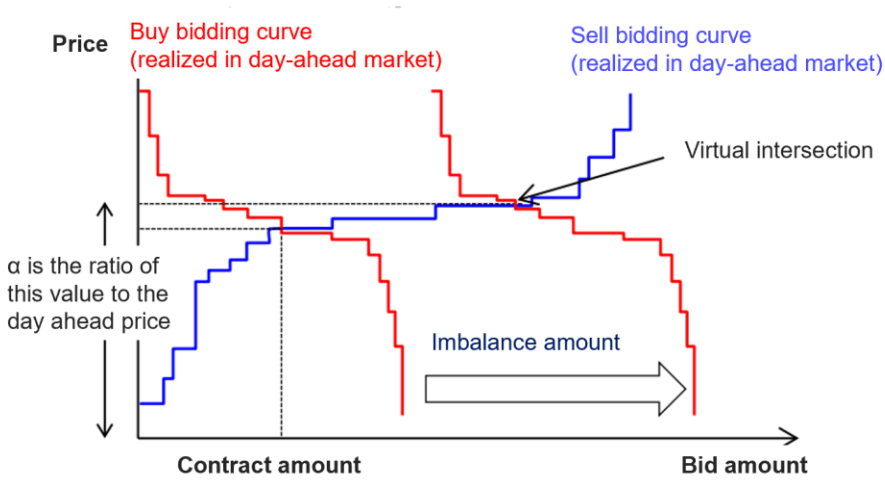

Source: METI (https://www.meti.go.jp/)

Figure 6.3: Calculation method of α

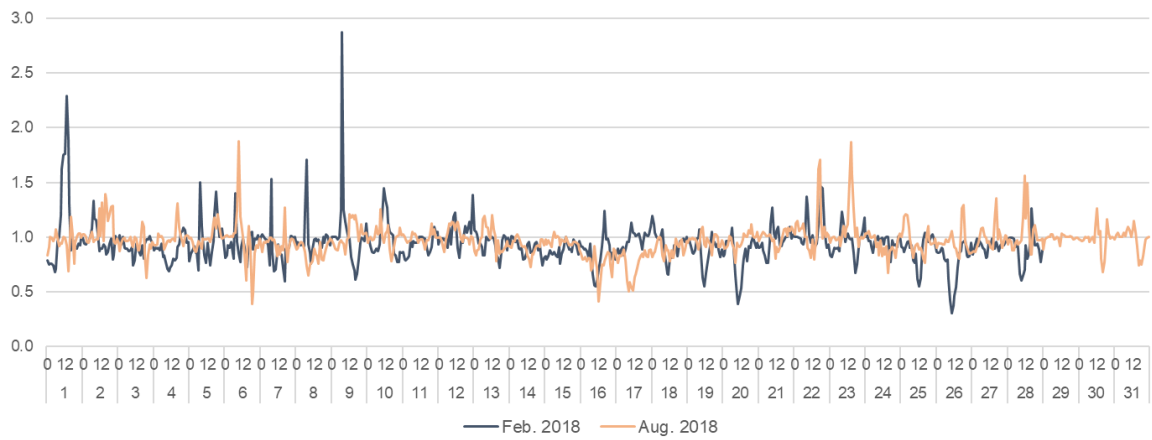

Data source: JEPX (http://www.jepx.org/)

Figure 6.4: Hourly shape of α (Feb. 2018 and Aug. 2018)

The penalty terms k and l generally range from 0.2 to 0.8 (Table 6.3), except in the case of the higher values observed in Hokkaido (this area's supply-demand scale is quite small). The demand weighted averages are calculated as $k = 0.53$ and $l = 0.51$. Note that these values are set at a level such that the "system operator in each area can recover the adjustment cost without excess or deficiency" (METI 2019).

In this study, the area correction term β is not taken into consideration, and modeling is performed by using a system price that means the national average. The reason for this is that the intraday price is published only as an average price for all areas, and we want to consider arbitrage

behavior at the national level through the JEPX. Since β compensates for the difference between each area price and the system price, its demand weighted average is set at 0.

6.3.2.2 Information Disclosure Schedule

Figure 6.5 summarizes the information disclosure timing of parameters, prices, imbalance volume, etc. In Japan, imbalance related data is disclosed around five days after the delivery time as quick estimation values; the final values are disclosed a few months later. Against this background, there was a policy of "anti-gaming" to incentivize individual operators not to produce imbalances by intentionally lowering the predictability of imbalance prices. However, considering that the most recent policy discussion is moving toward publishing such information in a timely manner (as mentioned in the previous section), this work performs simulations assuming a scenario in which the information disclosure lag is shorter (detailed in Section 6.4.1).

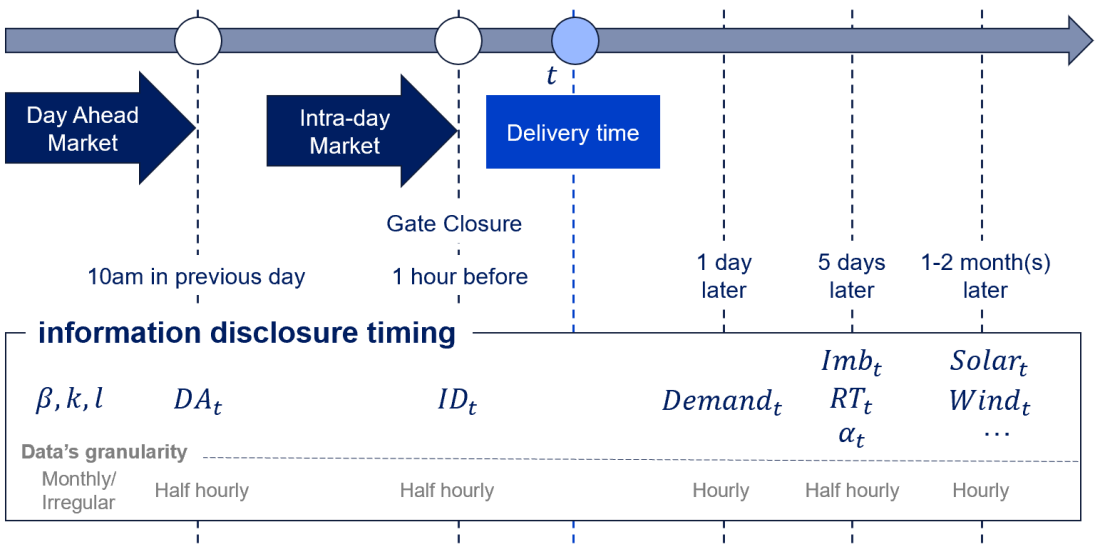

Figure 6.5: Timeline of market transactions and information disclosure

6.4 Statistical Arbitrage Model and Optimal Positions

In this section, we construct a statistical arbitrage model for the current imbalance system in Japan. After building the forecast model of the imbalance volume and price, we introduce the derivation method of the player's optimal strategy (i.e., optimal intraday transaction volume).

6.4.1 Quantile Prediction Models for Imbalance volume and Price

In building the arbitrage model for the Japanese market, considering that there is no deterministic function for the imbalance price on the volume, we need to treat imbalance price RT as a random variable in addition to imbalance volume Imb. In order to predict probability distributions for these two variables, we first consider the structure of the factors that influence them (Figure 6.6), based on the aforementioned calculation mechanism of α. The relationships between the two main random variables Imb / RT and their influencing factors are assumed to be indifferent to (i.e., independent of) each other. In other words, if the factors that affect imbalance volume would also affect the imbalance price, they always do so via the imbalance volume. Therefore, we can construct two independent prediction models for Imb and RT and then combine them to predict RT. For the prediction of each probability distribution, we use quantile regression (e.g., Davino et.al. 2014) because the shape of the densities and the interpolated forms of all the estimated quantiles are not restricted to a particular function.

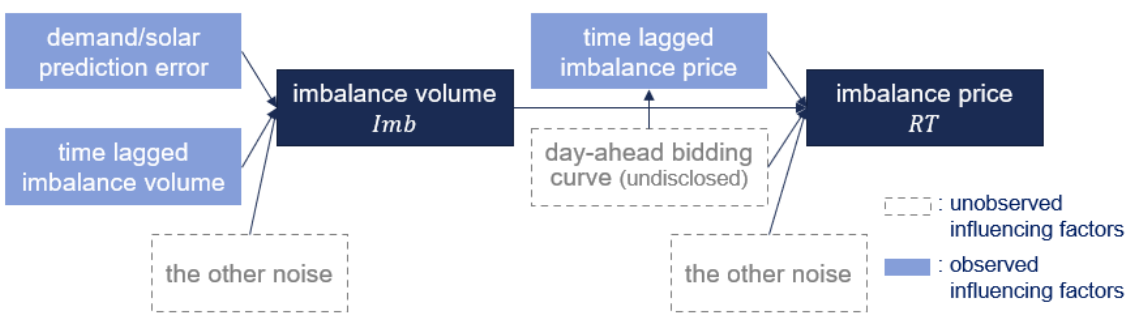

Figure 6.6: Factors that influence imbalance volume and imbalance price

6.4.1.1 Quantile Forecast Model for Imbalance Volume

First, we consider a quantile forecast model for imbalance volume. Recent research on imbalance forecasting shows that higher wind and solar forecast errors increase the absolute values of imbalance volumes (Goodarzi et al. 2019). In this study, considering that the amount of wind power generation in Japan is extremely small when compared to solar power (the ratio of installed capacity of wind to that of solar was 7.6% at the end of 2018), we focus on solar power generation as the renewable energy prediction error. Additionally, we also incorporate the demand prediction error since it has been confirmed as having a significant effect on the imbalance volume in many months and across many time zones (see Section 6.7.4). Moreover, because the forecasts of solar power

and demand are not publicly available, we separately construct forecast models that mimic how market participants might make such predictions for their own purposes (see Sections 6.7.2 and 6.7.3).

The specific forecast function for imbalance volume is given below. Using quantile regression, the below function can be estimated separately for discrete quantiles indexed through q[55]:

$$\widehat{Imb_{t,q}} = \gamma_{1,r,q} Imb_{t-r} + \gamma_{2,r,q} Imb_{t-24} + \gamma_{3,r,q} Solar_{t-r} + \gamma_{4,r,q} Demand_{t-r} + \gamma_{5,r,q} \tag{6.2}$$

where $\widehat{Imb_{t,q}}$ is forecast value of system imbalance (positive if shortage) at time $t \in \{1,2,\dots,N\}$. Imb_{t-r} (Imb_{t-24}) is the observed system imbalance volume with a time lag of r (24). $Solar_{t-r}$ ($Demand_{t-r}$) is the solar power (demand) forecast error, which is the difference between the latest values measured at $t-r$ and the day-ahead forecast values (see Appendix sections 6.7.2, 6.7.3, and 6.7.4 for details on $Solar_{t-r}$ and $Demand_{t-r}$). γ is the coefficient/constant term estimated by the quantile regression. In this work, quantile functions are estimated in a monthly rolling manner—when testing on out-of-sample data, forecast functions are estimated based on the previous month's data.

6.4.1.2 Quantile Forecast Model for Imbalance Price

Next, we similarly construct quantile forecast models for imbalance price. Japanese electricity market prices are always positive, and imbalance volume can be either negative or positive. Considering this, we apply a logarithmic transformation to price data, and the following quantile forecast function can be obtained:

$$Q_p\big(ln(RT_t)\big) = \theta_{1,p} ln(DA_t) + \theta_{2,p} ln(RT_{t-r}) + \theta_{3,p} Imb_t \tag{6.3}$$

where $Q_p(\cdot)$ is the forecast value on quantile p, RT_t (DA_t) is the imbalance (day-ahead) price at time t (which can be observed in the previous day), RT_{t-r} is the latest obtained imbalance price at $t-r$, and θ is a coefficient estimated by the quantile regression. The constant term was not

[55] The model is estimated separately by hour $h \in \{1,2,\dots,24\}$, month $m \in \{1,2,\dots,12\}$, and information time lag $r \in \{1,2,\dots,8\}$ (i.e., 2,304 models are estimated, but hour h and month m are omitted in the formula for simple notation). Also, hourly price/imbalance data is obtained by averaging/summing half-hourly data. In addition, information time lag scenarios are set as within eight hours based on the most recent policy discussion.

retained because small t-values were estimated. Also, RT_t refers to $\alpha_t DI_t$ (i.e., first term in (6.1)). The penalty term will be considered when solving optimization problems in Subsection 6.4.2. Here, from the quantile regression's property of "invariance to monotone transformations" (e.g., Koenker 2005), (6.3) is converted into the following formula:

$$\widehat{RT_{t,p}} := Q_p(RT_t) = DA_t{}^{\theta_{1,p}} \times RT_{t-r}{}^{\theta_{2,p}} \times exp\left(\theta_{3,p} Imb_t\right) \tag{6.4}$$

where $\widehat{RT_{t,p}}$ is the forecasted imbalance price at time t on quantile p. In (6.4), the explanatory variable Imb_t is unobserved at the forecasting time. Therefore, by using (6.2) as an input in (6.4), the following two-dimensional quantile forecast function is constructed:

$$\begin{aligned} \widehat{RT_{t,p,q}} &:= DA_t{}^{\theta_{1,p}} \times RT_{t-r}{}^{\theta_{2,p}} \times exp\left(\theta_{3,p} \widehat{Imb_{t,q}}\right) \\ &= DA_t{}^{\theta_{1,p}} \times RT_{t-r}{}^{\theta_{2,p}} \times exp\left[\theta_{3,p}\begin{pmatrix} \gamma_{1,r,q} Imb_{t-r} + \gamma_{2,r,q} Imb_{t-24} \\ +\gamma_{3,r,q} Solar_{t-r} + \gamma_{4,r,q} Demand_{t-r} + \gamma_{5,r,q} \end{pmatrix}\right]. \end{aligned} \tag{6.5}$$

where $\widehat{RT_{t,p,q}}$ is the forecasted imbalance price at time t on the quantile p (on quantile formula (6.4)) and on the quantile q of forecasted imbalance volume (on quantile formula (6.2)). In this way, the quantile forecast function for $\widehat{RT_{t,p}}$ can be expressed as $\widehat{RT_{t,p}} = \frac{1}{N}\sum_q \widehat{RT_{t,p,q}}$.

Then, a supplementary explanation is added to help with intuition deriving (6.5). First, Figure 6.7 shows a univariate cumulative distribution function $x(q)$ overlaid with a discrete step function $\widetilde{x(q)}$ with N equal domains serving as an approximate function. Here, the expected value of the random variable X with the inverse cumulative distribution function $x(q)$ (which is a smooth monotonically increasing function on the domain $q \in [0,1]$), can be approximated using the discrete step function $\widetilde{x(q)}$ as follows:

$$\begin{gathered} E[X] = \int_0^1 x(q)dq \approx \frac{1}{N}\sum_{n=1}^{N} \widetilde{x(q)} \\ \text{s.t. } \widetilde{x(q)} := \left\{x\left(\frac{2n-1}{2N}\right) \middle| \frac{n-1}{N} \le q < \frac{n}{N},\ n = 1,2,\dots,N\right\} \end{gathered} \tag{6.6}$$

where the approximation in (6.6) converges with N. Figure 6.8 shows the concept of the discrete approximation extended to two dimensions and applied to the bivariate random variables specified here. Note that t is omitted for simplicity of notation (i.e., $\widehat{Imb_q}$ stands for $\widehat{Imb_{t,q}}$, which is the

same for $\widehat{RT_{p,q}}$ and $\widehat{RT_p}$).[56] Here, we consider approximating the predicted value in each mesh with the value at the midpoint of the mesh when both quantiles of the imbalance volume and price are divided into N equal parts. Then, the prediction formula at the midpoint is obtained as $\widehat{RT_{p,q}} = \widehat{RT_p}\left(\widehat{Imb_q}\right)$ (i.e., (6.5)), which simultaneously holds $\widehat{Imb_q}$ and $\widehat{RT_p}(Imb)$ (i.e., (6.2) and (6.4)). The expected value of the imbalance price is obtained as the weighted average of values on each mesh (area $= 1/N^2$) as in the following formula. In this work, $N = 10$ is used to balance computational load and the required accuracy:

$$\widehat{RT_t} = \frac{1}{N}\sum_{p}\widehat{RT_{t,p}} = \frac{1}{N^2}\sum_{p,q}\widehat{RT_{t,p,q}}. \tag{6.7}$$

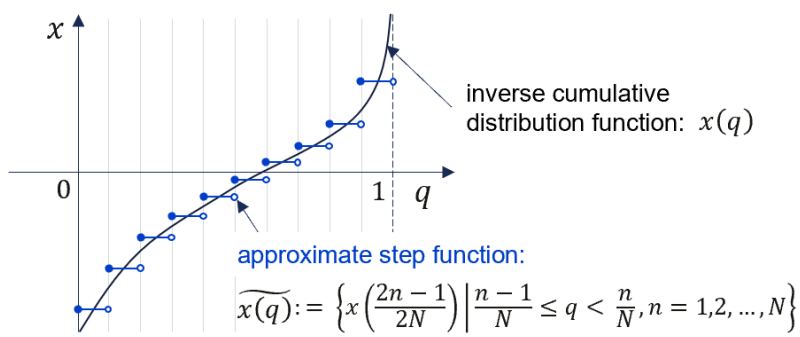

Figure 6.7: Concept of discrete approximation (univariate case)

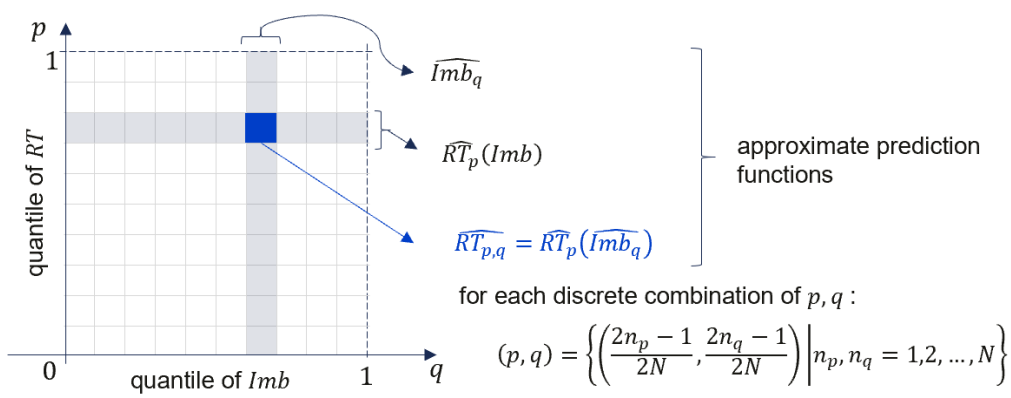

Figure 6.8: Discrete approximation for the bivariate quantile forecast functions

[56] The probability distribution in the two-dimensional coordinate here is assumed to be independent for each variable, as shown in Figure 6.6, and only the marginal distributions are considered.

6.4.2 Optimization of Participant Imbalance Positions

We formulate an optimization problem whereby participants make an arbitrage transaction using the intraday market to speculate the imbalance price. As mentioned earlier, imbalance price varies depending on the amount of imbalance, and if a participant has a deliberate long/short position (i.e., buy/sell electricity) in the intraday market, it contributes to surplus/shortage of system imbalance. That is, if a participant has a long position x_t (short position $-x_t$ if x_t is negative), the imbalance volume in (6.5) become smaller by x_t (larger by $-x_t$), so the quantile forecast function is formulated by the following equation:

$$\widehat{RT_{t,p,q}}\left(\widehat{Imb_{t,q}}, x_t\right) = DA_t{}^{\theta_{1,p}} \times RT_{t-r}{}^{\theta_{2,p}} \times exp\left[\theta_{3,p}\left(\widehat{Imb_{t,q}} - x_t\right)\right]. \tag{6.8}$$

Here, the participant's profit is formulated as a value obtained from the product of the imbalance price spread with the intraday price ID_t and the transaction volume as follows:

$$\pi_{t,p,q}(x_t) = \left\{\widehat{RT_{t,p,q}}\left(\widehat{Imb_{t,q}}, x_t\right) - ID_t\right\} \times x_t. \tag{6.9}$$

Thus, the optimization formulation is given by the following equation for the speculator to obtain the optimal position (decision variable) x_t that maximizes the expected profit of (6.9):

$$\max_{x_t}\left(\frac{1}{N^2}\sum_{p,q}\pi_{t,p,q}(x_t)\right) s.t. x_t \in [x_{min}, x_{max}]. \tag{6.10}$$

In (6.10), the decision variable x_t is defined as a continuous variable, meaning that it can be taken within a certain range (i.e., within the upper and lower limits of the tradeable amount).

6.4.2.1 Interpretation of the Optimal Solution

Before solving the optimization problem (6.10), we provide an interpretation for changing the optimal strategy in accordance with each variable using a mathematical analysis approach. First, the objective variable (i.e., expected profit $\widehat{\pi_t}$) of (6.10) is transformed as follows:

$$\begin{aligned} &\widehat{\pi_t} := \frac{1}{N^2}\sum_{p,q}\pi_{t,p,q}(x_t) = \frac{1}{N^2}\sum_{p,q}\left\{A_{p,q}x_t \times exp\left(-B_p x_t\right)\right\} - C_t x_t. \\ &\text{s.t.} \begin{cases} A_{t,p,q} := DA_t{}^{\theta_{1,p}} \times RT_{t-r}{}^{\theta_{2,p}} \times exp\left(\theta_{3,p}\widehat{Imb_{t,q}}\right) \\ B_p \quad := \theta_{3,p} \\ C_t \quad := ID_t \end{cases} \end{aligned} \tag{6.11}$$

To understand the general structure of the problem, consider the following simplified equation (using simplified profit variable $\tilde{\pi}(x)$), which does not consider the distinction of quantiles p and q:

$$\tilde{\pi}(x) := Rev(x) - Cost(x) = Ax \times exp(-Bx) - Cx$$
$$\text{s.t.} \begin{cases} Rev(x) := Ax \times exp(-Bx) \\ Cost(x) := Cx \end{cases} \tag{6.12}$$

where $Rev(x)$ corresponds to imbalance settlement income (expenditure if negative), and $Cost(x)$ corresponds to the procurement cost at intraday (sales gain if negative). In relation to (6.11), A denotes a prediction of imbalance price indifferent to position x, B denotes the sensitivity of the imbalance price to the amount, and C is the intraday price. Thus, $A, B,$ and C should all be positive values.

The functions $Rev(x)$ and $Cost(x)$ are plotted in Figure 6.9, which displays the relationship between the optimal position x^* and the optimal profit $\tilde{\pi}^*(x^*)$. Similarly, the relationship between the first derivative of both functions and optimal values (x^* and $\tilde{\pi}^*(x^*)$) is shown in Figure 6.10, depending on the cases of size relationships between A and C. Note that in this graph, the optimal profit, calculated as $\tilde{\pi}^*(x^*) = \tilde{\pi}(0) + \int_0^{x^*} \frac{\partial \tilde{\pi}}{\partial x} dx = \int_0^{x^*} \left(\frac{\partial Rev(x)}{\partial x} - \frac{\partial cost(x)}{\partial x} \right) dx$, corresponds to the shaded area. Also, the optimal decision $x^*$is found as the solution of the equation $\frac{\partial \pi}{\partial x} = \frac{\partial Rev(x)}{\partial x} - \frac{\partial cost(x)}{\partial x} = 0$ (i.e., the intersection of the two functions in Figure 6.10), and there is always one solution within the range $(-\infty,\ 1/B)$. The relationship between the optimal decision and profit when variables $A, B,$ and C vary is shown in Table 6.4 (the change of B in the case of $A = C$ is omitted in the table since it always satisfies $x^* = 0$ and $\tilde{\pi}^*(x^*) = 0$ regardless of B).

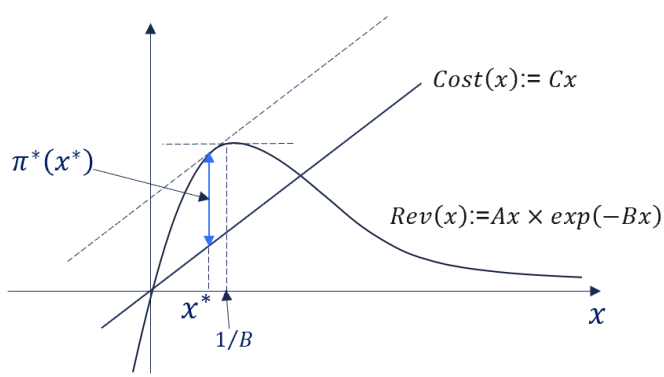

Figure 6.9: Relationship between revenue/loss functions and optimal profit/decision

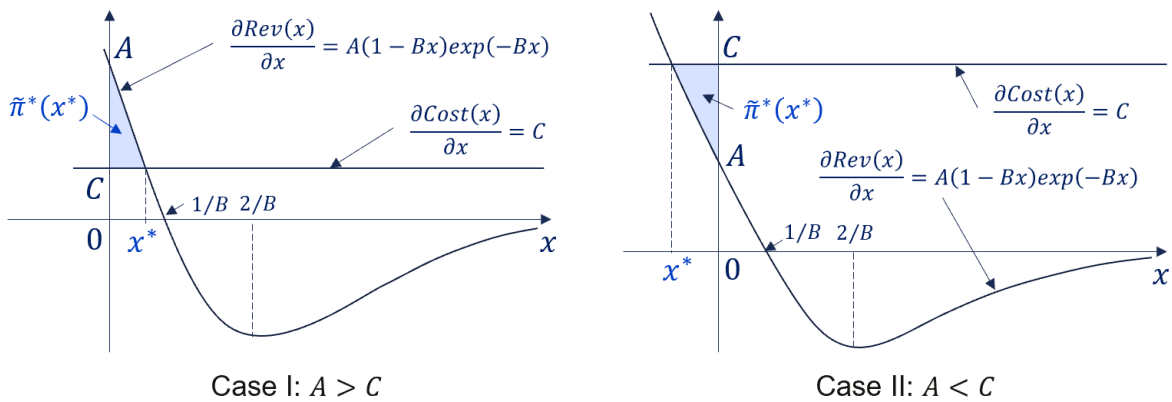

Figure 6.10: Relationship between the first derivatives of revenue/loss functions and optimal profit/decision

Table 6.4: Change of optimal decision and profit in relation to each variable A, B, and C

Relation to A

A	0	⋯	C	⋯	$+\infty$
x^*	$-\infty$	↗	0	↗	$1/B$
$\tilde{\pi}^*(x^*)$	$+\infty$	↘	0	↗	$+\infty$

Relation to B

Case I: $A > C$

B	0	⋯	$+\infty$
x^*	$+\infty$	↘	0
$\tilde{\pi}^*(x^*)$	$+\infty$	↘	0

Case II: $C > A$

B	0	⋯	$+\infty$
x^*	$-\infty$	↗	0
$\tilde{\pi}^*(x^*)$	$+\infty$	↘	0

Relation to C

C	0	⋯	A	⋯	$+\infty$
x^*	$1/B$	↘	0	↘	$-\infty$
$\tilde{\pi}^*(x^*)$	A/eB	↘	0	↗	$+\infty$

- *A (forecast value of RT indifferent to Imb).* The optimal intraday long position x^* increases along with A, and optimal profit $\tilde{\pi}^*(x^*)$ increases as A deviates from C. In other words, the higher/lower the imbalance price forecast value is in comparison to the intraday price, the more the optimal long/short positions at the intraday market can be increased (the profit can be increased accordingly).
- *B (sensitivity of RT to Imb).* If B is low, the impact on the imbalance price given by player's transaction is small. Therefore, optimal absolute intraday position (long if $A > C$, and short otherwise) increases, which generates profit. Conversely, if B is very high, the optimal intraday position and profit approach 0. This is because the chance of arbitrage is decreased, as the own transaction amount reduces the profit margin.
- *C (intraday price ID).* If C is a certain price (i.e., imbalance price forecast A), the optimal long position x^* and profit $\tilde{\pi}^*(x^*)$ will equal 0 because there is no chance of arbitrage. Optimal long position x^* monotonously decreases in response to C, which means that the higher intraday price urges more short positions. Optimal profit $\pi^*(x^*)$ increases as C

deviates from A because the profit margin increases with the price differential.

6.4.2.2 Derivation of Approximate Solution

Next, we consider an optimization problem (6.10) where quantile forecast values are considered. This problem corresponds to finding x_t when the first-order derivative of (6.11) (defined here as $f(x_t)$) is equal to 0.

$$f(x_t) := \frac{\partial \widehat{\pi_t}}{\partial x_t} = \frac{1}{N^2} \sum_{p,q} A_{p,q}(1 - B_p x_t) exp(-B_p x_t) - C_t = 0. \tag{6.13}$$

There is no closed-form solution in (6.13). Therefore, in this study, we use Newton's method (see Algorithm 1). The parameter $i_{max} = 5$ is used in the empirical analysis because sufficient convergence was obtained. Additionally, when the penalty term is considered, the algorithm should be as it is in Algorithm 2. For each long/short position scenario (penalty scenario), the obtained optimal solution should be judged whether it is consistent with the scenario condition or not. If it matches, the solution is valid; however, if none of the cases match, there is no optimal arbitrage transaction (i.e., the optimal transaction volume is 0).

Algorithm 1 Solution for the approximate optimal decision using Newton's method

Initialize: $x_{t,0} = 0$

for $i = 0 : i_{max}$ **do**

$$x_{t,i+1} = x_{t,i} - f(x_{t,i})/f'(x_{t,i}) = x_{t,i} - \frac{\frac{1}{N^2}\sum_{p,q} A_{p,q}(1 - B_p x_{t,i}) exp(-B_p x_{t,i}) - C_t}{\frac{1}{N^2}\sum_{p,q} -A_{p,q} B_p (2 - B_p x_{t,i}) exp(-B_p x_{t,i})}$$

end for

return $x_{t,i}$

Algorithm 2 Solution for the approximate optimal decision using Newton's method (considering penalty)

Initialize: $x_{t,0} = 0$
for $position \in \{"long", "short"\}$ **do**
  switch $(position)$
    case "$long$": define penalized marginal profit function $f_p(\cdot) \coloneqq f(\cdot) - l$
    case "$short$": define penalized marginal profit function $f_p(\cdot) \coloneqq f(\cdot) + k$
    for $i = 0: i_{max}$ **do**
      $x_{t,i+1} = x_{t,i} - f_p(x_{t,i}) / f_p{}'(x_{t,i})$
    end for
    case "$long$": **if** $x_{t,i} > 0$ **return** $x_{t,i}$
    case "$short$": **if** $x_{t,i} < 0$ **return** $x_{t,i}$
  end switch
end for
return 0

6.5 Empirical Analysis

In this section, actual data is used to simulate changes in profit and imbalance volume when participants make arbitrage transactions in the intraday market.

6.5.1 Precondition and Scenarios

For the empirical analysis, the following data will be used.

- System imbalance volume Imb [MWh]: sum of all nine areas in Japan[57]
- Day-ahead price DA, Intraday price ID, Imbalance price RT [JPY/kWh]: JEPX system price[58]
- Solar power forecast error $Solar$ [MWh]: calculated by a separately constructed solar forecast model using next-day weather forecast data (see Section 6.7.2)
- Demand forecast error $Demand$ [MWh]: calculated by a separately constructed demand forecast model using next-day weather forecast values (see Section 6.7.3)

The training period is each month between Dec. 2017 and Nov. 2018. For the simulations, out-of-sample data are collected from Jan. 2018 to Dec. 2018 (out-of-sample forecasts use the forecast model estimated from the previous month in a rolling manner).

[57] Downloaded from each electric power company's web page (e.g. TEPCO: http://www.tepco.co.jp/pg/consignment/retailservice/imbalance/index-j.html).

[58] All prices are downloaded from http://www.jepx.org/market/index.html.

6.5.1.1 Market Conditions and Scenarios

Here, we assume the market conditions and scenarios. First, as described above, we assume a typical speculative retailer as a player[59] who does not have physical generation but can arbitrage trades from the intraday market against the imbalance prices. Note that the upper and lower limits of players' positions are calibrated to the 90th percentiles of the actual imbalance volumes in 2018. As for information time lag scenarios, we assumed eight different time lags (from one- to eight-hour delays). Also, in the simulation, a perfect-foresight (PF) case is calculated for comparison. Regarding imbalance penalty scenarios, assuming that there is the same penalty for shortage and surplus (i.e., $k = l$), we set the following six scenarios: $k, l = \{0, 0.25, 0.5, 1.0, 2.0, 4.0\}$ [JPY/kWh]. As described in Section 6.3.2, the national averages (area demand weighted average) of k and l are 0.53 and 0.51, so $k = 0.5$ corresponds to the current system.

6.5.1.2 Construction of the Deterministic Function for Imbalance Price Depending on Player's Decision

In the empirical analysis, we want to find the profit obtained by the retailer's arbitrage transaction, but as mentioned earlier, there is no deterministic price function depending on imbalance volume in the Japanese system. Hence, we considered the following linear regression model and concluded that it is adequate for predicting imbalance prices (in the testing period of 2018, the R-squared was at least 0.997 for all 288 models for all months and hours):

$$ln(RT_t) = \vartheta_1 ln(DA_t) + \vartheta_2 ln(RT_{t-1}) + \vartheta_3 Imb_t + \epsilon_t. \tag{6.14}$$

Therefore, assuming the predictor part in (6.11) as a deterministic function on Imb_t, we have a function for profit based upon a trader's optimal decision x^*:

$$\begin{gathered} \pi_t(x^*) = \left\{\widehat{RT}_t(x^*) - ID_t\right\} \times {x_t}^* \\ \text{s.t. } \widehat{RT}_t(x^*) = {DA_t}^{\vartheta_{1,p}} \times {RT_{t-r}}^{\vartheta_{2,p}} \times exp\left[\vartheta_{3,p}\left(Imb_{t,q} - {x_t}^*\right)\right]. \end{gathered} \tag{6.15}$$

6.5.2 Simulation Result and Consideration

In this subsection, we calculate and consider the imbalance volume and the profits based on the

[59] Under the current Japanese system, physical players (former general electric utilities), in principle, are to put all the power supply exceeding its own demand into the intraday market as well as the day-ahead market. Therefore, simulation on physical player is not realistic, and we only assume non-physical players.

retailers' optimal decision based on the scenario of information disclosure lime lag and imbalance penalty. First, Figure 6.11 shows a graph of the absolute value and standard deviation of the system imbalance volume when the retailers are acting optimally. As the figure shows, the imbalance is reduced in accordance with the shortened information time lag. Conversely, if the information time lag is long (i.e., if the predictability is low), the imbalance will instead increase due to arbitrage. Additionally, when the time lag is short (around 1 to 2 hours), it can be confirmed that certain imbalance penalties contribute to further reducing the imbalance volume (both of the absolute value and standard deviation), but a large penalty enlarges it more than a no-penalty case. All in all, however, when arbitrage was performed under the same penalty strength as the current system (i.e., in the case where $k, l = 0.5$ [JPY/kWh]) and when the information was disclosed within one hour, the imbalance volume could be reduced by 7.7% in terms of absolute value and 10.7% in terms of standard deviation, if retailers were to act optimally.

Next, Figure 6.12 shows that retailers make a profit at all lags and under all penalties. Evidently, profit decreases with time lag and imbalance penalty. Interestingly, a small penalty (e.g., k and l range from 0.25 to 0.5 [JPY/kWh]) has little effect on the retailer's profit although it reduced imbalance volume as demonstrated above. This indicates that a small penalty could restrain players from arbitrage transactions with small margins. As a result, it could reduce imbalance volumes without reducing the retailer's profit.

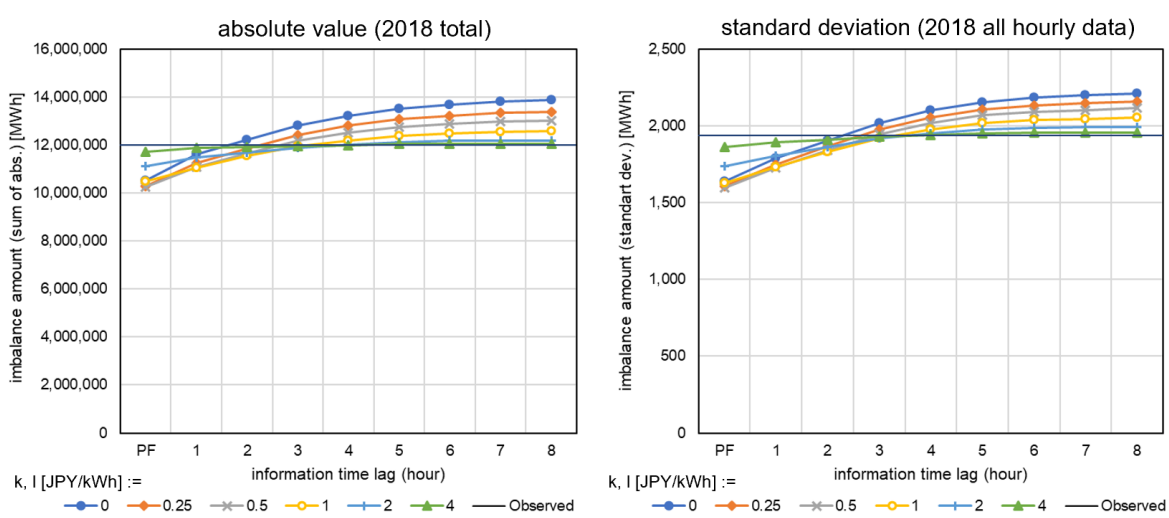

Figure 6.11: Simulated imbalance volume changing with time lag and penalty

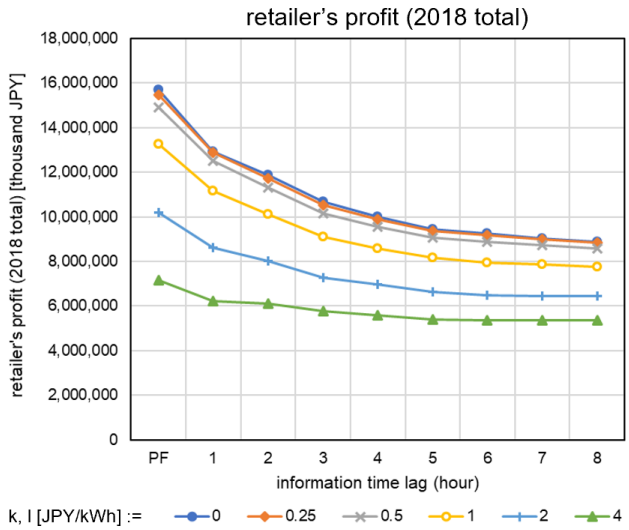

Figure 6.12: Arbitrage profit changing with time lag and penalty (2018 total)

To confirm the impact of the penalty on the arbitrage volume with hour granularity data, Figure 6.13 shows the simulated results for weekdays in mid-February when the price fluctuated. The graph on the left shows the case without penalty, and the graph on the right shows the case where the penalty is $k, l = 0.5$ [JPY/kWh]. In both cases, the information time lag is set as one hour. Overall, the retailer's optimal decision when system imbalance is positive (shortage) tends to be positive (long position), and the decision when the system imbalance is negative (surplus) tends to be negative (short position). On the other hand, there are some periods during which the directions are reversed or excessive arbitrage is performed (e.g., the part with the arrow on the left graph) due to extremes in the intraday price. Looking at the right graph with a penalty of 0.5 [JPY/kWh], it is evident that such a reverse or excessive arbitrage transaction is slightly mitigated. This means that a small imbalance penalty has an effect of reducing unsuitable or extreme arbitrage, which may move in the direction of increasing imbalance volume.

Figure 6.14 shows the monthly results of the imbalance volume as it changes with arbitrage transaction (the information time lag is set to one hour, and the penalty is 0.5 [JPY/kWh]). In general, the absolute value and standard deviation of the imbalance volume are suppressed by arbitrage in each month, and they are further reduced in the perfect forecast case. However, the absolute imbalance volume is increased in some months, including September. This is because the intraday price in September 2018 was significantly below the imbalance price (see Figure 6.1).

Therefore, the arbitrager could have been urged to adopt a long position that exceeded the appropriate level, thus expanding the level of imbalance.

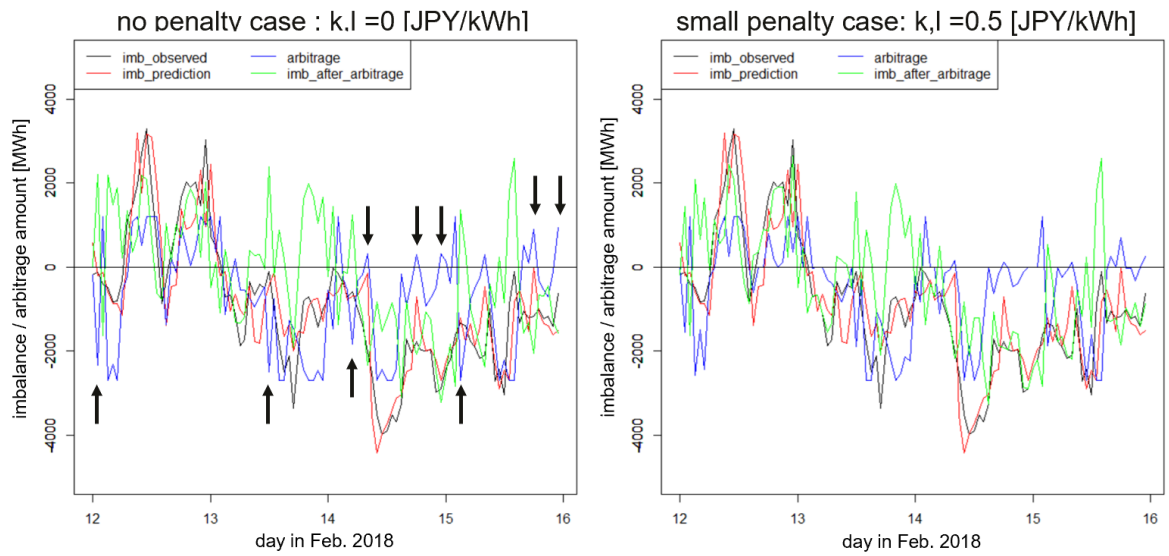

Figure 6.13: Simulated imbalance volume (example of mid-Feb. 2018)

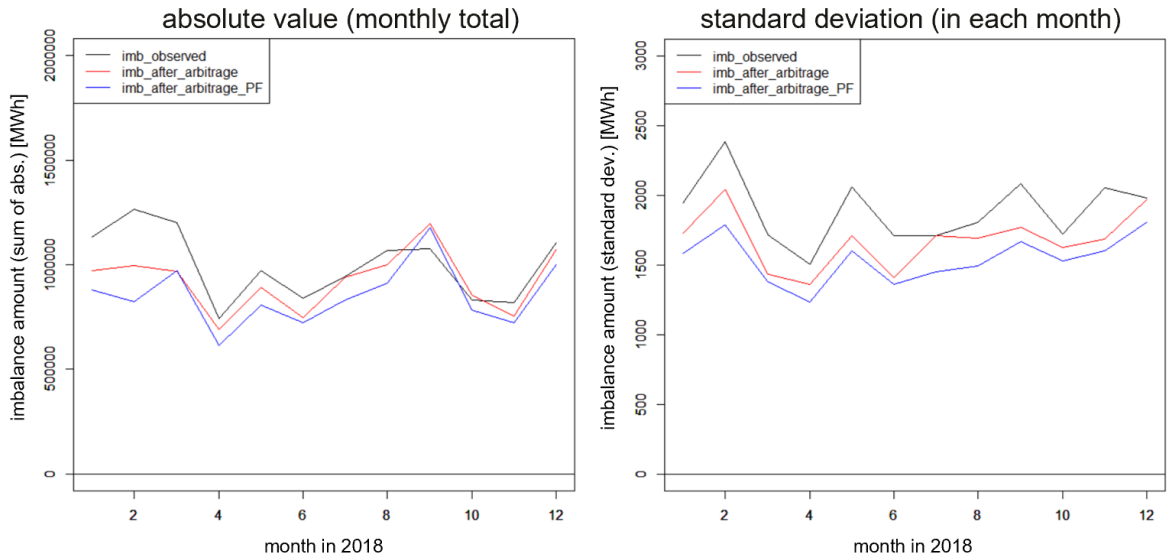

Figure 6.14: Simulated monthly imbalance volume

6.6 Conclusion

This work verified that the arbitrage effect shown in previous research in the Austrian market is

also present in the Japanese market. First, from a methodological perspective, the following items can be cited as the points that this research has contributed:

- To analyze a market mechanism where there is no deterministic relationship between imbalance price and imbalance volume (as is the case in most markets) but in a way that is unlike a similar application (Bunn and Kermer 2018), we developed a two-step quantile regression method that incorporates correlated asymmetric probability distributions.
- We refined the optimization problem put forth by Bunn and Kermer (2018) by assuming that the player's decision (trading position) is treated as a continuous variable instead of a discrete variable.
- We provided a simple interpretation using a mathematical analysis for the optimization problem and introduced an effective approximate solution method.

The following points are mentioned as policy-related suggestions for Japan's imbalance system:

- Permitting retailers in Japan to optimize imbalance arbitrage could contribute to both their profit earning and system stabilization as long as the imbalance related information disclosure time lag is sufficiently short
- The imbalance penalty newly introduced in 2019 in Japan enhances the arbitrage effects of reducing system imbalance volume, although it was not intended to do so.
- Policymakers need to be aware that in the illiquid market, where the intraday price can deviate largely from the imbalance price (as happened in September 2019), the imbalance volume may be increased by arbitrage transaction.

As mentioned earlier, in parallel with the current system update in 2019, the new policy review has just begun. This policy is intended to promote system users to forecast imbalance prices as a means of ensuring the system balance by publishing imbalance related information in a timely manner. This movement is consistent with the policy recommendation described in this work. However, the discussion is not necessarily considered from the viewpoint of optimizing market efficiency, assuming retailers' arbitrage. In the background of the Japanese electricity market liberalization, there is the concept of "aiming for efficient market formation using market mechanisms" as stated in the regulatory philosophy (EMSC 2018). In the long-term future, designing an imbalance system from the perspective of improving market efficiency would be an

effective approach, taking into account the use of the market mechanism of imbalance reduction effect by the arbitrager, as was demonstrated in this work.

6.7 Appendix

6.7.1 Realized Relationship Between α and Imbalance volume

Figure 6.15 shows a series of scatter plots of α and imbalance volume for each month of 2018 (all values are hourly values). There is a significant convex correlation between α and imbalance, although it is distributed within a specific range.

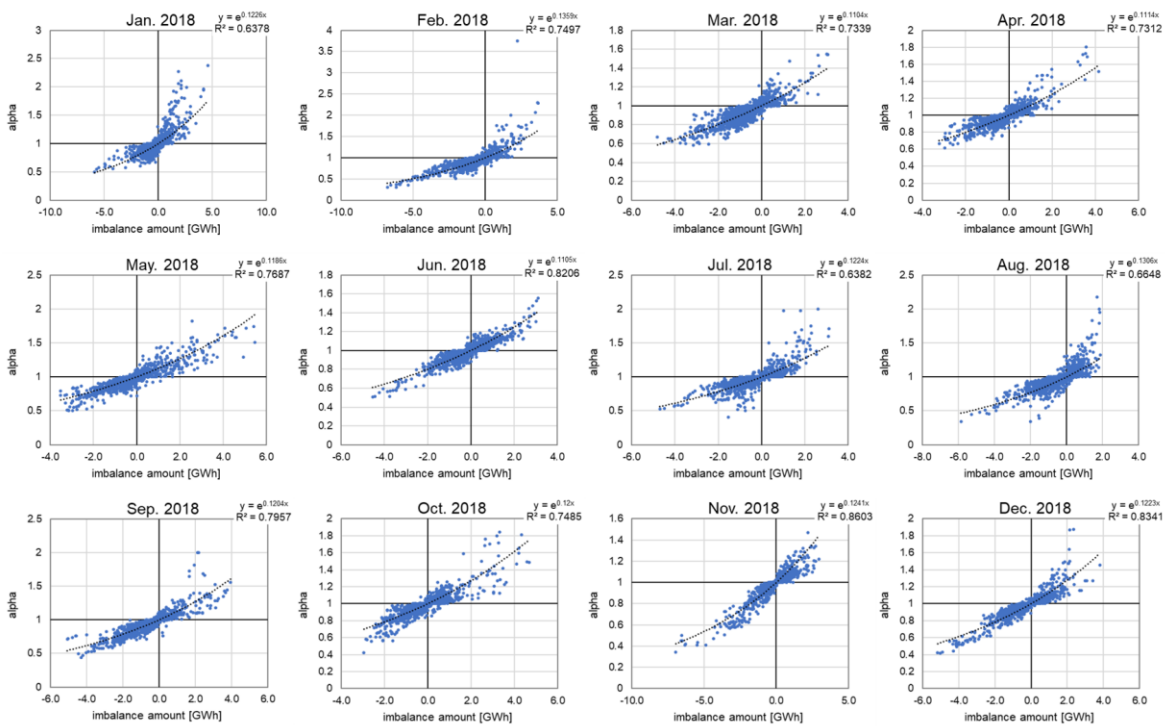

Figure 6.15: Scatter plot of α and imbalance

6.7.2 Prediction Method for Solar Power Output Using Previous Day Weather Forecasts

As mentioned at the beginning of Section 6.5, the solar power prediction error used for the imbalance prediction is not publicly available, so we obtained it by separately building the prediction model using measured values. In this section, we propose a practical modeling method that can predict solar power output easily (and robustly with small sample size data) using the

public weather forecast published on the previous day.

6.7.2.1 Model Construction

When constructing a prediction model using data from a very small sample size (of about a year and a half), the challenge is how to handle the strong seasonality and increasing trend in power generation due to the recently increased installation. Matsumoto and Yamada (2019a) propose a method that uses a GAM (Hastie and Tibshirani 1990) to estimate the smooth yearly cyclical trend that exists when the time series of solar power output are divided by hourly clock time and weather. To further enhance the robustness of the model, we use a two-dimensional tensor product spline function with a smoothing condition in the intraday time direction in addition to the seasonal direction considered in previous studies. In related research, Matsumoto and Yamada (2019b, 2019d) applied a tensor product spline function for the pricing of weather derivatives; the present research applies the same idea to the prediction model. In addition, to improve the prediction accuracy, this work considers temperature variables.

The specific construction procedure for the model used in this work is described below. Regarding the annual change trend, which depends on the increasing amount of installation, we separately model the linear trend of the installation capacity and estimate the trend for the "power output per unit" (obtained dividing the hourly output data by the capacity). First, solar power capacity (at day t) W_t is modeled by the following single linear regression:

$$W_t = w_1 Period_t + w_2 + \epsilon_{w,t} \tag{6.16}$$

where w_1 and w_2 are the coefficient and intercept, respectively, estimated by the OLS (6.16). $Period_t$ is the daily dummy variable representing the number of years that have passed. By using this equation, the prediction value of capacity $\widehat{W}_t$ can be obtained as follows:

$$\widehat{W}_t = w_1 Period_t + w_2. \tag{6.17}$$

Note that observed capacity W_t is monthly data (even with some missing values), but the prediction value $\widehat{W}_t$ can be obtained as daily granularity data.

Second, we define the unit power output (at date t, hour h) $U_{t,h}$ as solar power output volume $V_{t,h}$ divided by the estimated capacity $\widehat{W}_t$ and construct the following GAM:

$$U_{t,h} = u_{sunny}(t,h)I_{sunny,t,h} + u_{cloudy}(t,h)I_{cloudy,t,h} + u_{rainy}(t,h)I_{rainy,t,h} + u_{snowy}(t,h)I_{snowy,t,h} + u_{tmax}(t,h)\epsilon_{tmax,t,h} + u_{tmin}(t,h)\epsilon_{tmin,t,h} + \epsilon_{u,t,h} \quad (6.18)$$

where $u_{\cdot}(t,h)$ is the tensor product spline function estimated by the GAM, $I_{\cdot,t,h}$ is a dummy variable (which is 1 if the weather at date t hour h is the same as the suffix's weather and is 0 otherwise. The 'snowy' term is only included in the model for snowy areas. $\epsilon_{tmax,t}$ / $\epsilon_{tmin,t}$ is daily maximum/minimum temperature's "forecast differential" (observed forecast value minus its trend) obtained by the following GAM:

$$Tmax_t = f_{tmax}(t) + \epsilon_{tmax,t}, Tmin_t = f_{tmin}(t) + \epsilon_{tmin,t} \quad (6.19)$$

where $Tmax_t$/$Tmin_t$ is the maximum/minimum temperature prediction for the value at date t, which is forecasted on the previous day. $f_{tmax}(t)$ and $f_{tmax}(t)$ are the yearly cyclical trends estimated by the GAM. We estimate the cyclical trends as the spline functions $f_{\cdot}(Seasonal_t)$ in (6.19) and $u_{\cdot}(Seasonal_t, h)$ in (6.18) using yearly cyclical dummy variables $Seasonal_t$ $(= 1, \dots, 365\ (or\ 366))$, whose allocation method is proposed in Yamada et al. (2015). In this work, the starting point of the cyclical dummy variables is January 1, and from 1 to 365 (366 for leap years) are allocated in order. Additionally, we denote $f_{\cdot}(Seasonal_t)$ and $u_{\cdot}(Seasonal_t, h)$ as $f_{\cdot}(t)$ and $u_{\cdot}(t,h)$ to make the notation more concise.

6.7.2.2 Empirical Analysis

In the following, we use empirical data to estimate the solar power prediction model constructed above using the previous day weather forecast, and we verify the prediction error. A model is constructed for each of all the nine power areas, and the data used will be as follows:

- Solar power output volume $V_{t,h}$ [MW]: measured value published by nine electricity power companies [60]
- Solar power capacity W_t [MW]: month-end results published by METI [61]
- General weather condition $I_{\cdot,t,h}$, maximum/minimum temperature $Tmax_t$/ $Tmin_t$ [°C]: forecast values announced by the JMA on the previous morning (one major city in each of

[60] Downloaded from each electric power company's web page (e.g. TEPCO: http://www.tepco.co.jp/forecast/html/area_data-j.html.

[61] Calculated by using the data from https://www.fit-portal.go.jp/PublicInfoSummary.

the nine areas).[62]

Figure 6.16 shows the estimated trend (e.g., of the Tokyo area) for the data of the in-sample period, from April 2016 (when the data was released) to November 2017 (before the period used for estimating the imbalance prediction model). First, it can be confirmed that the output values are larger in order of sunny, cloudy, and rainy weather. Solar power generation decreases in efficiency during the summer due to high temperatures. As a reflection of this, trend (power output leevl) of sunny weather decline in the summer, and such a decrease is resolved in the case of cloudy and rainy. The drastic decline in the rainy trends in the winter coincides with the extreme darkening as the weather changes into sleet or snow. In addition, the maximum temperature contributes to increasing the output, and the minimum temperature contributes to decreasing the output. This could be due to the fact that under a fixed maximum temperature, the lower the minimum temperature (usually recorded in the early hours of the day), the greater the amount of solar radiation during the day (which should be needed to raise the temperature). Therefore, there is a negative correlation between the minimum temperature and solar power output.

We carried out an error analysis for the period from December 2017 to December 2018. The error is evaluated for each area, but the prediction error used in the main text is the total prediction error of all nine areas; the same applies to the demand prediction error in the next section. Figure 6.17 shows a summary of solar power output prediction errors. R-squared does not show any noticeable decline in the out-of-sample period, which means that the model has been built robustly. The same applies to mean absolute error (MAE). The slightly high MAE in Kansai was caused by the downward bias in the trend estimation due to the introduction of solar power being more advanced than expected. Also, in Hokkaido and Hokuriku, where the installed capacity amounts are relatively small (their ratios when compared to the nationwide amount were 3.0% and 2.0%, respectively at the end of December 2018) and discontinuous (unsmoothed), increased instruction trends led to raising the MAE. Additionally, for reference, compared with a model that does not include temperature variables (which we constructed separately to evaluate temperature terms' effects), the model in (6.18) had a higher R-squared by 1.1% (2.5% for in-sample) and a lower MAE by 0.7% (1.7% for in-samples). Both of these values were calculated as simple averages for

[62] Downloaded from http://weather-transition.gger.jp.

each area.

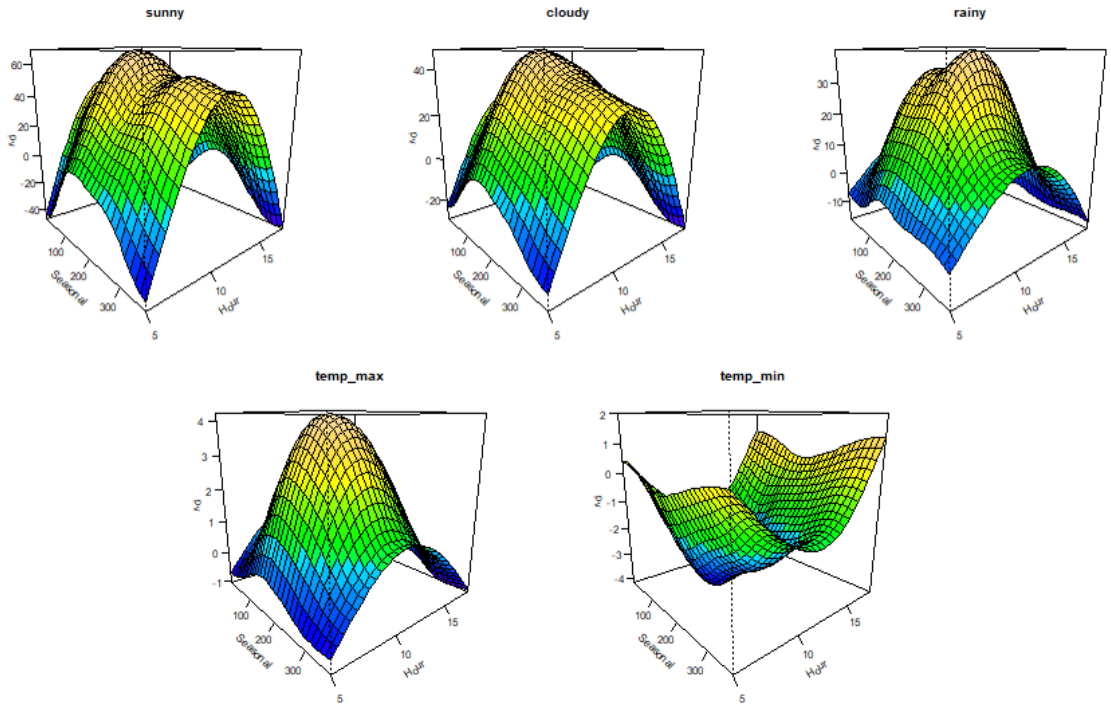

Figure 6.16: Estimated trends of solar power output (example of Tokyo area)

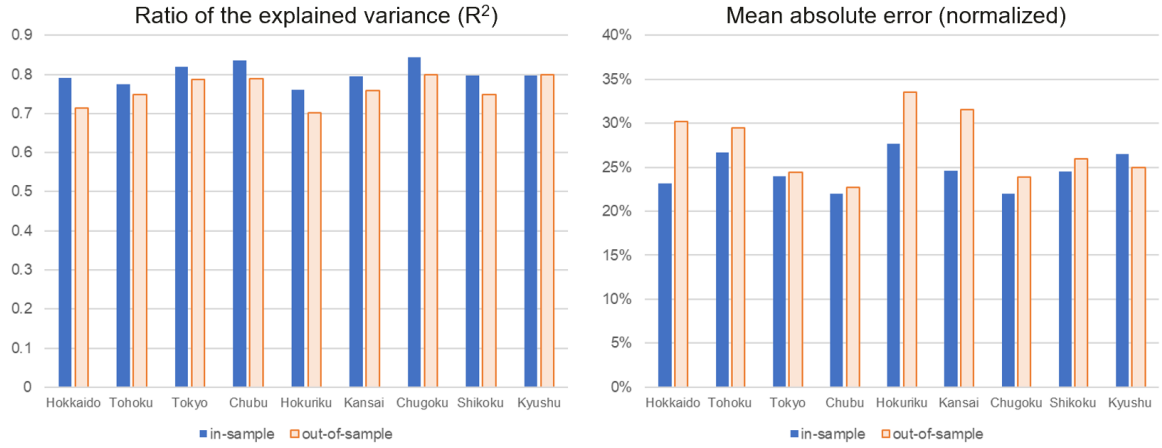

Figure 6.17: Evaluation of solar power output prediction error (Left: R-squared, Right: MAE)

6.7.3 Prediction Method for Demand Using Previous Day Weather Forecast

In this section, we propose a demand prediction method using previous day weather forecasts.

6.7.3.1 Model Construction

Since the obtained demand data is from a small sample size (i.e., the same period as the solar power model in the previous section), ensuring robustness is an issue. Therefore, we will use a tensor product spline function by incorporating a smooth condition of intraday time direction in the same manner as the solar model, thus expanding a previous method (Yamada et al. 2018), which estimated the demand trend by dividing it by time. By doing this, we overcome the problem of robustness and further refine the model by incorporating weather condition variables as well. We construct the following GAM for demand (at date t, hour h) $D_{t,\,h}$:

$$\begin{aligned} D_{t,\,h} = d(t,h) &+ d_{sat}(t,h)I_{sat,t,h} + d_{sun}(t,h)I_{sun,t,h} + d_{tmax}(t,h)\epsilon_{tmax,t,h} \\ &+ d_{tmin}(t,h)\epsilon_{tmin,t,h} + d_{sunny}(t,h)I_{sunny,t,h} \\ &+ d_{rainy}(t,h)I_{rainy,t,h} + d_{snowy}I_{snowy,t,h} + Period_{\,t} + \epsilon_{d,\,t,\,h} \end{aligned} \tag{6.20}$$

where $d_{\cdot}(t,h)$ is the tensor product spline function estimated by the GAM, $I_{\cdot,t,h}$ is a dummy variable (that is 1 if the weather corresponds to the suffix and is 0 otherwise). Therefore, in this model, the first term $d(t,h)$ represents the cloudy weekday's trend. Note that the 'snowy' term is included only in snowy areas, and its coefficient is a fixed value considering robustness. Also, $I_{sun,t,h}$ and $\epsilon_{tmax,t,h}$ are set to 0 whenever hour h is between 0 and 6 because they are not expected to affect the demand at this time.

6.7.3.2 Empirical Analysis

Here, we estimate the demand prediction model and verify the error using the following data:

- Electricity demand $D_{t,\,h}$[MW] : measured data published by OCCTO[63]
- General weather condition $I_{\cdot,t,h}$ maximum/minimum temperature $Tmax_t$ / $Tmin_t$ [°C]: forecast values announced by the JMA on the previous morning (one major city in each of nine areas)[64]

Figure 6.18 shows the estimated trend (e.g., of the Tokyo area) for the data of the in-sample period (from April 2016 to November 2017). First, looking at the trends by day-type, the effect of decreasing demand is strong in the order of Sunday (holidays) and Saturday. Next, as for the trends in the maximum/minimum temperatures, which correspond to the sensitivity of a one-degree rise

[63] Downloaded from http://occtonet.occto.or.jp/public/dfw/RP11/OCCTO/SD/LOGIN_login#.

[64] Downloaded from http://weather-transition.gger.jp.

in demand, the demand rises in the summer (positive sensitivity) and decreases in the winter (negative sensitivity) with each temperature. On the other hand, paying attention to the intraday time trend, the absolute value of sensitivity for the maximum temperature becomes the highest at around 15:00, and that for the minimum temperature is attenuated as the time becomes late (since the prediction horizon is longer). Finally, focusing on trends based on weather conditions, the sunny day trend has a similar shape as the trend of maximum temperature. However, it is different from the decrease in winter daytime, which seems to be because of self-generated solar power outputs (i.e., sunny weather does not only decrease demand but also increases the solar power supply, which deepens the "valley" of the sunny trend). The trend of rainy weather has an inverted U shape in the summer, perhaps because the overnight cooling effect causes a decline in demand, whereas during the daytime humidity increases demand (for dehumidification). For the rainy trend in winter, the demand rises from midnight until the morning (perhaps because of freezing), and the sensitivity decreases later in the day, as the prediction horizon is longer.

Figure 6.19 shows the results of the error analysis for the out-of-sample period from December 2017 to December 2018 in comparison to the in-sample data. For both R-squared and MAE, there was no noticeable decline in the out-of-sample period, and it was confirmed that the model was sufficiently robust.

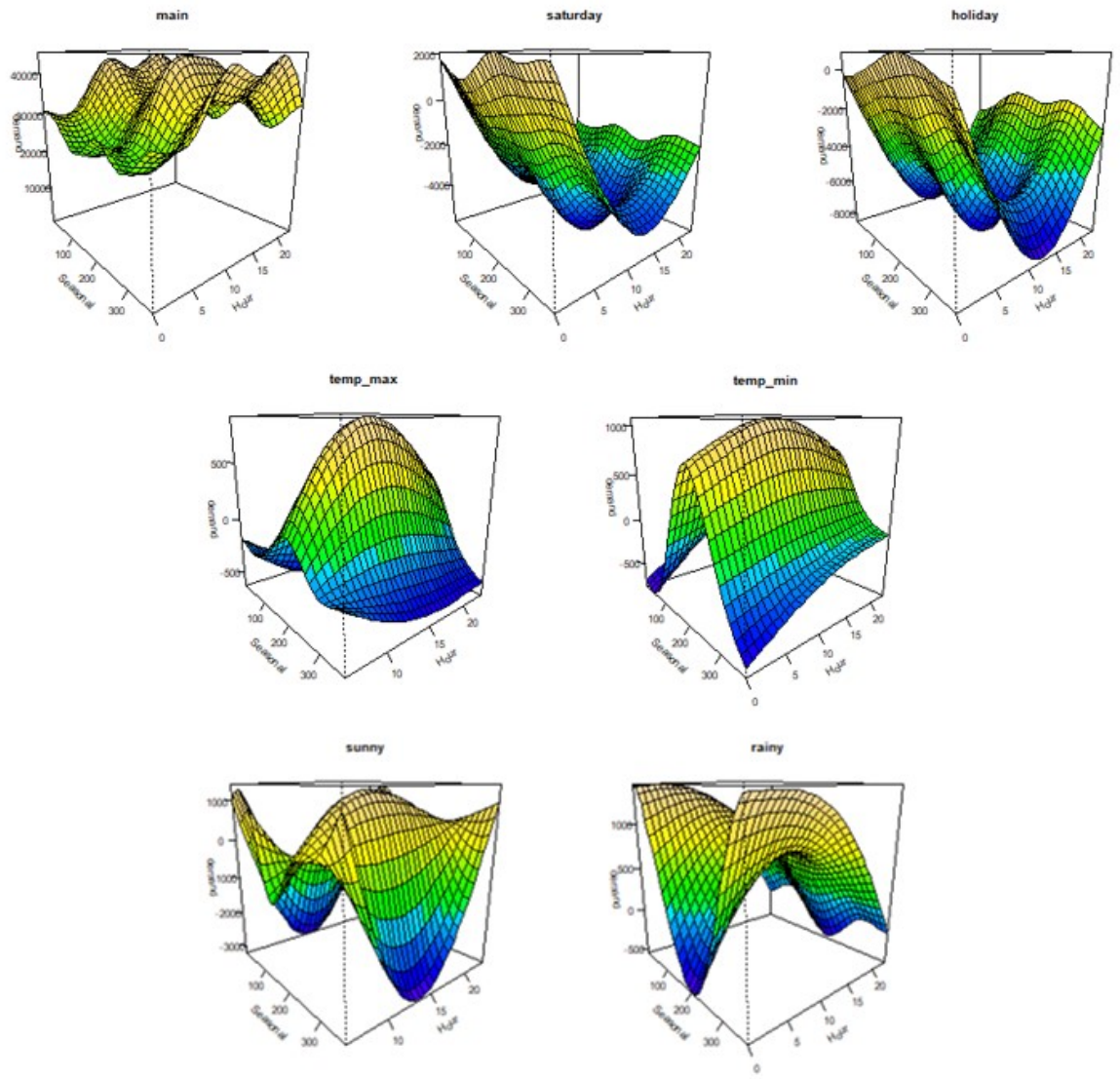

Figure 6.18: Estimated trend of demand (example of Tokyo area)

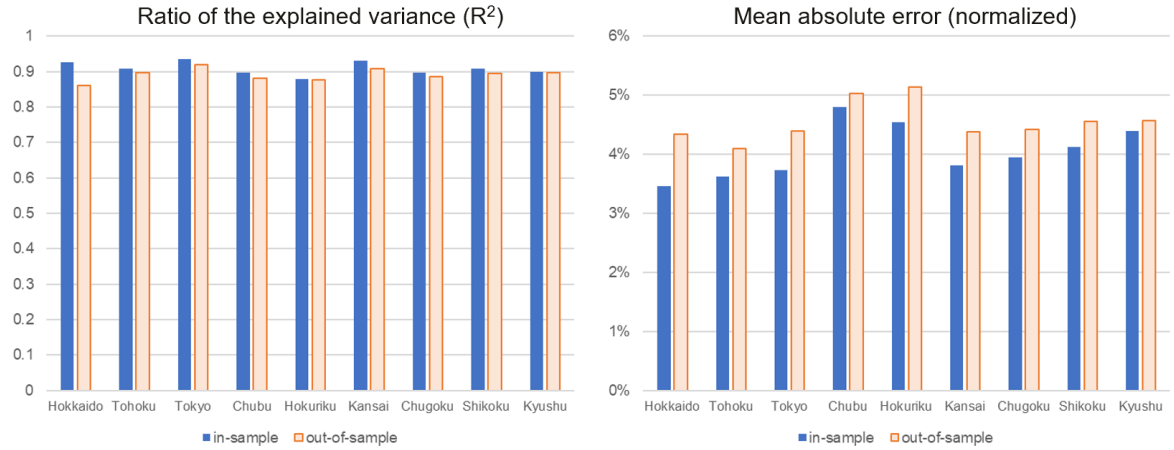

Figure 6.19: Evaluation of demand prediction error (Left: R-squared, Right: MAE)

6.7.4 Significant Evaluation of Demand/Solar Power Prediction Errors on Imbalance

In this section, we perform significance tests to confirm whether the prediction errors in solar power generation and demand calculated in the previous section are significantly influencing the imbalance volume. First, the following OLS estimation is performed with respect to prediction errors in solar power and demand:

$$Imb_t = \rho_s Solar_{t-1} + c_s + \epsilon_{s,t} \tag{6.21}$$

$$Imb_t = \rho_d Demand_{t-1} + c_d + \epsilon_{d,t} \tag{6.22}$$

where $Solar_{t-1}$ ($Demand_{t-1}$) is solar (demand) prediction error calculated as the differential of the latest measured values at $t-1$ and the day-ahead prediction. ρ_s (c_s) and ρ_d (c_d) are the estimated coefficients (constant terms), and $\epsilon_{s,t}$ and $\epsilon_{d,t}$ are the residual term with an average of 0. Of these, ρ_s (ρ_d) is a coefficient for the solar (demand) prediction error as the target of the significance test.

The significant signs that were calculated are shown in Table 6.5 and Table 6.6 (a double sign means the p-value is less than 0.05, and a single sign means it is less than 0.1). For the solar power generation prediction error, there is a significant negative correlation between the prediction error and the (deficit) imbalance volume throughout all seasons (two positive relationships were obtained, but these are in the small impact time zone). Also, the reason the significance in summer daytime periods is weakened could be that the demand prediction error has a large impact on imbalance

volume. Regarding the demand prediction error, there is a significant positive correlation between demand prediction error and the imbalance volume (especially in the winter and summer seasons, as well as during the night for most months).

As described above, since both prediction errors for solar power and demand significantly affect the overall imbalance volume, both variables are incorporated into the imbalance volume prediction model. Note that although obtained significances differ depending on the month and time zone, we do not elaborate on the imbalance forecasting model to distinguish them.

Table 6.5: Summary of Significant Sign for Coefficient of Solar Prediction Error

Month	Hour																							
	0	1	2	3	4	5	6	7	8	9	10	11	12	13	14	15	16	17	18	19	20	21	22	23
1										- -	- -	- -	- -	- -	- -	- -	- -							
2								- -	- -	- -	- -	- -	- -	- -	- -	- -	- -	- -						
3										- -				-	- -	-	- -	- -	- -					
4							- -			- -	- -	- -	- -	- -	- -	- -	- -		-					
5									-	- -	- -	- -			-				+ +					
6							- -			-		-	-	- -	- -	-	- -							
7						+ +				-		-	-	-					-					
8								-	-	-		-			- -									
9									-	- -	- -	- -												
10								- -	- -	- -	- -	- -	- -	- -	- -	- -								
11									- -	- -	- -	- -	- -	- -	- -	- -								
12										- -	- -	- -	- -	- -	- -	- -			- -					

Table 6.6: Summary of Significant Sign for Coefficient of Demand Prediction Error

Month	Hour																							
	0	1	2	3	4	5	6	7	8	9	10	11	12	13	14	15	16	17	18	19	20	21	22	23
1		++	++	++									+	++	++									
2	++		++				+	++	++	++	++	++	++	++	++	++		+	++	++	++	++	++	++
3						+	++			+									++	++	++	++	++	+
4																				+	++	++		
5	++		+																	++	++	++	++	++
6																			++		++	+		++
7	++	++	++	++	++	+			+	++	++	+	+	+	++	++	++	++	++					
8	++	++	++	++				++	++	++	++	++				+	++	++	++	++	++		+	++
9		+							++	++	+					+	+	++	++	++	++			
10										++	++	++	++		++	+	++	++	++	++	++	++	++	++
11																			++	++	++	++	++	++
12	++						++	++							++	+			+	+	++	++	++	++

Chapter 7

Conclusion

In this thesis, we proposed solutions for risk management in the electricity market from the three approaches: prediction methods, hedging methods, and market trading strategies. This chapter summarizes each study, states the conclusions, and offers suggested directions for future works.

7.1 Summary and Conclusion of Each Study

This section summarizes each study performed from Chapter 3 to Chapter 6 (refer to Table 7.1 for the key points of each study). First, in Chapter 3, we proposed a method for predicting solar radiation and solar power output using general weather forecasts reported by the JMA, taking particular note of the smooth yearly cyclical trend identified when dividing the measured value of solar radiation by the hourly clock time and weather. As for the methodology, by using GAM, we extracted the seasonal trends of solar radiation and solar power output for different general weather scenarios. Then, estimating the probability of each weather scenario, given a forecasted weather condition by using a multinomial logit model and combining it with seasonal trends estimated by GAM, we constructed a new prediction model that calculates the prediction values of solar radiation and power output. Finally, Chapter 3 also verifies the superiority of the proposed prediction method in the reduction of prediction error by comparing it with previous related methods and the prediction method that directly substitutes forecast scenarios. The contribution of this research lies particularly in the practical aspect. That is, the proposed modeling approach is relatively easy to construct, and the clarification of the bias that exists in the "forecast value substitution method," which may tend to be adopted in business scenes and could provide a useful perspective, especially for practitioners.

In Chapter 4, we provided prediction error weather derivatives to hedge the risks of loss caused by prediction errors related to solar power output. First, defining a certain loss function, we

measured the hedge effect of the derivative on solar radiation prediction error, thereby verifying that the existing hedging method for wind power can also be applied to solar power generation with strong seasonal trends. By introducing the temperature derivative on the absolute prediction error, we also proposed a cross-hedging method that demonstrated not only a further variance reduction effect when used with solar radiation derivatives but also a certain hedging effect even when only temperature derivatives are used. For the estimation of optimal contract volume of temperature derivatives, we proposed a method using a tensor-product spline function that simultaneously incorporates the smoothing conditions of both the direction of intraday time trend and the seasonal trend; we then verified its effectiveness. The main contributions of this work include the following three points: the application of existing hedging methods to a different target (solar power business), the diversification of underlying assets of derivatives (solar radiation and temperature), and the expansion of models incorporating different time trends (by using tensor product spline function). In recent years, the importance of the social issue of expanding balancing costs due to the prediction error of renewable energy outputs has been increasing and rapidly attracting attention worldwide. We believe that our approach could provide a possible solution for the issue.

Chapter 5 proposed simultaneous hedging strategies of price and volumetric risks using two different market models: (1) the revenue of solar power generation companies in the JEPX spot market and (2) the procurement cost of retail electricity business in the PJM market. In both cases, using a portfolio of derivatives whose underlying assets consist of fuel prices and weather derivatives (e.g., solar radiation and temperature), we proposed multilateral hedge modeling strategies that apply various non-parametric regression methods such as tensor product spline function, ANOVA decomposition, and spline function with cross variables. Through an empirical analysis, we demonstrated the effectiveness and versatility of the model, using data from JEPX and PJM. Also, we proposed new standardized derivatives whose underlying assets are the square of the temperature prediction error and verified significant hedging effects using empirical data. In this way, the contributions of this study can be summarized as expanding the previous method to support for estimating complex trends, verifying the robustness of hedging strategies using multiple market models, and proposing new standardized derivatives. The applicability and versatility demonstrated by this work indicate the potential for the further development of our approach.

Lastly, in Chapter 6, which was motivated by the system change in the Japanese electricity market in 2019, we examined the validity of the new balancing system from the perspective of retailers' arbitrage effects. There, we revealed that the system balancing effect brought by arbitragers, which is shown in the previous study in an Austrian market model, also present in the new Japanese system. In particular, we demonstrated that the arbitrager's profit and the system stabilization effect increase as the predictability of imbalance increases, and that a certain level of penalty is effective in further reducing the imbalance in the Japanese market with relatively low liquidity. In terms of modelling, we derived a discrete approximate prediction method that is based on two-step quantile regressions and considers both probability distributions of imbalance amount and price, which can be used for analyzing balancing markets in different countries without deterministic imbalance price formulae. We also proposed a high-resolution analytical method, for example, by constructing an optimization problem with the decision variable of the arbitrager as a continuous variable. Thus, in this work, we provided valuable suggestions not only regarding the bidding strategies of retailers but also the institutional decision making of policymakers. It is expected that this research will have beneficial implications for the future system design in the free electricity market aiming for stable supply and economic efficiency in the electricity market.

7.2 Concluding Remarks and Suggestions for Future Works

As mentioned at the beginning of Chapter 1, this study focused most intently on responding to needs in light of recent environmental changes. Each theme discussed in this thesis deals with current social issues. Such issues include the hedging methods for risks derived from the worldwide expansion of renewable energy, the effective modeling method for complex time series trends, the practical prediction method for new entrants into the solar power market, and the analysis of the market mechanism of the balancing system where the system design is reviewed in a groping state. A wide variety of our results, demonstrated by data from Japan with a large amount of solar power, may provide valuable case studies for markets in other countries, which may need to respond to such risks equally to a greater extent than Japan in the near future.

In terms of practical applications, this work emphasized the interpretability of the proposed model. GAM-based trend estimation, which has been covered in many studies, has several advantages, particularly in terms of providing intuitive interpretations with visualization and in

ensuring the robustness of model estimation and understandability in the calculation process. As mentioned at the end of Chapter 1, what matters in business implementation and policymaking is how the analysis results can provide useful suggestions for decision-making among many stakeholders. By focusing on such a point, this study emphasized interpretability for modeling analyses and pursued the meanings that can be extracted from each result by adding detailed explanations and illustrations.

As described above, we provided some suggestions related to the practical needs of recent social issues, but this study only addressed very limited issues in a highly complex electricity market system. It is expected that new risks due to the expansion of renewable energy will become more serious in the future. To cope with such challenges, it would be necessary to combine extensive hardware and software technologies. For example, as the use of distributed power generation that utilizes solar energy or small batteries progresses more and more in the future, the electricity transaction with new information and communication technologies such as P2P and blockchain will become more realistic components of further enhancing the trading efficiency. In such a changing environment, it is expected that the evolution of models in the aspect of risk management will become increasingly necessary.

In terms of the immaturity of the Japanese electricity market, there is also much to learn from overseas cases. Chapter 5 of this thesis presented an empirical study using the US-PJM market model, and Chapter 6 analyzed Japanese market mechanisms inspired by the institutional design of the European markets. The insight gained through these works is that cross-sectional analyses of the different markets sometimes result in new empirical findings or modeling ideas. In order to continue to obtain useful suggestions for electricity markets that are highly specific to individual countries, it could be beneficial to apply previous research on other countries' markets to the Japanese market and vice versa.

Risk management in the electricity market involves a very complex social issue. To tackle this challenge, it is essential to organically connect opposite concepts—such as research and practice, domestic and international, and business strategy and policy design—as has been done to some extent in this research. Such an integrated approach could be useful to further improving the efficiency of the energy market and maximizing social welfare.

Table 7.1: Key points for each study

Chapter/ Theme overview	Chapter 3: Prediction Method for Solar Power Business	Chapter 4: Prediction Error Weather Derivatives for Solar Power	Chapter 5: Hedging Strategy for Revenue/Cost Fluctuation	Chapter 6: Arbitrage Strategy and Effect in Imbalance System
Social background and research purpose	• Proposal of practical prediction method against the background of the increase in new entrants in the solar power business triggered by electricity liberalization and the feed-in tariff system (FIT)	• Proposal of a hedging method for predicting error loss caused by the recent increase in renewable energy (solar power) and the resulting supply-demand adjustment costs	• Proposal of alternative hedging strategies using multiple weather / fuel price derivatives portfolios in the absence of a liquid market for derivatives on prices	• Verification of the effect of the new market incentive triggered by the change in the balancing system • Market trading strategies for retailers exposed to new imbalance risks
Most relevant previous studies	Yamada et al. (2015) - Estimation of yearly cyclical trend using a GAM	Yamada (2018b) - Prediction error weather derivatives in wind power	Yamada (2019) - Simultaneous hedging of demand and price	Bunn and Kermer (2018) - Imbalance arbitrage in the Austrian market
Used model/method	• GAM • Multinomial logit model (MNL)	• GAM (tensor product spline and spline function with cross variable)	• GAM (tensor product spline and spline function with cross variable, ANOVA decomposition)	• Quantile regression • Optimization algorism using Newton's method • GAM
Viewpoints of modeling	• Modeled seasonality when time series were divided by clock time and weather using GAM • Focused on bias correction by separately estimating probability distributions of weather scenarios	• Modeled two different smoothing trends, such as time and date, with tensor product splines • Simultaneous estimation for payoff functions of multiple derivatives based on solar radiation and temperature	• Clarification of hedge modeling structure using ANOVA decomposition • Simultaneous estimation of trends with different features, such as date and underlying assets, as well as seasonality and annual change	• Proposal of a two-step quantile regression using the concept of mesh approximation • Derivation of optimal solutions for continuous decision variables based on Newton's method
Suggestions from the empirical analysis	• Enough prediction accuracy despite easy handling using public data • Reduction in bias and error by using MNL (pointed out the problem in "forecast value substitution method")	• Demonstrated the applicability of existing methods for wind power to solar power with strong seasonality • Confirmation of a high cross-hedge effect among temperature derivatives	• Demonstration of a strong cross-hedge effect by derivatives portfolio • High versatility of the models is proven by a demonstration using multiple market models, such as the JEPX and PJM	• Policy implications of retailers' arbitrage allowances to reduce imbalance amounts • Proved that new penalties have effective incentives for system stabilization

Reference

[1] Ang BW (1995) Decomposition methodology in industrial energy demand analysis. *Energy* 20(11):1081-1095.

[2] Antonanzas J, Osorio N, Escobar R, Urraca R, Martinez-de-Pison F, Antonanzas-Torres F (2016) Review of photovoltaic power forecasting. S*olar Energy* 136:78-111.

[3] Augustin NH, Beevers L, Sloan WT (2008) Predicting river flows for future climates using an autoregressive multinomial logit model. *Water Resources Research* 44(7).

[4] Bacher P, Madsen H, Nielsen HA (2009) Online short-term solar power forecasting. *Solar Energy*, 83(10):1772-1783.

[5] Benth FE, Benth JS, Koekebakker S (2008) *Stochastic modelling of electricity and related markets* Vol. 11 (World Scientific).

[6] Bessa RJ, Trindade A, Silva CS, Miranda V (2015) Probabilistic solar power forecasting in smart grids using distributed information. *International Journal of Electrical Power & Energy Systems* 72:16-23.

[7] Bhattacharya S, Gupta A, Kar K, Owusu A (2015) Hedging strategies for risk reduction through weather derivatives in renewable energy markets. *IEEE International Conference on Renewable Energy Research and Applications*: 1190-1195.

[8] Bhattacharya S, Gupta A, Kar K, Owusu A (2019) Risk Management of Renewable Power Producers from Co-dependencies in Cash Flows. *European Journal of Operational Research*.

[9] Blackmon BG (1985) A Futures Market for Electricity: Benefits and Feasibility. *Harvard Uni. Kennedy School of Gov., En. & Env. Policy Centre, Disc. Paper* E-85-07.

[10] Boogert A, Dupont D (2005) On the effectiveness of the anti-gaming policy between the day-ahead and real-time electricity markets in The Netherlands. *Energy Economics* 27(5):752–770.

[11] Brockett PL, Wang M, Yang C, Zou H (2006) Portfolio effects and valuation of weather derivatives. *Financial Review* 41:55–76.

[12] Browell J (2018) Risk Constrained Trading Strategies for Stochastic Generation with a Single-Price Balancing Market. *Energies* 11(6).

[13] Bunn DW (2000) Forecasting loads and prices in competitive power markets. *Proc. of the IEEE* 88(2):163-169.

[14] Bunn DW (2004) *Modelling Prices in Competitive Electricity Markets* (The Wiley Finance Series).

[15] Bunn DW, Kermer S (2018) Statistical arbitrage and information flow in an electricity balancing market. Available at SSRN 3101716.

[16] Bunn DW, Gianfreda A, Kermer S (2018). A trading-based evaluation of density forecasts in a real-time electricity market. *Energies* 11(10):2658.

[17] Burger M, Graeber B, Schindlmayr G (2008) *Managing energy risk: An integrated view on power and other energy markets* (John Wiley & Sons).

[18] Cao M, Wei J (2005) Stock market returns: a note on temperature anomaly. *Journal of Banking and Finance* 29:1559-1573.

[19] Carr P, Madan D (2001) Optimal positioning in derivative securities, *Quantitative Finance* 1:19-37.

[20] Charytoniuk W, Chen MS, Van Olinda P (1998) Nonparametric regression based short-term load forecasting *IEEE transactions on Power Systems* 13(3):725-730.

[21] Davino C, Furno M, Vistocco D (2014) *Quantile Regression: Theory and Applications* (John Wiley & Sons).

[22] Davis M (2001) Pricing weather derivatives by marginal value, *Quantitative Finance* 1(3):305-308.

[23] Ding H, Pinson P, Hu Z, Wang J, Song Y (2017) Optimal Offering and Operating Strategy for a Large Wind-Storage System as a Price Maker. *IEEE Transactions on Power Systems* 32(6):4904–4913.

[24] Deng SJ, Oren SS (2006) Electricity derivatives and risk management. *Energy* 31(6-7):940-953.

[25] Detyniecki M, Marsala C, Krishnan A, Siegel M. (2012) Weather-based solar energy prediction. *Proc. of the 2012 IEEE Congress on Computational Intelligence*, Brisbane, Australia: 587-593.

[26] Efron B, Stein C (1981) The jackknife estimate of variance. *The Annals of Statistics*:586-596.

[27] Electricity and Gas Market Surveillance Commission (2018) Management Philosophy and Medium-term Policy. https://www.emsc.meti.go.jp/activity/emsc_system/pdf/032_08_00.pdf. (in Japanese)

[28] Electricity and Gas Market Surveillance Commission (2019) Detailed design of imbalance fees from FY2021. https://www.emsc.meti.go.jp/activity/emsc_system/pdf/036_03_00.pdf. (in Japanese)

[29] Emery GW, Liu Q (2002) An analysis of the relationship between electricity and natural gas futures prices. Journal of Futures Markets. *Journal of Futures Market* 22(2):95-122.

[30] Eydeland A, Wolyniec K (2003) *Energy and power risk management: New developments in modeling, pricing, and hedging* (John Wiley & Sons).

[31] Feller W (1971) *An introduction to probability theory and its applications, volume II* (Wiley, New York, 1971).

[32] Fishbone LG, Abilock H (1981) Markal, a linear - programming model for energy systems analysis: Technical description of the bnl version. *International journal of Energy research* 5(4):353-375.

[33] Fonseca J, Oozeki T, Ohtake H, Shimose KI, Takashima T, Ogimoto K (2014) Regional forecasts and smoothing effect of photovoltaic power generation in Japan: an approach with principal component analysis. *Renewable Energy* 68:403-413.

[34] Gedra TW (1994) Optional forward contracts for electric power markets. *IEEE Transaction of Power Systems* 9(4):1766-1773.

[35] Greene WH (1993) *Econometric Analysis* (Engelwood Cliffs).

[36] Goodarzi S, Perera HN, Bunn DW (2019) The impact of renewable energy forecast errors on imbalance volumes and electricity spot prices. *Energy Policy* 134：110827.

[37] Haida T, Muto S (1994) Regression based peak load forecasting using a transformation technique. *IEEE Transactions on Power Systems* 9(4):1788-1794.

[38] Haque AU, Nehrir MH, Mandal P (2013) Solar PV power generation forecast using a hybrid intelligent approach. *In 2013 IEEE Power & Energy Society General Meeting*: 1-5.

[39] Hastie T, Tibshirani R (1990) *Generalized additive models* (Chapman & Hall).

[40] Hosoda Y, Namerikawa T (2012) Short-term Photovoltaic Prediction by using Switching Kalman Filtering and Clustering. *Japan Joint Automatic Control Conference*. (in Japanese)

[41] Hull J (2000) *Options, Futures, and Other Derivative. 4th ed* (Prentice-Hall).

[42] Janczura J, Trück S, Weron R, Wolff RC (2013) Identifying spikes and seasonal components in electricity spot price data: A guide to robust modeling. *Energy Economics* 38:96-110.

[43] Jimenez PA, Hacker JP, Dudhia J, Haupt SE, Ruiz-Arias JA, Gueymard CA, Thompson G, Eidhammer T, Deng A (2016) WRF-Solar: Description and clear-sky assessment of an augmented NWP model for solar power prediction. *Bulletin of the American Meteorological Society* 97(7):1249-1264.

[44] Kamo M, Kato A, Yoshimoto A (2013) Snow Damage Analysis by Discrete Regression Models. *Proceedings of the Institute of Statistical Mathematics* 61(2):189-200. (in Japanese)

[45] Kanamura T (2019) Volumetric Risk Hedging Strategies and Basis Risk Premium for Solar Power. Available at SSRN 3325755.

[46] Kanamura T, Ohashi K (2009) Pricing summer day options by good-deal bounds. *Energy Economics* 31:289–297.

[47] Kataoka Y, Fujiwara K, Ishihara Y, Funabashi T, Okuno Y, Nakashima H (2009) Study on Forecasting Irradiation by Using Cloudiness of Numerical Prediction Data. *Proceedings of JSES/JWEA Joint Conference*:127-130. (in Japanese)

[48] Kath C, Ziel F (2018) The value of forecasts: Quantifying the economic gains of accurate quarter-hourly electricity price forecasts. *Energy Economics 76*:411-423.

[49] Kato T (2017) Development of Forecasting Method of Photovoltaic Power Output. The *Journal of the IEEJ* 137(2):101-104. (in Japanese)

[50] Kaye RJ, Outhred HR, Bannister CH (1990) Forward contracts for the operation of an electricity industry under spot pricing. *IEEE Trans. Power Systems* 5(1):46-52.

[51] Kawasaki S, Taoka H, Nagao T, Onaka K (2015) Development of Insolation Forecasting Method by Genetic Algorithm. *IEEJ Transactions on Power and Energy* 135(2):89-96. (in Japanese)

[52] Kiesel R, Paraschiv F (2017) Econometric analysis of 15-minute intraday electricity prices. *Energy Economics 64*:77-90.

[53] Kim J, Kim D, Yoo W, Lee J, Kim YB (2017) Daily prediction of solar power generation based on weather forecast information in Korea. *IET Renewable Power Generation* 11(10):1268-1273.

[54] Klæboe G, Eriksrud AL, Fleten SE (2015) Benchmarking time series based forecasting models for electricity balancing market prices. *Energy Systems*, 6(1):43-61.

[55] Koenker R (2005) Quantile Regression, *Econometric Society monographs; no. 38* (Cambridge university press).

[56] Kristiansen T (2004) Congestion management, transmission pricing and area price hedging in the Nordic region. *Electrical Power and Energy Systems* 26:685-695.

[57] Krishnamurthy D, Uckun C, Zhou Z, Thimmapuram PR, Botterud A (2018) Energy Storage Arbitrage Under Day-Ahead and Real-Time Price Uncertainty. *IEEE Transactions on Power Systems* 33(1):84-93.

[58] Kudo M, Takeuchi A, Nozaki Y, Endo H, Sumita J (2007) Forecasting Electric Power Generation of Photovoltaic Power System for Energy Network. *IEEJ Transactions on Power and Energy* 127(7):847-853. (in Japanese)

[59] Kurokawa K, Wakamatsu K (1994) *Photovoltaic power generation system design guidebook* (Ohmusha). (in Japanese)

[60] Lee Y, Oren SS (2009) An equilibrium pricing model for weather derivatives in a multicommodity setting. *Energy Economics* 31, 70213.

[61] Liebl D (2013) Modeling and forecasting electricity spot prices: A functional data perspective. *The Annals of Applied Statistics* 7(3):1562-1592.

[62] Liu M, Wu FF, Ni Y (2006) A survey on risk management in electricity markets. *In 2006 IEEE Power Engineering Society General Meeting*.

[63] Li Y, Su Y, Shu L (2014) An ARMAX model for forecasting the power output of a grid connected photovoltaic system. *Renewable Energy* 66:78-89.

[64] Lorenz E, Hurka J, Karampela G, Heinemann D, Beyer HG, Schneider M (2007) Qualified Forecast of ensemble power production by spatially dispersed grid-connected PV systems. *Measurement*.

[65] Lorenz E, Remund J, Müller SC, Traunmüller W, Steinmaurer G, Pozo D, Ruiz Arias JA, Lara Fanego V, Ramirez L, Gastón M (2009) Benchmarking of different approaches to forecast solar irradiance. *In 24th European photovoltaic solar energy conference*. Hamburg, Germany: 21-25.

[66] Maciejowska K, Nitka W, Weron T (2019) Day-Ahead vs. Intraday - Forecasting the Price Spread to Maximize Economic Benefits. *Energies* 12(4):631.

[67] Mahoney D (2016) *Modeling and Valuation of Energy Structures: Analytics, Econometrics, and Numerics* (Springer).

[68] Mathiesen P, Collier C, Kleissl J. (2013) A high-resolution, cloud-assimilating numerical weather prediction model for solar irradiance forecasting. *Solar Energy* 92:47-61.

[69] Matsumoto T, Yamada Y (2018a) Design of solar radiation derivatives based on prediction errors and measurement of the hedge effect. *Abstracts of the 2018 Spring National Conference of the ORSJ.* (in Japanese)

[70] Matsumoto T, Yamada Y (2018b) Cross Hedging Using Prediction Error Weather Derivatives for Loss of Solar Output Prediction Errors in Electricity Market. *Asia-Pacific Financial Markets* 26(2):211-227.

[71] Matsumoto T, Yamada Y (2019a) Prediction method for solar power business based on forecasted general weather conditions and periodic trends by weather. *Transactions of the Operations Research Society of Japan.* 62:1-22. (in Japanese)

[72] Matsumoto T, Yamada Y (2019b) Cross Hedging Using Prediction Error Weather Derivatives for Loss of Solar Output Prediction Errors in Electricity Market. *Asia-Pacific Financial Markets* 26(2):211-227.

[73] Matsumoto T, Yamada Y (2019c) Integrated derivative portfolio for hedging the risk of fluctuations in solar power business revenue in the wholesale power trading market, *Proc. of the 51st JAFEE winter conference*. (in Japanese)

[74] Matsumoto T, Yamada Y (2019d) Hedging strategies for solar power businesses in electricity market using weather derivatives. *Proc. in 2019 IEEE 2nd International Conference on Renewable Energy and Power Engineering*.

[75] McFadden D (1974) Conditional Logit Analysis of Qualitative Choice Behavior. *Frontiers in Econometrics*: 105-142.

[76] Mellit A, Pavan AM (2010) A 24-h forecast of solar irradiance using artificial neural network: Application for performance prediction of a grid-connected PV plant at Trieste, Italy. *Solar Energy* 84(5): 807-821.

[77] Meier J, Schneider S, Le CH (2019) Short-term Electricity Price Forecasting Using Generalized Additive Models, *Proc. of 15th Int. Conf. on ICT in Education, Research and Industrial Applications*.

[78] Ministry of Economy, Trade and Industry (2017a). The influence of solar power generatio n forecast failure in the supply and demand adjustment service of general transmission and distribution business operators, http://www.emsc.meti.go.jp/activity/emsc_system/pdf/025_08_00.pdf. (in Japanese)

[79] Ministry of Economy, Trade and Industry (2017b) Immediate review of imbalance fees, https://www.meti.go.jp/shingikai/enecho/denryoku_gas/denryoku_gas/seido_kento/pdf/007_04_00.pdf. (in Japanese)

[80] Ministry of Economy, Trade and Industry (2018) Improving the institutional environment t o ensure efficient and stable power supply and demand balance, https://www.meti.go.jp/shingikai/enecho/denryoku_gas/denryoku_gas/pdf/010_05_00.pdf. (in Japanese)

[81] Ministry of Economy, Trade and Industry (2019) Appropriate market mechanism and the way of securing supply and demand, https://www.meti.go.jp/shingikai/enecho/denryoku_gas/denryoku_gas/pdf/020_07_00.pdf. (in Japanese)

[82] Moghram I, Rahman S (1989) Analysis and evaluation of five short-term load forecasting techniques. *IEEE Transactions on power systems* 4(4):1484-1491.

[83] Monteiro C, Ramirez-Rosado I, Fernandez-Jimenez L, Conde P (2016) Short-term price forecasting models based on artificial neural networks for intraday sessions in the Iberian electricity market. *Energies 9*(9):721.

[84] Mori H, Okada M (2016) An ANN-based design for weather derivatives in consideration of meteorological uncertainties. *In 2016 IEEE Innovative Smart Grid Technologies-Asia*: 1002-1007.

[85] Nakamura N, Mishima Y (2013) Forecasting Next Day's Photovoltaic Generation Output Using the Cloud Amount Information. *Annual Meeting Record of IEEJ*: 191-192. (in Japanese)

[86] OFGEM (2014) *Electricity Balancing Significant Code Review*. https://www.ofgem.gov.uk/electricity/wholesale-market/market-efficiency-review-and-reform/electricity-balancing-significant-code-review.

[87] Omasa K, Tsunekawa A, Machida A (1999) Study on future prediction of vegetation distribution in the Asia-Pacific region by climate change. *Chikyu-kankyo* 4(1):105-113. (in Japanese)

[88] Orita S, Kemmoku Y, Nakagawa S, Sakakibara T (1997) Insolation Forecasting by a Multi-Stage Neural Network. *IEEJ Transactions on Power and Energy* 117(8):1146-1151. (in Japanese)

[89] Papalexopoulos AD, Hesterberg TC (1990) A regression-based approach to short-term system load forecasting. *IEEE Transactions on Power Systems* 5(4):1535-1547.

[90] Pedro HT, Coimbra CF (2012) Assessment of forecasting techniques for solar power production with no exogenous inputs. *Solar Energy 86*(7):2017-2028.

[91] Pelland S, Remund J, Kleissl J, Oozeki T (2013) Photovoltaic and Solar Forecasting: State of the Art. *International Energy Agency, Report PVPS T14-10*.

[92] Peura H, Bunn DW (2018) Strategic forward trading and technology. Available at SSRN 2738703.

[93] PJM (2014) *Analysis of Operational Events and Market Impacts During the January 2014 Cold Weather Events*. https://www.pjm.com/~/media/library/reports-notices/weather-related/20140509-analysis-of-operational-events-and-market-impacts-during-the-jan-2014-cold-weather-events.ashx.

[94] Platen E, West J (2004) A fair pricing approach to weather derivatives. *Asia-Pacific Financial Markets* 11:23–53.

[95] Powell A (1993) Trading Forward in an Imperfect Market: The Case of Electricity in Britain. *The Economic Journal* 103(417):444-453.

[96] PricewaterhouseCoopers (2011) *Weather Risk Derivative Survey Prepared for the Weather Risk Management Association.* https://wrma.org/wp-content/uploads/2014/07/WRMA-2010-2011-Industry-Survey-Results.pdf.

[97] Qing X, Niu Y (2018) Hourly day-ahead solar irradiance prediction using weather forecasts by LSTM. *Energy* 148:461-468.

[98] Ramsami P, Oree V (2015) A hybrid method for forecasting the energy output of photovoltaic systems. *Energy Conversion and Management* 95:406-413.

[99] Rana M, Koprinska I, Agelidis VG (2015) 2D-interval forecasts for solar power production. *Solar Energy* 122:191-203.

[100] Sasaki S, Fukunaga S, Ota Y (2017) Evaluation of kWh Value of Photovoltaic Generation by Application of Simplified Method using Numerical Factor of Weather. *Journal of Japan Society of Energy and Resources* 38(5):1-9. (in Japanese)

[101] Shankar V, Mannering F (1996) An exploratory multinomial logit analysis of single-vehicle motorcycle accident severity. *Journal of Safety Research* 27(3): 183-194.

[102] Sharma N, Sharma P, Irwin D, Shenoy P (2011) Predicting solar generation from weather forecasts using machine learning. *In 2011 IEEE international conference on smart grid communications*: 528-533.

[103] Shimada S, Liu Y, Yoshino J, Kobayashi T, Wazawa Y (2013) Solar irradiance forecasting using a mesoscale meteorological model: Part II: Increasing the accuracy using the Kalman filter. *Solar energy* 39(3):61-67. (in Japanese)

[104] Shimada T, Kurokawa K (2007) Insolation Forecasting Using Weather Forecast with Weather Change Patterns. *IEEJ Transactions on Power and Energy* 127(11):1219-1225. (in Japanese)

[105] Shirakami K, Kawahara K (2016) Study on Predicting Solar Radiation Using Pattern Matching for Searching Similar Weather. *The Journal of the Institute of Electrical Installation Engineers of Japan* 36(12):875-880. (in Japanese)

[106] Simonov M, Mussetta M, Grimaccia F, Leva S, Zich R (2012) Artificial intelligence forecast of PV plant production for integration in smart energy systems. *International Review of Electrical Engineering* 7(1):3454-3460.

[107] Smith LD, Lawrence EC (1995) Forecasting losses on a liquidating long-term loan portfolio. *Journal of Banking & Finance* 19(6):959-985.

[108] Smith LD, Sanchez SM, Lawrence EC (1996) A comprehensive model for managing credit risk on home mortgage portfolios. *Decision Sciences* 27(2):291-317.

[109] Suganthi L, Samuel AA (2012) Energy models for demand forecasting - A review. *Renewable and sustainable energy reviews* 16(2):1223-1240.

[110] Takeuchi K (1979) Form and method of statistical forecast. *Journal for ORSJ Members*, 24(1):31-34. (in Japanese)

[111] Tamura H, Hiraguchi H, Nishizawa K (2014) Development of a solar irradiance forecasting method for PV systems (Part 2) Analysis of prediction errors and investigation for accuracy improvement. *Central Research Institute of Electric Power Industry Annual Reports*: 13013. (in Japanese)

[112] Tanlapco E, Lawarree J, Liu CC (2002) Hedging with futures contracts in a deregulated electricity industry. *IEEE Transactions on Power Systems* 17(3):577-582.

[113] Turvey CG (2001) Weather derivatives for specific event risks in agriculture. *Review of Agricultural Economics* 23(2):333-351.

[114] Veen RA, Hakvoort RA (2016) The electricity balancing market: Exploring the design challenge. *Utilities Policy* 43:186-194.

[115] Weber C, Just S (2012) Strategic Behavior in the German Balancing Energy Mechanism: Incentives, Evidence, Costs and Solutions. *Journal of Regulatory Economics* 48(2): 218-243.

[116] Weron R (2007) *Modeling and forecasting electricity loads and prices: A statistical approach* (John Wiley & Sons).

[117] Weron R (2014) Electricity price forecasting: A review of the state-of-the-art with a look into the future. *International journal of forecasting* 30(4):1030-1081.

[118] Woo CK, Horowitz L, Olson A, DeBenedictis A, Miller D, Moore J (2011) Cross-hedging and forward-contract pricing of electricity in the Pacific Northwest. *Managerial and Decision Economics* 32(4):265-279.

[119] Woo CK, Moore J, Schneiderman B, Ho T, Olson A, Alagappan L, Zarnikau J (2016) Merit-order effects of renewable energy and price divergence in California's day-ahead and real-time electricity markets. *Energy Policy 92*:299-312.

[120] Wood SN (2013) Thin plate regression splines. *Journal of the Royal Statistical Society: Series B (Statistical Methodology)* 65(1):95-114.

[121] Wood SN (2017) *Generalized additive models: an introduction with R* (Chapman and Hall).

[122] Wood SN (2019) *Package 'mgcv' v. 1.8-28*. https://cran.r-project.org/web/packages/mgcv/mgcv.pdf.

[123] Yamada F, Wazawa Y, Kobayashi K, Miwa Y, Kinno T, Yukita K, Goto Y, Ichiyanagi K (2014) Prediction of Next Day Solar Power Generation by Gray Theory and Neural Networks. *IEEJ Transactions on Power and Energy* 134(6):494-500. (in Japanese)

[124] Yamada Y (2008a) Optimal design of wind derivatives based on prediction errors. *JAFEE Journal* 7:152-181. (in Japanese)

[125] Yamada Y (2008b) Optimal hedging of prediction errors using prediction errors. *Asia-Pacific Financial Markets* 15(1):67-95.

[126] Yamada Y (2016) The Importance of Weather Prediction in the Field of Photovoltaic Power Generation. *Journal of Japan Society of Fluid Mechanics* 35(1):7-11. (in Japanese)

[127] Yamada Y (2017) Construction of JEPX forward pricing model based on spot price prediction. *RIETI Discussion Paper Series, 17-J-072*: 1-21.

[128] Yamada Y (2018) Hedge of JEPX spot price considering periodicity error correlation by weather derivatives. *Proceedings of the JAFEE winter conference* 60-71. (in Japanese)

[129] Yamada Y (2019) Simultaneous hedging of demand and price by temperature and power derivative portfolio: consideration of periodic correlation using GAM with cross variable. *Proc. of the 50th JAFEE winter conference*. (in Japanese)

[130] Yamada Y, Iida M, Tsubaki H (2006) Pricing of weather derivatives based on trend prediction and their hedge effect on business risks. *Proceeding of the Institute of Statistical Mathematics* 54(1):57-78. (in Japanese)

[131] Yamada Y, Kurahashi S, Yamaguchi N (2018) Demand forecasting model construction for electricity market trading simulation experiment. *Abstracts of the 2018 Spring National Conference of the ORSJ.* (in Japanese)

[132] Yamada Y, Makimoto N, Takashima R (2015) JEPX price predictions using GAMs and estimations of volume-price functions. *JAFEE Journal* 14:8-39. (in Japanese)

[133] Yamada Y, Makimoto N, Takashima R, Goto J (2016) Estimation of JEPX spot power supply / demand function based on parametric expression. *JAFEE Journal* 15:64-93. (in Japanese)

[134] Yamagishi Y, Saji K, Aoki I, Tanikawa R, Fujii Y (2012) Accuracy Verification of Irradiance Forecast using Numerical Weather Prediction Data by Japan Meteorological Agency. *IEEJ Transactions on Power and Energy* 132(4):334-340. (in Japanese)

[135] Yona A, Senjyu T, Funabshi T, Sekine H (2008) Application of Neural Network to 24-hours-Ahead Generating Power Forecasting for PV System. *IEEJ Transactions on Power and Energy* 128(1):33-40. (in Japanese)

[136] Yukawa M, Asaoka M, Takahara K, Ohshiro T, Kurokawa K (1996) Estimation of Photovoltaic Module Temperature Rise. *IEEJ Transactions on Power and Energy*, 116(9):1101-1110.